NTNU

Norwegian University of
Science and Technology

# Dynamic Real-Time Optimisation of an Amine-Based Post-Combustion $CO_2$ Capture Facility using Single-Level Nonlinear Model Predictive Control

**Mathilde Hotvedt**

Master of Science in Cybernetics and Robotics
Submission date: June 2018
Supervisor: Lars Imsland, ITK
Co-supervisor: Svein Olav Hauger, Cybernetica AS
Fredrik Gjertsen, Cybernetica AS

Norwegian University of Science and Technology
Department of Engineering Cybernetics

# Preface

This Master's thesis was written in collaboration with *Cybernetica AS*, who suggested the research questions investigated in this thesis. *Cybernetica AS* has made their software tools Modelfit, CENIT and RealSim available for investigation of the research questions and have provided assistance for utilisation of the tools. The thesis has utilised previous work done in a Project thesis during autumn 2017, which has been enclosed for the interested reader, although contents relevant for this thesis have been included in condensed form for completeness. Further description of *Cybernetica AS* involvement may be found in Chapter 1, in particular Sections 1.3-1.5, and a deeper explanation of software tools and for what task they have been applied may be found in Chapter 3. For the interested reader, has it been decided with support from *Cybernetica AS*, to write a conference paper based on the result in this thesis. The conference paper is in progress, a draft may be found in Appendix B, and will hopefully be published in 2019.

June 1, 2018, Trondheim, Norway
Mathilde Hotvedt

# Abstract

A complete model of a $CO_2$ capture facility has been optimised with the aid of Dynamic Real-Time Optimisation (DRTO) utilising single-level, Nonlinear Model Predictive Control to merge regulatory and economic objectives. The goal has been to, during 24 hours, minimise the cost related to the energy consumption in the reboiler by variable solvent regeneration, whilst achieving a specified accumulated, or overall, capture ratio of $CO_2$ at the end of the simulation horizon. An hourly varying price of energy with a period of 24 hours have been included in the optimisation problem.

The complete model is based on a previous model from *Cybernetica AS*, the original model, with model reductions suggested by Hotvedt (2017) for the absorber, desorber and heat exchanger. The suggestions included modelling using molar amounts as state variables for each substance in the facility and discretising the unit models in space using control volumes. The complete reduced model has been validated against the original model in addition to instrumental measurements from an existing test facility at Tiller in Trondheim (SINTEF, 2017). It was found the reduced model yielded adequate behaviour although with deviations from both the original model responses and instrumental measurements. Introduction of simple estimator; bias updating, removed the deviations significantly. Eigenvalue analysis of the original and the reduced model were performed, and results show that the reduced model yielded only minor reductions in stiffness. On the other hand, the reductions decreased the dimension of the state space with 225 states, resulting in a simulation time reduction of $\approx 73\%$.

The DRTO was designed using the infeasible soft-constraint method where constraints on the energy costs have been set infeasible. Results from simulation show that the DRTO is able to achieve the reference accumulated capture ratio after 24 hours in addition to utilise the time varying price of energy to minimise cost. The performance was compared to a basic case where the accumulated capture ratio of $CO_2$ was forced constant during the prediction horizon, obtaining a constant solvent regeneration, and a cost reduction of 13.0% and 10.9% was found using a reference value for the accumulated capture ratio of 85% and 91% respectively. The DRTO was further tested for robustness by firstly inducing a step change in inlet conditions of the flue gas, secondly by abruptly increasing the price of energy and lastly by applying stricter constraints on the reboiler duty. The DRTO accomplished the capture goal in all cases, except for a step in inlet conditions close to the end of the simulation horizon. Lastly, the optimal solution resulted in unnecessary use of reboiler duty analysing a simulated plant replacement model, and consequently was bias updating introduced to enhance cost minimisation.

# Sammendrag

En fullstendig modell av et $CO_2$ fangstanlegg har blitt optimalisert ved bruk av en Dynamisk Sanntids Optimeringsalgoritme (DRTO) hvor et ett-nivås Ulinær Model Prediktiv Regulator (MPC) kombinerer økonomiske og regulatoriske mål. Hensikten har vært å minimere kostanden relatert til energibehovet i kokeren i løpet av et døgn ved bruk av variabel regenerering av aminløsingen, samt å nå et referansemål for fangstgraden av $CO_2$ etter 24 timer. Optimering har tatt hensyn til en tidsvarierende energipris med periode på 24 timer.

Den fullstendige modellen er basert på en tidligere modell fra *Cybernetica AS*, den originale modellen, med modellreduksjoner fra Hotvedt (2017) for absorberen, desorberen og varmeveksleren. Reduksjonene besto i å modellere enhetene med molare mengder som tilstandsvariable for hver av substansene i anlegget, samt å diskretisere likningene romlig ved bruk av kontrollvolum. Den fullstendige reduserte modellen har blitt sammenlignet med responsen til den originale modellen i tillegg til instrumentelle målinger fra et eksisterende testanlegg på Tiller i Trondheim (SINTEF, 2017). Resultatene viste god respons for den reduserte modellen, men med avvik fra den originale modellen og målinger. Introduksjon av en enkel estimator; bias-oppdatering, fjernet avvikene tilstrekkelig. En egenverdianalyse av både den reduserte modellen og den originale modellen viste at den reduserte modellen kun ga små reduksjoner i stivheten til systemet. Derimot minket den reduserte modellen tilstandsrommet med 225 tilstander sammenlignet med den originale modellen, noe som førte til at simuleringstiden ble redusert med $\approx 73\%$.

DRTO algoritmen ble designet ved bruk av infeasible soft-constraint metoden hvor begrensingene på energikostnaden ble satt uoppnåelige. Resultatene viste at algoritmen oppnådde referansemålet for fangstgrad av $CO_2$ i tillegg til å utnytte den varierende energiprisen til å redusere kostandene. Resultatene ble sammenlignet med et tilfelle der fangstgraden ble holdt på et konstant nivå igjennom hele døgnet, som resulterte i en konstant regenerering av aminløsningen, og kostnadsreduksjonen ble henholdsvis 13.0% og 10.9% med et referansemål på 85% og 91% fangst. Robustheten til optimeringsalgoritmen ble testet, først med et sprang i innløpsbetingelsene til røykgassen, så med en økning i energipris for deretter å innføre strengere begrensinger for energiforbruket i kokeren. Resultatene viste at algoritmen var robust i de aller fleste tilfeller, med unntak av sprang i innløpsbetingelser mot slutten av simuleringshorisonten, der målet for fangst ikke ble nådd. Til slutt, analyse av et simulert $CO_2$ anlegg viste at den optimale løsningen ga et unødvendig høyt forbruk av energi i kokeren. Derfor ble bias-oppdatering innført for å minke kostnadene ytterligere.

# Acknowledgement

I would like to extend my greatest appreciation to *Cybernetica AS* for granting me the opportunity to work with such an important topic as CCS. Knowing that the work I do benefits the technology in a global sense has motivated and encouraged me to work hard on the assignment to achieve useful results.

I would further like to express my gratitude towards my co-supervisors at *Cybernetica AS*; Svein Olav Hauger and Fredrik Gjertsen for support and assistance on a challenging and demanding subject. Without their guidance, this task could not have been completed.

Lastly, I would like to extend my thankfulness to my supervisor at NTNU, Lars Imsland, for important advice during guidance sessions and to Peter Singstad at *Cybernetica AS*, for valuable input during meetings.

# Table of Contents

# List of Figures

# List of Tables

# Nomenclature

**Abbreviations**

| | |
|---|---|
| $CCS$ | Carbon Capture and Storage |
| $CR$ | Capture Ratio |
| $CV$ | Controlled Variable |
| $DRTO$ | Dynamic Real-Time Optimisation |
| $DV$ | Disturbance Variable |
| $EMPC$ | Economic Model Predictive Control |
| $ETS$ | Emissions Trading System |
| $MEA$ | Monoethanolamine |
| $MIMO$ | Multiple-Input Multiple-Output |
| $MINLP$ | Mixed Integer Nonlinear Program |
| $MPC$ | Model Predictive Control |
| $MV$ | Manipulated Variable |
| $NMPC$ | Nonlinear Model Predictive Control |
| $ODE$ | Ordinary Differential Equation |
| $QP$ | Quadratic Program |
| $RD$ | Reboiler Duty |
| $RTO$ | Real-Time Optimisation |

| | | |
|---|---|---|
| $SQP$ | Sequential Quadratic Programming | |
| $SR$ | Stiffness Ratio | |
| $WMO$ | World Meteorological Organization | |

**Greek symbols**

| | | |
|---|---|---|
| $\epsilon$ | Perturbation variable | |
| $\varepsilon$ | Set of equality constraints | |
| $\lambda$ | Eigenvalue | |
| $\phi$ | Decision variable | |
| $\psi$ | Price of energy | $[\frac{NOK}{kWs}]$ |

**Symbols**

| | | |
|---|---|---|
| $A$ | Cross-sectional area | $[m^2]$ |
| $A_{g/l}$ | Interfacial area between gas and liquid | $[m^2]$ |
| $C$ | Concentration | $[\frac{kmol}{m^3}]$ |
| $c_p$ | Specific heat capacity | $[\frac{kJ}{kmolK}]$ |
| $\tilde{D}$ | Deviation | |
| $F$ | Molar flow | $[\frac{kmol}{s}]$ |
| $\hat{h}$ | Heat transfer coefficient | $[\frac{kW}{m^2K}]$ |
| $h$ | Molar enthalpy | $[\frac{kJ}{kmol}]$ |
| $I$ | Identity matrix/set of inequality constraints | |
| $J$ | Jacobian matrix | |
| $J_{g/l}$ | Gas-liquid interface molecular flux | $[\frac{kmol}{m^2s}]$ |
| $L$ | Length | $[m]$ |
| $N$ | Molar amount | $[kmol]$ |
| $N$ | Prediction horizon | |
| $n$ | Number of control volumes | |

| | | |
|---|---|---|
| $\dot{q}$ | Heat flux | $[\frac{kJ}{m^2 s}]$ |
| $T$ | Temperature | $[K]$ |
| $u$ | Input variable | |
| $V$ | Volume | $[m^3]$ |
| $v$ | Velocity | $[\frac{m}{s}]$ |
| $x$ | State variable | |
| $y$ | Measured variable | |
| $z$ | Derived variable | |

**Subscript and Superscripts**

| | |
|---|---|
| 0 | Initial value |
| $abs$ | Property of the absorber |
| $acc$ | Accumulated |
| $avg$ | Average |
| $cv$ | Control volume |
| $des$ | Property of the desorber |
| $g$ | Property of gas/vapour |
| $hex$ | Property of the heat exchanger |
| $in$ | Property of input |
| $init$ | Initial value |
| $k$ | Discrete time index/ component in substance |
| $l$ | Property of liquid |
| $lean$ | Property of lean liquid |
| $lm$ | Logarithmic mean |
| $local$ | Local property |
| $max$ | Maximum value |

| | |
|---|---|
| $min$ | Minimum value |
| $nc$ | Number of components |
| $opt$ | Optimal objective |
| $org$ | Property of original model |
| $out$ | Property of output |
| $red$ | Property of reduced model |
| $ref$ | Reference point/trajectory |
| $rich$ | Property of rich liquid |
| $surr$ | Property of surroundings |
| $tot$ | Total |
| $trac$ | Tracking objective |

# Chapter 1

# Introduction

According to World Meterological Organization (2017), was 2017 not only a year with numerous weather and climate events such as devastating hurricanes, floods, heatwaves, draughts and fires, but also among the third warmest years on record. WMO states that the extreme weather is most likely caused by the steadily increasing average global temperature, which is further caused by the human made emissions of greenhouse gases into the atmosphere, whereby the most prominent gas is carbon dioxide ($CO_2$). In fact, Olivier et al. (2017) reports that the global greenhouse gas emissions reached 49.3 gigatonnes of $CO_2$ equivalents in 2016, which is an increase of shockingly 50% compared to 1990. Three economic sectors stand out when it comes to greenhouse gas emissions to the atmosphere on a global basis. Production of electricity and heat by the use of fossil fuels, agriculture along with forestry and land use, and industry such as cement and fertiliser production (Olivier et al., 2017). In addition, transportation utilising fossil fuels together with emissions from buildings are also contributing greatly. In Norway, emissions due to electricity production are only minor as most of the production utilise renewable sources such as water. However, numbers from 2016 (SSB, 2017) show that Norway contributed with 53.3 million tonnes to the global emissions, in which most of it comes from oil- and gas production, industry and transportation. If Norway and the rest of the world are to contribute towards stalling of the global warming and its devastating consequences, a higher focus on decreasing human made greenhouse gas emissions is essential.

In 2015, Norway was among the 196 countries that established The Paris agreement (European Commission, 2018b), a legally binding climate deal with a long term goal of keeping the global temperature increase below $2°C$ compared to pre-

industrial levels. The goal of the agreement was to limit the severe consequences that global warming could bring. In order to meet this goal, the global emissions of greenhouse gases to the atmosphere, and especially $CO_2$, have to be reduced extensively in the coming years, and in the end be abolished completely. Even though the numbers from 2016 show that Norway largely contributes to the global greenhouse gas emissions, they also show that the percentage change in emissions from the oil and gas, industrial and transportation sector have been reduced since 2015 (SSB, 2017). This fact suggest that Norway's increased focus on reducing greenhouse gas emissions is successful.

Norway focuses on reduced emissions of greenhouse gases in several ways. Norway is for instance a part of the EU Emission Trading System (ETS). This is a system in which maximum amounts of allowable greenhouse gas emissions exists, and the countries within the system will have to trade amongst themselves for emission allowances (European Commission, 2018a). Further, the maximum amount will decrease each year, forcing a reduction in the overall emissions. Several industries in Norway, such as the oil and gas industry and cement and fertiliser production, are covered by the EU ETS. On the other hand, does there exist technologies that may significantly reduce the $CO_2$ emissions without trading for emission allowances. Carbon Capture and Storage (CCS) is one such technology. According to Carbon Capture and Storage Association (2018), is CCS a technology able to capture approximately 90% on average of the $CO_2$ from exhaust gas of power plants and other industrial processes. Considering the numbers from SSB (2017) which suggest that approximately 26 million tonnes of $CO_2$ were in 2016 released into the atmosphere due to the aforementioned industries in Norway, will CCS installed in all these industries reduce emissions with approximately 23.4 million tonnes. This amount is approximately twice the amount of Norway's predicted reductions within the transportation sector if all suggested preventive actions are introduced (EnergiNorge, 2016). Unfortunately, it is highly unlikely that all industries in Norway will invest in a carbon capture plant, as the plant is associated with a large operational energy demand in addition to establishing costs. In fact, Smith et al. (2013) showed that for a gas-fired power generation plant, a connected $CO_2$ capture plant would not only increase the operational cost of the plant but also decrease the power plant efficiency. Consequently, many factories will not afford having a capture plant attached to their exhaust outlet and will rather choose to pay for emission allowances from EU ETS.

In order to make CCS a more desirable investment for power and industrial plants, the operational costs related to the carbon capture process must be reduced. This thesis therefore investigates the development of control technology to minimise the cost in relation to the energy requirement of the $CO_2$ capture process, over a time horizon of 24 hours. With this time horizon in mind, the natural periodicity

of the energy price during 24 hours with high and low peaks may be exploited. The solvent regeneration, which is the most energy demanding process in the plant, may thus be varied regarding the energy price, allowing less regeneration during high peaks of the energy price and high regeneration during the low peaks. Consequently, will also the capture ratio of $CO_2$ in the facility vary as a high amount of regeneration results in a high capture ratio and vice versa. Additionally, such control technology enables a more automatic system without the necessity of operators, obtaining a further reduction of the total operational costs. Hopefully, will the results of this thesis contribute towards a more desirable carbon capture technology such that companies will choose to invest in a capture plant rather than trading for emission allowances. If so, greenhouse gas emissions to the atmosphere may be reduced, possible stalling global warming and prevent severe climate changes and extreme weather conditions.

## 1.1 Background

The model of the $CO_2$ capture facility that has been used in this thesis to investigate cost minimisation is a model of an existing test facility located in SINTEF's laboratories at Tiller in Trondheim (SINTEF, 2017). Even though the real facility is a test facility, the model is generic and may be used for full-scaled facilities by changing certain constants and parameters. The test facility is a post-combustion facility, which in contrary to a pre-combustion facility that attempts removal of $CO_2$ from the fuel used in industrial plants, removes the $CO_2$ component from the exhaust gas of industrial processes (Carbon Capture and Storage Association, 2018). The technique used to remove $CO_2$ from the exhaust gas in the Tiller facility is absorption using the solvent monoethanolamine (MEA). According to Wang et al. (2017), is absorption with MEA a suitable way to remove $CO_2$ from exhaust gas, and most used due to a high reaction rate between the MEA and the $CO_2$. The MEA is mixed with $H_2O$ and referred to as the lean liquid solution. In contrary, is the liquid solution with absorbed $CO_2$ referred to as the rich solution. Figure 1.1 illustrates the unit models and connections of the Tiller facility.

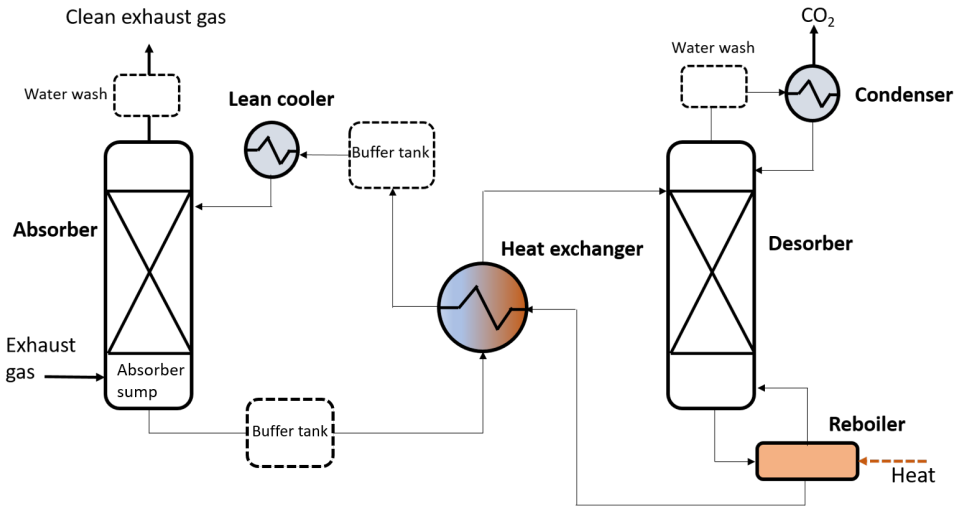


Figure 1.1: Overview of the unit models in the $CO_2$ capture facility at Tiller and connections between the models (Hotvedt, 2017)

In the absorber or absorption tower, the exhaust gas consisting of the components $H_2O$ vapour, $CO_2$, MEA, $N_2$ and $O_2$ is inlet at the bottom of the column and flows upwards. In the top of the absorber, the lean liquid solution that is pre-cooled by the lean cooler is inlet and will flow counter currently to the exhaust gas. The MEA in the liquid and the $CO_2$ in the exhaust gas will thus be exposed to each other and a reaction occur such that the $CO_2$ is absorbed into the MEA. The rich solution will leave the absorber sump and enter the heat exchanger counter currently with the relatively hotter lean solution coming from the desorber or stripping tower. The rich solution is hence preheated before it enters the top of the desorber where the MEA is to be regenerated. The regeneration is the most energy demanding process in the facility. In the desorber, the reboiler adds heat such that the temperature of the rich liquid solution increases. Resultantly, will the MEA release the absorbed $CO_2$ and a stream of $CO_2$, $H_2O$ vapour and some MEA vapour will enter the condenser, and a leaner liquid solution will exit the desorber. In the reboiler the leaner solution is additionally boiled such that more $CO_2$ is released from the MEA and the MEA may be circulated back to be used anew in the absorber. In the condenser, $H_2O$ and MEA gas is condensed such that an approximately 99% pure $CO_2$ gas stream exits the condenser and may later be compressed and transported away for storage (Wang et al., 2017). In the test facility at Tiller, two buffer tanks, one for lean and one for rich liquid solution, also exist for storage if necessary.

The complete $CO_2$ capture facility at Tiller has previously been modelled by Flø (2015), and further details about the real facility may be found in her thesis (Flø, 2015, p. 27). The modelling has been performed using sequential modular modelling (Westerberg and Piela, 1994), where each of the unit models of the facility has been modelled separately, and consequently are routines for calculation of internal inputs to each of the connected unit models also present. Each of the unit models in Flø (2015) were dynamically modelled using first principle conservation laws and the use of the orthogonal collocation method for discretization of the differential equations in space (Arora et al., 2005).

A version of the complete model in Flø (2015) was further developed by *Cybernetica AS*. This version will be thoroughly used in this thesis to compare the responses of the new developed model and will henceforth be referred to as the original model. *Cybernetica AS* is a company that specialises in advanced process control solutions, for instance Model Predictive Control (MPC) for online estimation and optimisation (Cybernetica AS, 2018). *Cybernetica AS* found that the large and complex state space of the original model, with more than 400 states, induced a high computational effort when performing online estimation and optimisation, and the model was resulting not well suited for optimisation using large time horizons. In an attempt at making the model of the facility more suitable for such conditions, Hotvedt (2017) experimented with model reductions of three of the unit models, the absorber, desorber and heat exchanger. The collocation method for discretization in space was substituted with the simpler control volume method, and additionally were the state space changed from using molar flows to molar amounts as state variables for each of the substances in the liquid and gas. The responses of the reduced unit models in Hotvedt (2017) were compared to the responses of original unit models, and an adequate correspondence was found using 10 control volumes in the absorber and desorber, and 2 control volumes in the heat exchanger. In this thesis, the suggested model reductions for the three unit models have been incorporated in the original model and the resulting complete model will hereafter be referred to as the reduced model. The reduced model have been analysed and validated against the original model considering modelling errors, system stiffness and simulation time, before it has been used in optimisation with a time horizon of 24 hours considering costs related to the energy requirement in the reboiler for MEA regeneration. This thesis however, is not the first to experiment with long term optimisation of an amine-based post-combustion $CO_2$ capture facility which have been explained in the following, Section 1.2.

## 1.2 Literature review

As mentioned in Chapter 1, the amine based post-combustion carbon capture process is able to capture more than 90% of the $CO_2$ in the flue gas from industrial processes or power plants (Carbon Capture and Storage Association, 2018). However, the stripping process in the desorber requires high amounts of energy supplied from the reboiler and will consequently induce extra costs on the industrial plant with the $CO_2$ capture facility attached. Several studies in literature have tried to minimise the energy requirement, and thus the cost, related to the stripping process. Flø et al. (2015) used basic PI controllers in order to minimise the reboiler duty with the presence of a variable energy marked, both for a variable energy demand and for a variable energy price during 24 hours. The study investigated several different flexible modes; load following, exhaust gas venting, a varying degree of solvent regeneration and solvent storage. However, Flø et al. (2015) found that due to the basic controllers, the goal of an average capture ratio of 90% was not reached in some of the modes. Other studies utilises more advanced control techniques such as Model Predictive Control (MPC) to increase the performance of the capture facility.

MPC is an highly beneficial technology that are able to handle large multiple-input multiple-output (MIMO) systems, system constraints and regulatory objectives in addition to utilising feedback from the system response (Foss and Heirung, 2016). The control technology is also able to handle nonlinear constraints, which is the concept of a Nonlinear MPC (NMPC). Several types of (N)MPC have been explored in literature to minimise the energy consumption related to the $CO_2$ capture. Some have utilised standard (N)MPC where the objective function consists of regulatory objectives. For instance, Laird et al. (2012) investigated the use of NMPC to minimise the energy consumption in the reboiler. However, only a reduced-order model implementing the separation unit consisting of desorber, reboiler and condenser was utilised. The study found that the control solution minimised the energy consumption adequately, however, as the study only included the separation unit, effects the rest of the facility might inflict on the energy consumption was not examined. Sahraei and Ricardez-Sandoval (2014) on the other hand, used a complete model of an amine-based post-combustion $CO_2$ facility together with a linear MPC to prove the superiority of the MPC over basic PI-controllers. The study showed how the control solution could consider energy and environmental constraints and stated that the solution could be suitable for inclusion of economic objectives as well as regulatory objectives.

When economic objectives are to be included in the optimisation design, quite common in literature is the use of multilevel controllers. The upper level will

typically solve the economic objectives providing setpoints to the lower level controlling the regulatory performance of the plant. For instance, Arce et al. (2012) studied the use of a multilevel MPC on the reboiler of a $CO_2$ capture facility. The upper layer included a variable price of both $CO_2$ emission fees and electricity to find the optimal energy utilisation during 24 hours for operational cost minimisation. The upper layer provided setpoints to the the lower level controller which regulated the level of liquid solution within the reboiler. The study found that the use of such a multilevel MPC resulted in a reduction of up to 10% in energy costs. However, as with Laird et al. (2012), only parts of the complete capture facility were included in the optimisation analysis, and consequently were possible downstream effects from the rest of facility ignored. Manaf et al. (2017) however, investigated the effect of a multilevel hybrid optimisation algorithm on a full-scale capture facility. A mixed integer nonlinear program (MINLP) were used on the top level to calculate the optimal carbon capture profile for maximising the plant's revenue considering both electricity prices and carbon prices, whereas a linear MPC were use at the lower level to control the performance of the capture plant. The results showed a plant net average revenue increase of 6%. Nonetheless, Maree and Imsland (2011) points out that several difficulties of the multilevel controller may lead to sub-optimal economic performance. Suggested instead by several papers including Maree and Imsland (2011), is the use of an integrated, single-level (N)MPC whereby both economic and regulatory performance are optimised. This kind of optimisation is often referred to as an Economic MPC (EMPC) or Dynamic Real-Time Optimisation (DRTO) (Willersrud et al., 2013).

Maree and Imsland (2011) used a DRTO on a simplified non-linear model of a multi-well oil production plant and found the DRTO to give optimal economic performance as well as satisfactory control performance. Willersrud et al. (2013) used two designs of a DRTO to optimise the control of an offshore oil and gas production plant and found that both designs were able to find the economically optimal point. However, to the authors' knowledge, no studies in literature have experimented with a DRTO on a full-scaled amine-based post-combustion $CO_2$ capture facility. Therefore, in this thesis the performance of such a controller will be experimented with on a reduced model of the $CO_2$ capture plant at Tiller.

## 1.3 Assumptions

There are several assumptions made in this thesis that the reader should be made aware of. Firstly, the original model provided by *Cybernetica AS* has been utilised under the perfect model assumption. That is, any modelling errors from the true facility are ignored. This is done for simplicity, as the original model is the best

model of the Tiller facility so far regarding performance and fit to measurements. Further, by the use of another model instead of measurements from a true plant, one has access to all states for direct comparison of the reduced model to the original model. One must keep in mind however, that the original model is likewise a model, and deviations from responses of the true facility may occur. Consequently, will measurements from a test run at the Tiller facility (courtesy of SINTEF) be included in the validation of the reduced model against the original model. These measurements have been assumed to reflect the reality well and be appropriate for analysis. Furthermore, the suggested reductions from Hotvedt (2017) only concerned the absorber, desorber and heat exchanger unit models. It has therefore been assumed that the remaining unit model behaviours, such as the reboiler and condenser, are adequate. Moreover, has optimisation of the $CO_2$ capture facility been performed assuming that the low-level controllers adjusting liquid levels, amount of water, mass flow rates, reboiler duty and temperatures in lean cooler and reboiler behaves flawlessly. That is, the low-level controllers will ensure that the optimal inputs calculated by the optimisation algorithm are implemented on the real system. Lastly, due to the design of the objective function for optimisation, it has been assumed that the local optimum found by the optimisation algorithm is also a global optimum. If the optimal solution deem inadequate, global analysis of the optimisation problem should be performed.

## 1.4 Thesis

The goal of this thesis has been to develop a Dynamic Real-Time Optimisation Algorithm to minimise the cost related to the energy consumption in the reboiler for MEA regeneration in a full-scaled, amine-based, post-combustion $CO_2$ capture facility whilst achieving an accumulated, or overall, specified capture ratio after 24 hours. The model of the $CO_2$ capture facility will be created based on an already existing model from *Cybernetica AS* with the suggestions for model reductions by Hotvedt (2017). The models will further be validated against each other, and parameter adjustments performed for a better fit of the reduced model to the original model. The DRTO will be constructed as a single-level Nonlinear Model Predictive Controller utilising the infeasible soft-constraint method for merging regulatory and economic objectives. To achieve both cost minimisation and the reference accumulated capture ratio and the end of the simulation horizon, has time-varying solvent regeneration been experimented with in accordance to an hourly varying price of energy with a periodicity of 24 hours.

## 1.5 Contributions

The work done in this thesis has been in collaboration with *Cybernetica AS* who has made their own tools Modelfit, RealSim and CENIT, in addition to C-code interfaces for communication with the tools, available in order to investigate the topic of this thesis. *Cybernetica AS* has furthermore provided guidance regarding utilisation of the tools. Additionally has the original model of the $CO_2$ capture facility been provided to use as a starting point for development of the reduced model and as a plant replacement model for both validation of the reduced model and for simulation of the capture facility during optimisation.

The main contributions of the work done in this thesis are five-fold

- **Model validation** of the new developed model of the $CO_2$ capture facility at Tiller with model reductions from Hotvedt (2017) integrated. Modelfit has been utilised for comparison of the reduced model to the original model and instrumental measurements from the test facility at Tiller. The measurements have been provided by SINTEF for additional analysis of the model responses and utilised for inclusion of a simple estimator, bias updating. Parameter adjustment has been performed.
- **Analysis of the stiffness** of the reduced model compared to the original model. MATLAB has been used for estimation of the Jacobian matrix and analysis of the eigenvalues. A MATLAB interface to the C-code of the original model, provided by *Cybernetica AS*, has been utilised to obtain the derivatives of the model.
- **Development of a Dynamic Real-Time Optimisation Algorithm** using a single-level Nonlinear Model Predictive Controller considering both regulatory and economic objectives. The DRTO has been designed using the infeasible soft-constraint method to include economic objectives in the optimisation problem.
- **Analysis of the performance of the DRTO with a time varying price of energy** in two modes of operation. A fixed mode, keeping the accumulated capture ratio at a specified reference throughout the simulation horizon, thus inducing a constant MEA regeneration, and a flexible mode utilising time-varying solvent regeneration such that a specified accumulated capture ratio is achieved after 24 hours. The two modes were compared to each other considering cost related to the energy requirement in the reboiler. Bias updating was introduced to enhance performance. *Cybernetica AS* tools RealSim and CENIT were utilised for simulation.

- **Analysis of the robustness of the DRTO** by inducing a step change in the composition of $CO_2$ in inlet exhaust gas, increasing the energy price, and lastly, enforcing strict constraints on the reboiler duty.

## 1.6 Outline

The thesis is structured such that firstly, in Chapter 1, will the reader be introduced to the importance of the research questions in this thesis considering global aspects. A brief introduction to the model of $CO_2$ capture facility at Tiller along with recent investigations of it will be given in Section 1.1, whereas a literature review of earlier research on optimising $CO_2$ capture facilities, or parts of it, with different control techniques are introduced in Section 1.2. Following in Section 1.3 is a description of important assumptions being made in order to complete this thesis, while the problem description is shortly given in Section 1.4. A list of contributions that have been provided is further given in Section 1.5.

The reader will moreover be given an introduction to the important theoretical aspects necessary to understand the results of this thesis in Chapter 2. The model equations for the unit models integrated into the original model are summarised in Section 2.1, theory related to system stiffness and integration routine is given in Section 2.2 and theory related to optimisation in general and the specific optimisation problem for the DRTO is introduced in Section 2.3. In Chapter 3, have code implementation and utilised software tools been described and illustrated such that the reader will be made aware of the extent of help given by *Cybernetica AS* and which parts have been implemented during the work with this thesis. The result of the validation of the reduced model against the original model considering modelling errors and analysis of the two system's stiffness and simulation time have been given in Chapter 4, whereas the analysis of the performance and robustness of the DRTO have been illustrated and discussed in Chapter 5.

An overall discussion of the assumptions made during this thesis and their influence on the results for the model validation and optimisation may further be found in Chapter 6, and a conclusion to the work done may be found in Chapter 7. Lastly, suggestions for future work are discussed in Chapter 8.

# Chapter 2

# Theory

This chapter will introduce relevant theory that have been used completing the thesis and will be of importance for the reader to understand the results in the following chapters of this thesis. The first task done in this thesis has been the implementation of the unit models for the absorber, desorber and heat exchanger from Hotvedt (2017) in the original model to obtain a model more suitable for optimisation using large time horizons. Consequently for the completeness of this thesis, a short description and summary of the balance equations for the three unit models have been included in Section 2.1. Section 2.2 contains theory related to eigenvalue analysis, system stiffness and choosing of an appropriate integration routine. This will be important theory for the model validation of the reduced model performed in Chapter 4. Lastly, in Section 2.3 has a presentation of general optimisation theory along with advanced control techniques been included in order for the reader to understand how the specific optimisation problem with a DRTO may be set up for the $CO_2$ capture facility, and to understand the result of the optimisation in Chapter 5.

## 2.1 Unit models

In Hotvedt (2017), were balance equations for the heat exchanger and general column of an amine-based post-combustion $CO_2$ capture facility developed. The development was based on first-principle conservation laws, and used the same approach as in Flø (2015). However, there were two important differences from the equations in Flø (2015). Firstly, molar amounts were used as state variables

in the mass balance equations instead of molar fractions, and secondly, the control volume method to approximate spatial derivatives was utilised instead of the collocation method. As the balance equations for both energy and mass in the heat exchanger and general column are highly dependent on the mass flow through the system, a relationship between molar amounts and molar flows was found such that the differential equations could be written in terms of the state variables. The relationship was established assuming constant gas and liquid velocity $v_g, v_l$ in each unit model and may be seen in equation 2.1.

$$F_{cv} = vAC_{tot,cv} = vA\frac{N_{tot,cv}}{V_{cv}} = vA\frac{N_{tot,cv}}{AL_{cv}} = \frac{nvN_{tot,cv}}{L} \tag{2.1}$$

Here $L_{cv} = \frac{L}{n}$ is the length of each control volume where $L$ is the total length of the unit and $n$ is the number of control volumes. $F$ is the molar flow, $N_{tot,cv}$ is the total molar amount in each control volume, $V_{cv}$ is the volume and $A$ is the cross-sectional area which is assumed constant for each control volume. For the completeness of this thesis, a short description of the heat exchanger and general columns have been included in the subsections below, together with a summary of the balance equations of each unit model using control volumes.

### 2.1.1 Heat exchanger

The heat exchanger in the capture facility at Tiller is a counter current exchanger where the lean and rich liquids enter at opposite ends to each other as in Figure 2.1.

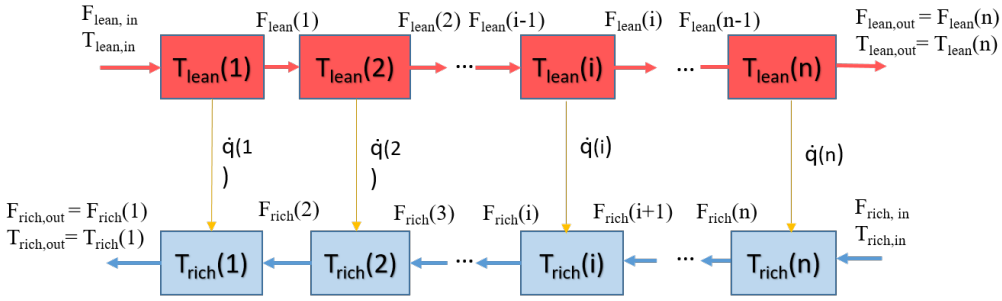


Figure 2.1: Illustration of the counter current heat exchanger divided into control volumes (Hotvedt, 2017). Here the lean and rich liquid solution enter at opposite ends to each other.

A wall separates the two liquids from each other such that mass is conserved and only heat exchange occur between the two liquids from the relatively hotter side to the relatively colder side. The heat flux $\dot{q}$ may be described using either a local temperature difference approach or using the logarithmic mean temperature in each control volume according to the equations in 2.2 and 2.3 respectively. Here $\hat{h}$ is the heat transfer coefficient. The molar amount and temperature balance equations for the heat exchanger taken from Hotvedt (2017) are summarised in equations 2.4-2.7. $T$ is the temperature and $c_p$ is the specific heat capacity. Here $k$ refers to the components in the liquid, $CO_2$, $H_2O$ or MEA and $i$ indicates the current control volume.

$$\dot{q}_{local} = \hat{h}(T_{lean} - T_{rich}) \tag{2.2}$$

$$\begin{aligned} \dot{q}_{lm} = \hat{h}\Delta T_{lm} &= \hat{h}\frac{\Delta T_2 - \Delta T_1}{\ln \frac{\Delta T_2}{\Delta T_1}} \\ &= \hat{h}\frac{(T_{lean,out} - T_{rich,in}) - (T_{lean,in} - T_{rich,out})}{\ln\left(\frac{T_{lean,out} - T_{rich,in}}{T_{lean,in} - T_{rich,out}}\right)} \end{aligned} \tag{2.3}$$

$$\begin{aligned} \frac{dN_{lean,k}}{dt}(i) &= F_{lean,k,in} - F_{lean,k,out} \\ &= \frac{nv_l}{L}(N_{lean,k,in} - N_{lean,k,out}) \\ &= \frac{nv_l}{L}(N_{lean,k}(i-1) - N_{lean,k}(i)) = 0 \\ k &= 1,2,3 \quad i = 1..n \end{aligned} \tag{2.4}$$

$$\begin{aligned} \frac{dN_{rich,k}}{dt}(i) &= F_{rich,k,in} - F_{rich,k,out} \\ &= \frac{nv_l}{L}(N_{rich,k,in} - N_{rich,k,out}) \\ &= \frac{nv_l}{L}(N_{rich,k}(i+1) - N_{rich,k}(i)) = 0 \\ k &= 1,2,3 \quad i = 1..n \end{aligned} \tag{2.5}$$

$$\begin{aligned} \frac{dT_{lean}}{dt}(i) = \frac{1}{N_{lean,tot}(i)c_{p,lean}(i)} \times \Big[&\frac{nv_{lean}}{L}N_{lean,tot}(i-1) \\ &\Big(c_{p,lean}(i-1)T_{lean}(i-1) - c_{p,lean}(i)T_{lean}(i)\Big) - \frac{A}{n}\dot{q}(i)\Big] \\ i = 1..n& \end{aligned} \tag{2.6}$$

$$\frac{dT_{rich}}{dt}(i) = \frac{1}{N_{rich,tot}(i)c_{p,rich}(i)} \times \Big[\frac{nv_{rich}}{L}N_{rich,tot}(i+1) \Big(c_{p,rich}(i+1)T_{rich}(i+1) - c_{p,rich}(i)T_{rich}(i)\Big) + \frac{A}{n}\dot{q}(i)\Big] \quad (2.7)$$
$$i = 1..n$$

### 2.1.2 General Column

Both the absorber and the desorber in the $CO_2$ capture facility are represented by the differential equations for a general column, however, the normal operating conditions regarding temperature and molar amounts will be different in the two units models. There are two fluids present, and they are inlet at opposite ends of the column and flowing counter currently to each other. The liquid solvent, which has components $CO_2$, $H_2O$ and MEA and a gas with at most five components; $CO_2$, $H_2O$, MEA, $N_2$ and $O_2$. An illustration of how the column has been divided into control volumes may be found in Figure 2.2.

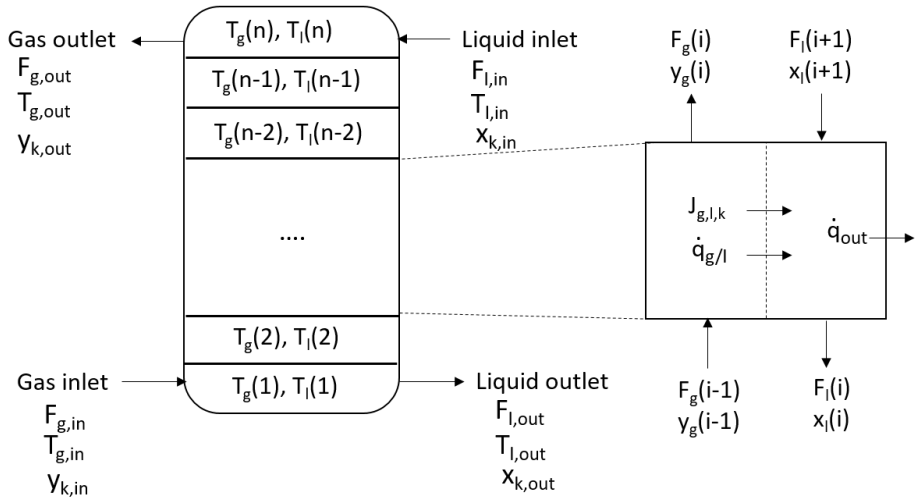


Figure 2.2: Illustration of the general column divided into control volumes (Hotvedt, 2017). Here the liquid enters at the top of the column in control volume $n$ whereas the gas enters at the bottom of the column in control volume 1. In each control volume, both mass and heat may diffuse.

Both mass and energy are allowed to diffuse from one fluid to another, and to describe the diffusion of mass the two-film theory has been utilised (Withman, 1923). In the absorber, flue gas consisting of all five components will encounter the lean amine flow, and a reaction between the MEA in the liquid and the $CO_2$ in the gas occurs such that the MEA absorbs the $CO_2$. This reaction is described by Xie et al. (2010) and for the interested reader repeated below in equation 2.8, where $RNH_2$ is a primary amine.

$$CO_2 + 2RNH_2 = RNHCOO^- + RNH_3^+ \tag{2.8}$$

The desorber on the other hand, is the reverse process of the absorber, (Geankoplis, 1993, p. 610), and by applying enough heat through the reboiler is the MEA stripped of $CO_2$. Further assumptions that have been made modelling the general column may be found in Hotvedt (2017).

The differential equations for the general column using control volumes developed in Hotvedt (2017) have been summarised below. The molar balance equations for each liquid and gas component may be found in equation 2.11 and 2.12 respectively. Here $nc_l = 3$ and $nc_g = 5$ in the absorber whereas $nc_g = 3$ in the desorber where the gas components $O_2$ and $N_2$ has been neglected due to small amounts. Equations 2.13 and 2.14 describes the differential energy balance of the liquid and gas. The heat flux between the two phases has been described using the local temperature difference in equation 2.9 where positive direction is assumed from the gas to the liquid. However, heat flux to the surrounding has been assumed to only leave the liquid phase and may therefore be described by 2.10. Here $J_{g/l}$ represents the mass diffusion through the gas-liquid interface $A_{g/l}$ and $h_g, h_l$ refers to the enthalpy in the gas and liquid respectively.

$$\dot{q}_{g/l} = -\hat{h}(T_l - T_g) \tag{2.9}$$

$$\dot{q}_{surr} = \hat{h}_{surr}(T_l - T_{surr}) \tag{2.10}$$

$$\begin{aligned} \frac{dN_{l,k}}{dt}(i) &= \frac{nv_l}{L}\Big(N_{l,k}(i+1) - N_{l,k}(i)\Big) + A_{g/l}J_{g/l,k}(i) \\ k &= 1..(nc)_g \quad i = 1..n \end{aligned} \tag{2.11}$$

$$\begin{aligned} \frac{dN_{g,k}}{dt}(i) &= \frac{nv_g}{L}\Big(N_{g,k}(i-1) - N_{g,k}(i)\Big) - A_{g/l}J_{g/l,k}(i) \\ k &= 1..(nc)_l \quad i = 1..n \end{aligned} \tag{2.12}$$

$$\frac{dT_l}{dt}(i) = \frac{1}{N_{l,tot}(i)c_{p,l}(i)} \times \Bigg[\frac{nv_l}{L}N_{l,tot}(i+1)\Big(c_{p,l}(i+1)T_l(i+1) - c_{p,l}(i)T_l(i)\Big) + A_{g/l}\sum_{k=1}^{nc_l} J_{g/l,k}(i)(h_{g,k}(i) - h_{l,k}(i)) + A_{g/l}\dot{q}_{g/l}(i) - A_{surr}\dot{q}_{surr}(i)\Bigg] \quad i = 1...n \tag{2.13}$$

$$\frac{dT_g}{dt}(i) = \frac{1}{N_{g,tot}(i)c_{p,g}(i)} \times \Bigg[\frac{nv_g}{L}N_{g,tot}(i-1)\Big(c_{p,g}(i-1)T_g(i-1) - c_{p,g}(i)T_g(i)\Big) - A_{g/l}\dot{q}_{g/l}(i)\Bigg] \qquad i = 1...n \tag{2.14}$$

## 2.2 Integration routine, eigenvalue analysis and system stiffness

According to Gravdahl and Egeland (2002, p. 560), do highly nonlinear systems often exhibit large variations in the eigenvalues of the system. This fact may cause several problems when solving the system, and will often limit which solvers may be used. For instance, constant step solvers such as Explicit Euler may be difficult to utilise as the step size must be small enough to account for the fastest dynamics, corresponding to the eigenvalue with the largest absolute real value $\lambda = max(abs(real(\lambda_i)))$ (Gravdahl and Egeland, 2002, 535). In highly nonlinear systems, the fastest eigenvalue may change from sample to sample and consequently may a small step size often be required for stability, increasing the solving time.

The same problem arises for so-called stiff systems where there is a large spread in the system eigenvalues (Gravdahl and Egeland, 2002, p. 534). In such systems, will there exist both fast and slow dynamics and consequently must the step size again be reduced to obtain stability. Resultantly, having a constant step size whilst obtaining a stable and accurate solution may be difficult to achieve. In fact, *Cybernetica AS* found that the original model was non-solvable with Explicit Euler even with a very small step size. This suggests that the original model is very stiff.

Even though the model investigated and used for optimisation in this thesis is a

reduction of the original model, is it still nonlinear and of high order. Whether or not the stiffness has been reduced due to the model reductions will be investigated in Chapter 4. If sufficient reductions in stiffness is achieved, Explicit Euler may be used as an integration routine to solve the system. On the other hand, in most cases with a complex system, will a variable step method increase accuracy, reduce computation time and account for possible stiffness. One such integration routine is CVODE. CVODE is a solver for both stiff and non-stiff Ordinary Differential Equations (ODE) (Computation, 2018). An advantage with CVODE is the use of both variable-order and variable-step multistep methods for integration. This will ensure better accuracy and less simulation time. For instance, according to Gravdahl and Egeland (2002, p. 518) may the ability to vary the order of the method decrease the local error and thus increase accuracy. Further, will the ability to vary the step size throughout the simulation decrease the total simulation time because larger steps may be taken where it is possible and smaller steps where it is necessary, in order to obtain stability. Multistep methods may further increase the accuracy due to utilisation of several previous points to estimate the solution (Gravdahl and Egeland, 2002, p. 560, p. 576). However, CVODE is also a quite complex system solver and do have its disadvantages. For instance, will CVODE have to estimate the system matrix, the Jacobian, and if the system has a large state space, this may be very time consuming.

How stiff a system is may be investigated through an eigenvalue analysis using the evaluation variable Stiffness Ratio (SR) (Moody, 2007). The Stiffness Ratio is defined as in equation 2.15, where $\lambda_i$ are the eigenvalues of the system Jacobian matrix J, defined in equation 2.16, where $m$ is the number of states in the system. Here $\boldsymbol{g} = \boldsymbol{g}(t, \boldsymbol{x}, \boldsymbol{u})$ describes the system differential equations. Moody (2007) defines a system as stiff if $SR >> 1$.

$$SR = \frac{\max\limits_i |\Re(\lambda_i)|}{\min\limits_i |\Re(\lambda_i)|} \tag{2.15}$$

$$J = \begin{bmatrix} \frac{\partial \boldsymbol{g}}{\partial x_1} \\ \frac{\partial \boldsymbol{g}}{\partial x_2} \\ \vdots \\ \frac{\partial \boldsymbol{g}}{\partial x_m} \end{bmatrix}_{|\boldsymbol{x}_0, \boldsymbol{u}_0} \tag{2.16}$$

The Jacobian of the system equations may be difficult to find analytically if the model is nonlinear and has a large state space. A numerical approximation of the Jacobian may thus be calculated using the following equation for finite differences, equation 2.17, for each $i = 1..m$ (Nocedal and Wright, 2000, p. 195). $\boldsymbol{e}$ is here a

vector with 1 at position $i$ but zeros elsewhere and $\epsilon$ is the perturbation parameter.

$$\frac{\partial \boldsymbol{g}}{\partial x_i} \approx \frac{\boldsymbol{g}(\boldsymbol{x} + \epsilon \cdot \boldsymbol{e}_i) - \boldsymbol{g}(\boldsymbol{x})}{\epsilon} \tag{2.17}$$

According to Nocedal and Wright (2000, p. 196), choosing the perturbation parameter as

$$\epsilon = 10^{-8} \tag{2.18}$$

is close to optimal if the problem is well scaled. However, in the reduced model of the $CO_2$ capture facility there are very many states with different units and ranges of values. Ideally should the states be scaled, for instance with a typical reference value, before approximating the Jacobian. In the original model on the other hand, are all states scaled to yield dimensionless variables, and consequently may the Jacobian approximation for the original model yield more accurate results than for the reduced model. This should be kept in mind while performing the eigenvalue analysis. Other approximations of the Jacobian matrix may also be used if the results deem inaccurate, for instance the central differences scheme (Nocedal and Wright, 2000, p. 196). Using equation 2.17 together with the perturbation parameter in 2.18, the simple for-loop in Listing 2.1 may be set up to calculate the Jacobian matrix in MATLAB.

```
% Initialise
J = zeros(m);
x_perturbed = x0;
% Pertubation parameter
epsilon = 10^(-8);
% Find function value of unperturbed state
gx = g(t,x0,u0);

for k = 1:m
    % Perturb state vector
    x_perturbed(k) = x_perturbed(k) + epsilon;
    % Find function value of perturbed state
    gx_perturbed = g(t,x_perturbed,u);
    % Estimate jacobian
    J(:,k) = (gx_perturbed-gx)/epsilon;
    % Reset state vector
    x_perturbed(k) = x0(k);
end
```

Listing 2.1: Finding the Jacobian numerically in MATLAB

The eigenvalues of the Jacobian may further be found by using the MATLAB command $eig(J)$ which calculates the roots of the characteristic polynomial

$$det(J - \lambda I) = 0 \tag{2.19}$$

and thus may the Stiffness Ratio be found with equation 2.15. An eigenvalue analysis of both the original model and the reduced model have been performed in Chapter 4.

## 2.3 Optimisation

An optimisation problem is, according to Foss and Heirung (2016), a problem in which an objective function is to be minimised or maximised with respect to certain decision variables and constraints. In general, may the optimisation problem be formulated as in equation 2.20, where $f(\boldsymbol{\phi})$ is the objective function to be minimised (or maximised), $\boldsymbol{\phi}$ the decision variables and $c_i(\boldsymbol{\phi})$ the constraints of the optimisation problem. The optimal solution to the problem will thus be the minimum (or maximum) of $f(\boldsymbol{\phi})$ within the constraints. The constraints are of two types, equality constraints $i \in \boldsymbol{\varepsilon}$ and inequality constraints $i \in I$.

$$\begin{aligned} &\min_{\boldsymbol{\phi} \in \mathbb{R}^n} f(\boldsymbol{\phi}) \\ &\text{subject to} \\ &c_i(\boldsymbol{\phi}) = 0 \quad i \in \boldsymbol{\varepsilon} \\ &c_i(\boldsymbol{\phi}) \geq 0 \quad i \in I \end{aligned} \tag{2.20}$$

In a dynamic nonlinear system, the system equations are described with a set of nonlinear differential equations dependent on time $t$, previous states $\boldsymbol{x}$ and inputs $\boldsymbol{u}$, equation 2.21, and is an example of equality constraints that must be satisfied in order to solve the problem. Here both $\boldsymbol{x}$ and $\boldsymbol{u}$ will be decision variables, and $\boldsymbol{x}_0$ is the initial point for the state variables.

$$\dot{\boldsymbol{x}} = \boldsymbol{g}(t, \boldsymbol{x}, \boldsymbol{u}), \quad \boldsymbol{x}(0) = \boldsymbol{x}_0 \tag{2.21}$$

An example of inequality constraints may for instance be the set $\boldsymbol{\phi} \geq 0$ which are common if the decision variables represent non-negative variables such as products produced in a factory. In order to formulate an optimisation problem for such a system, the system is discretised and solved at a time interval of interest $k \in [0, N]$. Here $N$ is called the prediction horizon, due to optimising and predicting the system over $N$ discrete time samples into the future. According to Seborg et al. (2004, p. 429), is it common to choose the prediction horizon $N$ in such a way that the last input has completely taken effect, that is, the dynamics of the state variables $\boldsymbol{x}$ have settled after a change in input. Foss and Heirung (2016) also

states that the prediction horizon influences the stability of the solution and a larger horizon typically produce better stability. The time between $k$ and $k+1$, $\Delta k$, is usually equidistant for simplicity, but may also be variable. The differential equations for the system in discrete time may be described using equation 2.22.

$$\boldsymbol{x}_{k+1} = \boldsymbol{g}(\boldsymbol{x}_k, \boldsymbol{u}_k), \quad \boldsymbol{x}(0) = \boldsymbol{x}_0, \quad k = 0, ..., N-1 \tag{2.22}$$

The optimisation problem for a dynamic, nonlinear system such as in equation 2.22, will have the same shape as the general optimisation problem in 2.20 with both equality and inequality constraints and are illustrated in equation 2.23 (Foss and Heirung, 2016). Here, the rate of change of the inputs represented by $\Delta \boldsymbol{u}_k$.

$$\begin{aligned}
&\min_{\boldsymbol{\phi} \in \mathbb{R}^n} f(\boldsymbol{\phi}) = \sum_{k=0}^{N-1} f_k(\boldsymbol{x}_{k+1}, \boldsymbol{u}_k) \\
&\text{subject to} \\
&\quad \boldsymbol{x}_{k+1} = \boldsymbol{g}(\boldsymbol{x}_k, \boldsymbol{u}_k), \qquad k = 0, ..., N-1 \\
&\quad \boldsymbol{x}_0, \boldsymbol{u}_{-1} = \text{given} \\
&\quad \boldsymbol{x}^{low} \leq \boldsymbol{x}_k \leq \boldsymbol{x}^{high}, \qquad k = 1, ..., N \\
&\quad \boldsymbol{u}^{low} \leq \boldsymbol{u}_k \leq \boldsymbol{u}^{high}, \qquad k = 0, ..., N-1 \\
&\quad \Delta \boldsymbol{u}^{low} \leq \Delta \boldsymbol{u}_k \leq \Delta \boldsymbol{u}^{high}, \qquad k = 0, ..., N-1 \\
&\quad \text{where} \\
&\qquad \boldsymbol{x} \in \mathbb{R}^{n_x} \\
&\qquad \boldsymbol{u} \in \mathbb{R}^{n_u} \\
&\qquad \Delta \boldsymbol{u}_k = \boldsymbol{u}_k - \boldsymbol{u}_{k-1} \\
&\qquad \boldsymbol{\phi}^T = (\boldsymbol{x}_1^T, ..., \boldsymbol{x}_N^T, \boldsymbol{u}_0^T, ..., \boldsymbol{u}_{N-1}^T) \\
&\qquad \boldsymbol{\phi} \in \mathbb{R}^n, \quad n = N \cdot (n_x + n_u)
\end{aligned} \tag{2.23}$$

The algorithm solving the optimisation problem will, at time $t_0$, find a set of inputs $\boldsymbol{u}_k, k = 0...N-1$, which will minimise the function $f$ over the prediction horizon $N$, while keeping within the boundaries specified by the constraints. The design of the objective function plays a crucial role to the solution of the optimisation problem. In fact, nonlinear optimisation problems are non-convex due to the nonlinear constraints, usually yielding several regions with several local extrema. Choosing $f$ wrongly may result in a large solving time of the optimisation problem, and worst-case scenario not being able to find the optimal solution at all (Foss

and Heirung, 2016). A general way of representing the objective function $f(\boldsymbol{\phi})$ in equation 2.23 with state and input variables may be seen in equation 2.24, in which the matrices Q and R at each time sample should be positive semi-definite $Q_k, R_k \succeq 0$.

$$f(\boldsymbol{\phi}) = \sum_{k=0}^{N-1} \frac{1}{2}\boldsymbol{x}_{k+1}Q_{k+1}\boldsymbol{x}_{k+1} + d_{x,k+1}^T\boldsymbol{x}_{k+1} + \frac{1}{2}\boldsymbol{u}_k^T R_k \boldsymbol{u}_k + d_{u,k}^T\boldsymbol{u}_k \tag{2.24}$$

The design of the objective function in equation 2.24 makes it easy to penalise or minimise certain states and inputs in the function more than other. For instance, if the term $\frac{1}{2}\boldsymbol{x}_{k+1}Q_{k+1}\boldsymbol{x}_{k+1}$ becomes increasingly larger than the other terms, will the optimisation algorithm focus on decreasing the state variables sufficiently such that $f$ also decreases sufficiently. Additionally, will the design of separate elements in the matrices $Q, R$ and vectors $d_x, d_u$ in the objective function make it possible to penalise states relative to other states or inputs relative to other inputs. For instance, may a high value of the first element in the Q matrix, force the algorithm to focus more on minimising state $x_1$ relatively to the other states in order to minimise the complete objective function.

According to Foss and Heirung (2016), does the objective function also exists with several modifications. For instance, if the states are to follow a reference trajectory, changing $\boldsymbol{x}_k \rightarrow (\boldsymbol{x}_k - \boldsymbol{x}_k^{ref})$, will lead to the objective function penalises deviations away from reference as the optimum $\boldsymbol{x}_k = \boldsymbol{x}_k^{ref}$ would lead to the corresponding term becoming zero in the objective function. Another quite common modification is the use of derived variables instead of the actual state, $\boldsymbol{x}_k \rightarrow \boldsymbol{z}_k = h(\boldsymbol{x}_k)$. In the model of the $CO_2$ capture facility, a natural derived variable to use for optimisation is the capture ratio of $CO_2$ in the absorber column. Furthermore, in a physical system, there will often be limitations to how fast actuators may move, such as opening of a valve. Including terms for the rate of change of input, $\frac{1}{2}\Delta\boldsymbol{u}_k^T R_{\Delta k}\Delta\boldsymbol{u}_k$, may thus enable the inclusion of such limitations in the control problem and penalise wear and tear on the actuators.

A disadvantage with the formulation in 2.23, is that for nonlinear systems, the constraints may sometimes render the solution infeasible; outside the bounds given by the constraints. In order to avoid infeasibility, soft constraints are often added for the state or derived variables through slack variables $\boldsymbol{\varepsilon}$ (Foss and Heirung, 2016, p. 44). Changing the constraints

$$\boldsymbol{x}^{low} \leq \boldsymbol{x}_k \leq \boldsymbol{x}^{high}, \quad \Rightarrow \quad \boldsymbol{x}^{low} - \boldsymbol{\varepsilon}_k \leq \boldsymbol{x}_k \leq \boldsymbol{x}^{high} + \boldsymbol{\varepsilon}_k$$

(or similarly for $\boldsymbol{z}_k$) and including the slack variables $\boldsymbol{\varepsilon}_k$ in the objective function

for minimisation, will ensure feasibility but minimise the violations as much as possible. Including the aforementioned modifications, the objective function may be represented by equation 2.25. The matrices and vectors $Q_k, R_k, \rho_k$ and $S_k$ may vary with time $k$ but is also quite common to set constant in time.

$$\begin{aligned}\min_{\boldsymbol{\phi}\in\mathbb{R}^n} f(\boldsymbol{\phi}) = \sum_{k=0}^{N-1} \Bigg( & \frac{1}{2}(\boldsymbol{x}_{k+1} - \boldsymbol{x}_{k+1}^{ref}) Q_{k+1} (\boldsymbol{x}_{k+1} - \boldsymbol{x}_{k+1}^{ref}) \\ & + d_{x,k+1}^T (\boldsymbol{x}_{k+1} - \boldsymbol{x}_{k+1}^{ref}) \\ & + \frac{1}{2}\boldsymbol{u}_k^T R_k \boldsymbol{u}_k + d_{u,k}^T \boldsymbol{u}_k + \frac{1}{2}\Delta\boldsymbol{u}_k^T R_{\Delta k} \Delta\boldsymbol{u}_k \\ & + \rho_{k+1}^T \boldsymbol{\varepsilon}_{k+1} + \frac{1}{2}\boldsymbol{\varepsilon}_{k+1}^T S_{k+1} \boldsymbol{\varepsilon}_{k+1} \Bigg)\end{aligned} \tag{2.25}$$

where

$$\begin{aligned} Q_k &\succeq 0, \qquad k = 1, ..., N \\ R_k &\succeq 0, \qquad k = 0, ..., N-1 \\ \boldsymbol{\varepsilon}_k \in \mathbb{R}^{n_x} &\succeq 0, \quad k = 1, ..., N \\ \rho_k \in \mathbb{R}^{n_x} &\succeq 0, \quad k = 1, ..., N \\ S_k \in \mathrm{diag}\{s_1, .., s_{n_x}\}, s_i &\succeq 0, i = 1, ..., n_x \end{aligned}$$

### 2.3.1 Nonlinear Model Predictive Control

The general optimisation problem described above and in equations 2.23 and 2.24 is according to Foss and Heirung (2016) an open loop optimisation problem. This is due to the optimal input $\boldsymbol{u}_k$ being calculated at time instant $t_0$ for the whole prediction horizon without feedback of the states during simulation. Model Predictive Control (MPC) is on the other hand a closed loop optimisation problem in which feedback is taken into consideration. MPC solves the general dynamic optimisation problem using the current state as initial state $\boldsymbol{x}_0 = \boldsymbol{x}_k$, yielding an optimal input $\boldsymbol{u}$ for the prediction horizon at each time instant $k = k+1, .., k+N-1$. However, only the first control move is used. As an illustration, the pseudo-algorithm for the state feedback MPC procedure from Foss and Heirung (2016, p. 40) is stated below. This algorithm assumes that the actual state is available for feedback. If the dynamic system is nonlinear, the algorithm will be referred to as Nonlinear Model Predictive Control (NMPC) Algorithm.

**Algorithm: State feedback (N)MPC procedure**

**for** k = 0,1,2,... **do**
  Get the current state $x_k$;
  Solve a dynamic optimisation problem on the prediction horizon from k to k+N with $x_k$ as the initial condition;
  Apply the first control move $u_k$ from the solution above;
**end for**

An illustration of the state feedback (N)MPC procedure, courtesy of *Cybernetica AS*, may be found in Figure 2.3. In the figure may one see how the controlled variables (CV) and manipulated variables (MV), $\boldsymbol{z}_k$ and $\boldsymbol{u}_k$ respectively, have varied in the past history and how the predicted trajectory $N$ time samples ahead looks like at the current time instant. The predictions show how the CV's will change given that the optimal MV's calculated are applied. However, only the first optimal control move $\boldsymbol{u}_k$ is applied, and a new solution will be calculated at the next time instant possible changing the optimal predicted solution and trajectory towards reference point. Consequently, as a constant $N$ is used at each time step, will the prediction horizon move in time, a so-called receding prediction horizon. What is less common, but sometimes utilised, is a shrinking prediction horizon where $N$ decreases by one time sample each sample $N_{k+1} = N_k - \Delta k$.

The (N)MPC algorithm will be solved for time steps $k = 0, 1, ..$ possible to infinity, and it is therefore common to discard the summation over $k$ in the problem formulation of the (N)MPC and use $i$ for summation over the prediction horizon. Using $\boldsymbol{z}$ as the control variable in the objective function and assuming constant weight matrices and vectors, the complete (N)MPC problem formulation may be written as in equation 2.26. Several variants of the objective function $f(\boldsymbol{\phi})$ exists, but the one in equation 2.26 includes the most common terms.

$$
\begin{aligned}
\min_{\boldsymbol{\phi}\in\mathbb{R}^n} f(\boldsymbol{\phi}) = \sum_{i=0}^{N-1} \Bigg( & \frac{1}{2}(\boldsymbol{z}_{k+i+1} - \boldsymbol{z}^{ref}_{k+i+1}) Q (\boldsymbol{z}_{k+i+1} - \boldsymbol{z}^{ref}_{k+i+1}) \\
& + d_z^T (\boldsymbol{z}_{k+i+1} - \boldsymbol{z}^{ref}_{k+i+1}) \\
& + \frac{1}{2}\boldsymbol{u}^T_{k+i} R \boldsymbol{u}_{k+i} + d_u^T \boldsymbol{u}_{k+i} + \frac{1}{2}\Delta\boldsymbol{u}^T_{k+i} R_\Delta \Delta\boldsymbol{u}_{k+i} \\
& + \rho^T \boldsymbol{\varepsilon}_{k+i+1} + \frac{1}{2}\boldsymbol{\varepsilon}^T_{k+i+1} S \boldsymbol{\varepsilon}_{k+i+1} \Bigg)
\end{aligned}
$$

subject to

$$
\begin{aligned}
\boldsymbol{x}_{k+i+1} &= \boldsymbol{g}(\boldsymbol{x}_{k+i}, \boldsymbol{u}_{k+i}), \qquad i = 0, ..., N-1 \\
\boldsymbol{z}_{k+i} &= \boldsymbol{h}(\boldsymbol{x}_{k+i}, \boldsymbol{u}_{k+i}), \qquad i = 1, ..., N \\
\boldsymbol{x}^{low} - \boldsymbol{\varepsilon}_{k+i} &\le \boldsymbol{x}_{k+i} \le \boldsymbol{x}^{high} + \boldsymbol{\varepsilon}_{k+i}, \qquad i = 1, ..., N \\
\boldsymbol{u}^{low} &\le \boldsymbol{u}_{k+i} \le \boldsymbol{u}^{high}, \qquad i = 0, ..., N-1 \\
\Delta\boldsymbol{u}^{low} &\le \Delta\boldsymbol{u}_{k+i} \le \Delta\boldsymbol{u}^{high}, \qquad i = 0, ..., N-1 \\
0 &\le \boldsymbol{\varepsilon}_{k+i} \le \boldsymbol{\varepsilon}_{max}, \qquad i = 1, .., N-1
\end{aligned}
\tag{2.26}
$$

where

$$
\begin{aligned}
\Delta\boldsymbol{u}_{k+i} &= \boldsymbol{u}_{k+i} - \boldsymbol{u}_{k+i-1} \\
\boldsymbol{x} &\in \mathbb{R}^{n_x} \\
\boldsymbol{z} &\in \mathbb{R}^{n_z} \\
\boldsymbol{u} &\in \mathbb{R}^{n_u} \\
\boldsymbol{\phi}^T &= (\boldsymbol{z}_1^T, ..., \boldsymbol{z}_N^T, \boldsymbol{u}_0^T, ..., \boldsymbol{u}_{N-1}^T) \in \mathbb{R}^n, \quad n = N \cdot (n_z + n_u) \\
Q &\in \mathbb{R}^{n_z \times n_z}, R \in \mathbb{R}^{n_u \times n_u}, R_\Delta \in \mathbb{R}^{n_u \times n_u}, S \in \mathbb{R}^{n_z \times n_z} \\
d_z &\in \mathbb{R}^{n_z}, d_u \in \mathbb{R}^{n_u}, \rho \in \mathbb{R}^{n_z}
\end{aligned}
$$

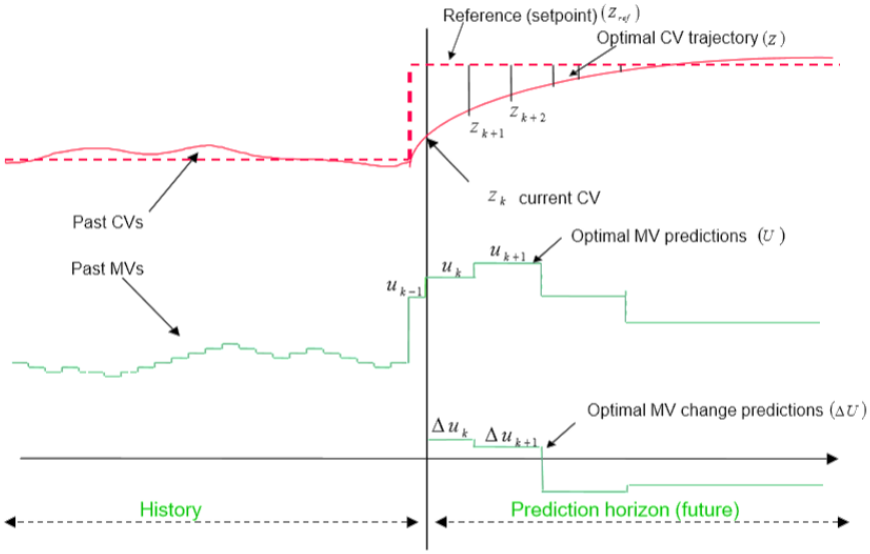


Figure 2.3: Illustration of (N)MPC procedure with history and predictions for manipulated and controlled variables. Also illustrated is the concept of CV evaluation points and input blocking. Courtesy of Svein Olav Hauger at *Cybernetica AS*

Also illustrated in Figure 2.3, are two methods for variable elimination to obtain a simpler problem with fewer degrees of freedom; input blocking and controlled variable evaluation points. Input blocking is according to Foss and Heirung (2016) a way of structuring the input variables to an adjacent-in-time structure, such that the number of optimal predicted inputs becomes smaller than in the original problem. For the original problem will the number of decision variables emanating from the input equal to $N \cdot n_u$. That is, one variable for each time sample for each $\boldsymbol{u}$. Using input blocking, one are able to specify the number of time samples desired before the next change in input, and keep the input constant between the two time instants. Consequently, will there be a reduction of input variables and hence the degree of freedom. Keeping the input constant in each input block is referred to as zero-order hold. According to Zhang et al. (2011) however, does zero-order hold not provide high accuracy if the time between each input blocks is large. First-order hold may instead be utilised, which linearly interpolates two recurrent input values instead of keeping it constant in the block interval. According to Zhang et al. (2011), will first-order hold improve accuracy very much while only insignificantly affecting the computational effort. According to Foss

and Heirung (2016), has input blocking worked well in industrial applications. The number of input blocks may vary from 1 to N, however, an important factor is that the $\boldsymbol{u}$ with fewer blocks should be able to approximate the optimal $\boldsymbol{u}$ without input blocking. The number of input blocks may be specified independently for each MV. How many blocks are needed will depend on how fast the inputs needs to change in order to reach optimum within the prediction horizon. According to Strand and Sagli (2004), are 4 to 8 blocks for standard MPC very common. However, Strand and Sagli (2004) considers a linear dynamic system and may thus use many blocks without affecting the simulation time in equal scale as if a nonlinear system was to be optimised due to the complexity and iterative style of the nonlinear solver. A large number of input blocks will result in a large simulation time. Resultantly, if NMPC is used in online optimisation where the solving time per sample must be less than the time between each sample, will the highest number of input block tolerated, be constrained by the time between each sample.

Controlled variable evaluation points is also a technique used to reduce the degrees of freedom of an optimisation problem by reducing the number of constraints (Strand and Sagli, 2004). Instead of having the objective function evaluated at each time instant $k$, a smaller number of time instants between the current and $N$ are chosen and the objective function only evaluated at these points in time. How many evaluation points are needed and where to place them will be dependent on the system and the wanted behaviour of the controller. In addition may different CV have a different number of evaluation points, and they may be specified independently. Strand and Sagli (2004) states that 5 to 20 evaluation points is common in standard MPC algorithms. For large nonlinear systems, such as the system in this thesis, input blocking and controlled variable evaluation points will be very important techniques in order to reduce the computational effort and speed up the solving time. The decision variables in equation 2.26, $\boldsymbol{\phi}^T = (\boldsymbol{z}_1^T, ..., \boldsymbol{z}_N^T, \boldsymbol{u}_0^T, ..., \boldsymbol{u}_{N-1}^T)$, will with these techniques include fewer variables, but the rest of the formulation will stay the same.

In the above description of the (N)MPC procedure, a plant replacement model of a physical system have been used in the closed loop optimisation in which all states, $\boldsymbol{x}_k$, are known and may be fed back at each time sample. However, if the (N)MPC scheme is to control a real physical plant, some kind of feedback from the true plant should exist as there for several reasons almost always exist modelling errors between the model and the true process. Consequently, will an estimator be necessary to remove modelling errors such that the (N)MPC procedure may provide a more optimal solution in accordance with the true plant. Such an (N)MPC scheme is often referred to as an output feedback procedure and is illustrated in Figure 2.4. In addition to the CV's and MV's, the diagram in

Figure 2.4 includes disturbance variables (DV), which are inputs not calculated by the controller, for instance noise. There exist several variants of the estimator, but in general will an estimator compare measurements from instruments of the plant, $\boldsymbol{y}$, against predicted measurements from the model, $\bar{\boldsymbol{y}}$, and use the deviation between the two to update the model and reduce modelling errors. An example of a simple and effective estimator is bias updating. In bias updating, the deviation between instrumental and modelled measurements are multiplied with a factor, quite often constant, and introduced additively back into the model. Which measurements to use in bias updating, must be determined in advance of starting the optimisation. For instance, the $CO_2$ capture facility at Tiller provides instrumental measurements for the mass flow of $CO_2$ out of the condenser. The deviation between this measurement and the calculated measurement in the model be used to update the predicted measurement variable in the model, and consequently will the model reflect the true conditions in the plant better. In addition should this deviation be used to update the capture ratio in the absorber column as there is a direct relationship with the absorbed $CO_2$ in the absorber and the outflow of $CO_2$ from the condenser.

There are however, several downsides with bias updating. Firstly, the updates of the model will not occur in the states of the system but rather in derived variables used for optimisation or variables for calculated measurements. Secondly, the update factor must be manually adjusted to achieve appropriate updating of variables. Lastly, which variables should be updated must be made in advance of starting the optimisation. A more advanced estimator such as (Extended) Kalman Filter may on the other hand, by using measurements observed over time and statistical analysis, automatically determine which states or parameters should be updated, and actually update the states and not derived or calculated measurement variables in the system. Further, the gain factor may be automatically calculated at each time sample without manual tuning, and additionally, is the Kalman Filter also able to estimate time varying parameters which may be beneficial for the predictions of the system (Brown and Hwang, 2012, p. 257). However, advanced estimators such as the Kalman Filter are very time consuming and may cause complications in online optimisation where the solving time per sample must be less than the time between samples. In fact, *Cybernetica AS* found that when the original model of the $CO_2$ capture facility were to be used for online optimisation, the solving of the model was too time consuming by itself to be able to include an estimator for parameter and state estimation. Additionally, a Kalman Filter may sometimes result in parameter adjustments that renders the system stiffer than original. Resultantly, has bias updating been utilised to reduce errors in the most important variables and for optimisation of the reduced model, as a Kalman Filter should be properly experimented with before inclusion in online estimation

of real facilities.

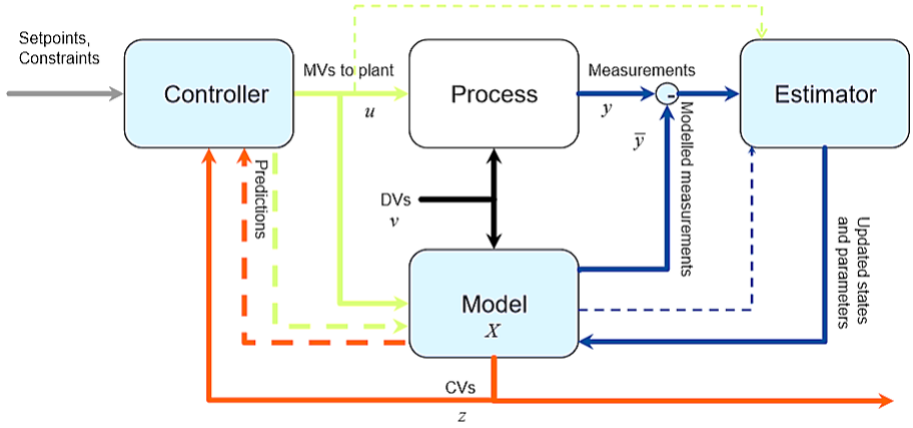


Figure 2.4: Illustration of the output feedback (N)MPC procedure with feedback from measurements through the estimator. Courtesy of Svein Olav Hauger at *Cybernetica AS*.

### 2.3.2 Dynamic Real-Time Optimisation

The dynamic optimisation problem that will be experimented with for the $CO_2$ capture facility in this thesis will be different from a standard (N)MPC problem as economic aspects will be taken into consideration. As stated in Section 1.2, common in literature is the use of a two-level control hierarchy in which the economical optimisation problem is solved at an upper level, often called Real-Time Optimisation (RTO), providing set points for the advanced regulatory controller at the level below. Oliveira (2016) points out that using a two-layer approach will have the advantage of a less complex problem because there will be a clear separation between the economic and regulatory objectives causing simpler sub-problems. Quite often however, will the upper level optimisation problem utilise steady state, non-linear models, which results in new setpoints being found only when the model has reached steady-state (Maree and Imsland, 2011). In line with the computer becoming increasingly faster, dynamic models to solve the economic objectives became common. However, often were different sample times for the two layers utilised in which the RTO had a larger sample time than the MPC for regulatory control. Both Maree and Imsland (2011) and Willersrud et al. (2013) suggested merging of the two-level hierarchy into one-level,

in which the objective function evaluates both regulatory and economic objectives of the plant, for instance reference tracking in addition to cost minimisation. Such an optimisation problem is sometimes referred to as an Economic MPC (EMPC) (Maree and Imsland, 2011) or a Dynamic Real-Time Optimisation Problem (DRTO) (Willersrud et al., 2013). As the two objectives are to be merged, a small sample time will be utilised also for the economic objectives. Willersrud et al. (2013) points out that this is one of the advantages of a one-level control hierarchy, as the algorithm will obtain faster reactions to disturbances. Additionally, direct comparison of the control and economic objectives will be available, and the importance of the two objectives may be weighed against each other. Two-level and one-level control hierarchy are illustrated in Figure 2.5.

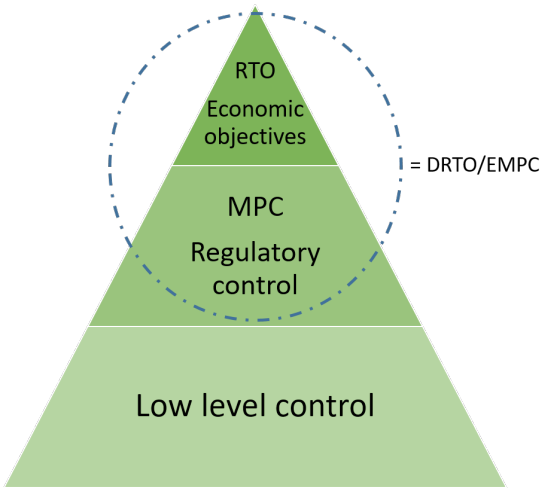


Figure 2.5: Illustration of a two-level advanced control hierarchy being merged into a single-level advanced controller on top of low-level controllers.

Willersrud et al. (2013) suggested two methods to include economic optimisation variables in the objective function. Firstly, by the use of an unreachable setpoint and secondly by the use of infeasible soft-constraints. The two methods have been illustrated in Figure 2.6 for both maximisation and minimisation problems. Unreachable setpoint is a method where a high or low unrealistic setpoint is used for the variable that will be maximised or minimised respectively. Using the division of decision variables as in Willersrud et al. (2013), $\boldsymbol{z}_{trac}$ for tracking objectives and $\boldsymbol{z}_{opt}$ for the optimisation variables, like cost, the following objective function in equation 2.27 was utilised for the unreachable setpoint method. Here, $Q$, $R_\Delta$, $\rho$ and $z^{ref}$ have been assumed constant in time with $\boldsymbol{z}_{opt}^{ref}$ unreachable, MV

penalisation's and linear CV penalisation's together with quadratic CV variable violations through slack variables have been omitted.

$$\begin{aligned}\min_{\boldsymbol{\phi}\in\mathbb{R}^n} f(\boldsymbol{\phi}) = &\sum_{i=0}^{N-1}(\boldsymbol{z}_{trac,k+i+1} - \boldsymbol{z}_{trac}^{ref})Q_{trac}(\boldsymbol{z}_{trac,k+i+1} - \boldsymbol{z}_{trac}^{ref}) \\ &+ (\boldsymbol{z}_{opt,k+i+1} - \boldsymbol{z}_{opt}^{ref})Q_{opt}(\boldsymbol{z}_{opt,k+i+1} - \boldsymbol{z}_{opt}^{ref}) \\ &+ \Delta\boldsymbol{u}_{k+i}^T R_\Delta \Delta\boldsymbol{u}_{k+i} + \rho^T \boldsymbol{\varepsilon}_{k+i+1}\end{aligned} \tag{2.27}$$

However, as Willersrud et al. (2013) states, may the value of the optimal setpoint affect the solution of the (N)MPC, even though it is set arbitrarily. This is due to the setpoint appearing in the gradient of the objective function that is used in the conditions for optimality. Infeasible soft-constraints on the other hand, utilise slack variables instead of setpoints to penalise deviations away from reference. By setting both the bounds on the variable out of reach but including slack variables in the objective function will yield a feasible solution and still minimise or maximise the variable in question. In a minimisation problem, the following will always hold

$$\begin{aligned}\boldsymbol{z}_{opt,min} \leq \boldsymbol{z}_{opt,max} \leq \boldsymbol{z}_{opt,k+i} \\ \boldsymbol{\varepsilon}_{opt,k+i} = \boldsymbol{z}_{opt,k+i} - \boldsymbol{z}_{opt,max} \geq 0 \\ \rho_{opt}^T \boldsymbol{\varepsilon}_{opt,k+i} = \rho_{opt}^T(\boldsymbol{z}_{opt,k+i} - \boldsymbol{z}_{opt,max})\end{aligned}$$

Consequently, as the term $-\rho_{opt}^T \boldsymbol{z}_{opt,max} \leq 0$ as long as $\rho_{opt}^T$ and $\boldsymbol{z}_{opt,max}$ are non-negative, this term may be omitted in the objective function and the objective function will no longer be dependent on the optimal value as it was in the unreachable setpoint method. $\boldsymbol{z}_{opt,max}$ non-negative is usually safe to assume if the optimisation variable represent cost. The objective function may thus be written as in equation 2.28, now with a linear penalisation term for the optimal (often economic) decision variable.

$$\begin{aligned}\min_{\boldsymbol{\phi}\in\mathbb{R}^n} f(\boldsymbol{\phi}) = &\sum_{i=0}^{N-1}(\boldsymbol{z}_{trac,k+i+1} - \boldsymbol{z}_{trac}^{ref})Q_{trac}(\boldsymbol{z}_{trac,k+i+1} - \boldsymbol{z}_{trac}^{ref}) \\ &+ \Delta\boldsymbol{u}_{k+i}^T R_\Delta \Delta\boldsymbol{u}_{k+i} + \rho_{trac}^T \boldsymbol{\varepsilon}_{trac,k+i+1} + \rho_{opt}^T \boldsymbol{z}_{opt,k+i+1}\end{aligned} \tag{2.28}$$

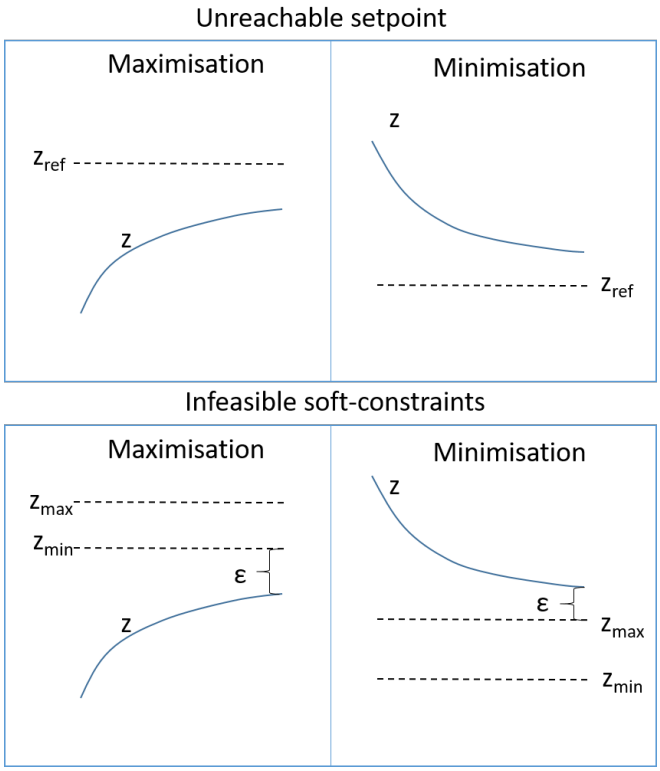


Figure 2.6: Illustration of the Unreachable setpoint and Infeasible soft-constraint method for maximisation and minimisation problems.

Willersrud et al. (2013) found by experimenting with both methods for production optimisation of an offshore oil and gas facility, that both solutions were able to find the economic optimal point. On the other hand, Willersrud et al. (2013) also state that the infeasible soft-constraint method was easier to tune due to fewer tuning parameters.

In this thesis, the cost related to the energy consumption in the reboiler will be attempted minimised while keeping an overall capture ratio of $CO_2$ in the absorber at a specified reference level after 24 hours. Consequently, may both the unreachable setpoint and infeasible soft-constraint method be utilised for this problem. Which is the better method for the model of the $CO_2$ capture facility will be experimented with in Chapter 5.

### 2.3.3 Solving nonlinear optimisation problems

As previously mentioned, for nonlinear systems in an NMPC scheme must a more complex nonlinear solver, often iterative in nature, be utilised at each time sample to solve the optimisation problem. One such algorithm, which has been used in this thesis, is Sequential Quadratic Programming (SQP). In SQP, the nonlinear optimisation problem will be formulated as a sequence of smaller quadratic problems which are approximation to the nonlinear objective function (Nocedal and Wright, 2000). The number of QP iterations will define how many quadratic sub-problems will be solved in an iterative fashion in the search of a more optimal solution. Using for instance two QP-iterations, the algorithm will firstly approximate the nonlinear objective function around the current point with a quadratic approximation, and find the optimum of this sub-problem. The algorithm will next use the point on the nonlinear curve closes to the found optimum and use this to approximate the second quadratic sub-problem. The point on the nonlinear curve closest to the second optimum will then be used to step one sample in the NMPC scheme. The SQP algorithm with one QP iteration is illustrated in Figure 2.7. In practice, will a higher number of QP iterations result in the optimal solution being found faster, with the consequence of higher solving time per sample. However, if the time between each sample is small, a somewhat slower convergence to the optimal solution is often accepted. On the other hand, if the time between samples are large, is it of higher importance to find the optimal solution fast, thus will a higher number of QP iterations be required. Further, one QP iteration is often accompanied with a line search. In a line search, several points on the nonlinear curve between the start point and the optimum of the approximation is tested before choosing the point on the nonlinear curve giving the most optimal value of the objective function so far. This is necessary because the algorithm sometimes steps too far when choosing the point on the nonlinear curve nearest to the optimal value of the quadratic problem and thus overlooks a better optimal value of the nonlinear curve. Unfortunately, the SQP algorithm may only guarantee convergence to a local optimum if the problem is non-convex, as most nonlinear problems are (Nocedal and Wright, 2000). Dependent on the starting point may therefore the SQP algorithm find itself stuck in a local optimum different from the global optimum. There are methods for also finding a global optimal solution for non-convex problems, for instance the Multistart methods (FrontlineSolvers, 2018), where a local optimal solver such as SQP is run from several different starting points to see if the optimal solution converges to the same extrema. Other methods may utilise different Branch and Bound methods where the region of interest is divided into smaller sub-regions such that the local optimisation solver may be utilised in each region (FrontlineSolvers, 2018). However, methods for global optimisation of nonlinear

problems may be very time consuming. On the other hand, proper design of the objective function may often avoid unnecessary many local optimum such that, in practise, the local optimum found by the SQP is also the global optimum.

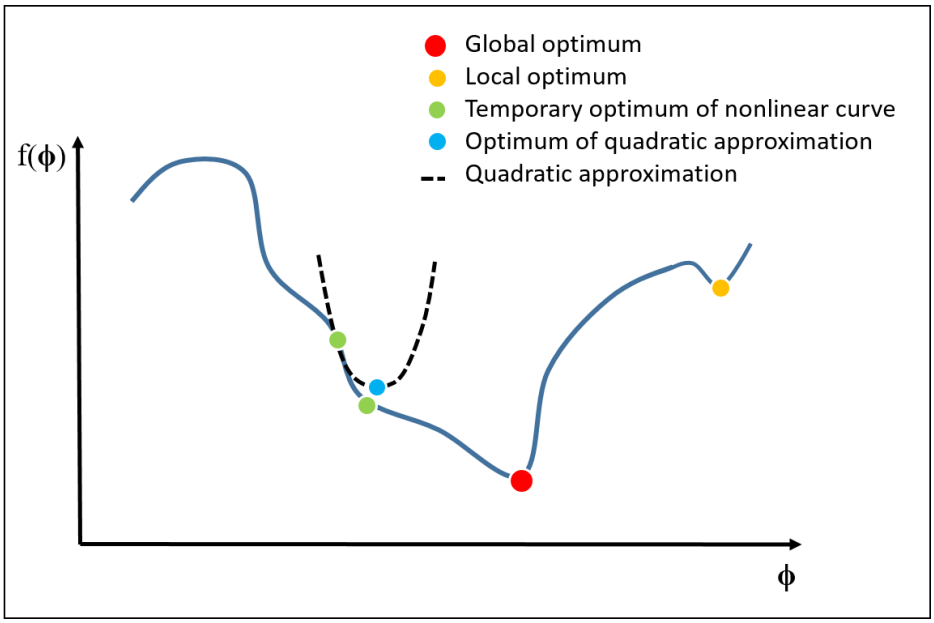


Figure 2.7: Illustration of the Sequential Quadratic Programming algorithm with one QP iteration. A quadratic approximation to the nonlinear curve in the current point is established, and the point on the nonlinear curve closest to the optimum of the approximation is used as the new, so far best, optimum of the nonlinear problem.

# Chapter 3

# Implementation and Software

As mentioned in Section 1.5, *Cybernetica AS* has provided software tools for investigation of the topic in this thesis, namely Modelfit, RealSim and CENIT. Interfaces developed to communicate with the software have also been provided such that the setup of the model validation in Chapter 4 and optimisation algorithm in Chapter 5 was manageable. In addition, has the original model been provided to use as plant replacement model for analysing the performance of the reduced model. Consequently, has *Cybernetica AS* provided a complete framework as a starting point for both development of the reduced model in addition to development of the DRTO algorithm. An overview of the different software, interfaces and code provided, and communication links between them may be found in Figure 3.2. However, the framework provided will need extensive changes in order to investigate this thesis.

First, will the model reductions from Hotvedt (2017) for the absorber, desorber and heat exchanger be integrated in the original model. Consequently, will the state space and complexity of the new reduced model be quite different from the original model. The reduced unit models integrated are summarised in Section 2.1. Since the complete model is built using sequential modular modelling, mentioned in Section 2.1, was the substitution of the reduced unit models effortlessly completed. On the other hand, routines calculating inputs to each unit model based on the output of other and routines calculating measurements, $\boldsymbol{y}$, and derived variables, $\boldsymbol{z}$, had to be changed due to different state variables in the reduced unit models and the original unit models. Additionally, it was decided to keep external inputs to the model equal to those in the original model such that a direct comparison of the responses of the models could be performed. Consequently, were inclusion

of several conversions between molar flows and molar amounts using equation 2.1 necessary.

After the new state space and model equations were implemented in addition to adjustments of the routines calculating inputs, measurements and derived variables, the new complete model of the facility could be validated against both instrumental measurements available from the real $CO_2$ facility at Tiller, courtesy of SINTEF, and the original model. The validation is done in Chapter 4 by the use of Modelfit, which is a tool designed by *Cybernetica AS* for offline estimation and model validation (Cybernetica AS, 2018). Input to Modelfit is a large, pre-generated data set with input and measurement vectors for each time sample of the simulation horizon. In Chapter 4, most of the simulations performed in Modelfit are ballistic, which means that no controllers nor parameter estimations are turned on. Modelfit uses the program flow illustrated in Figure 3.1 for ballistic simulations. Here "Calculate additional inputs" is the routine calculating inputs to each unit model based on the outputs of other unit models as explained above. Both measurements and derived variables are calculated, yet not used in the next loop of simulations because of running the simulations ballistic. However, if an estimator is included, the dashed line in Figure 3.1 will take effect.

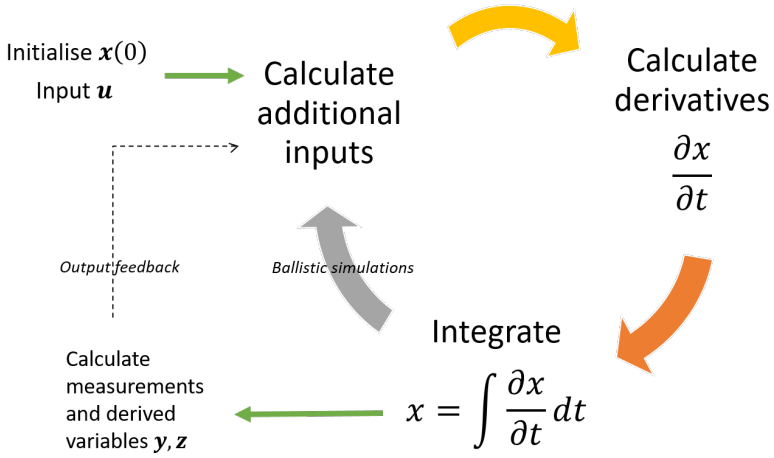


Figure 3.1: Program flow of ballistic simulations in Modelfit. The dashed line will take effect if an estimator is included for feedback of measurements to the system.

An eigenvalue analysis has also been performed in Chapter 4, to analyse the stiffness of the original and reduced model. The analysis was performed in MATLAB using the implemented estimation of the Jacobian matrix in Listing 2.1, in addition to built-in functions in MATLAB to obtain the eigenvalues. However, a MATLAB interface to the C-code of the model was necessary to acquire the model derivatives. This interface was also provided by *Cybernetica AS*.

For optimisation purposes, two other software applications from *Cybernetica AS* have been utilised, and consequently were there several other interfaces from the provided structure and code that had to be modified. RealSim is one of the applications, and is used as a plant replacement process simulator (Cybernetica AS, 2018). That is, simulation of the capture facility using a model if instrumental measurements from the actual plant is unavailable. CENIT is the second software used, which handles the controller of the optimisation problem along with the estimator (Cybernetica AS, 2018). Consequently, the controller interface had to be changed such that the one-level Dynamic Real-Time optimisation algorithm with both economic and regulatory objectives was implemented. The accumulated capture ratio and the cost related to the reboiler duty had to be included into the objective function and the appropriate CV evaluation points had to be chosen and set. Additionally, as the optimisation would proceed over 24 hours, the prediction horizon and the number and length of input blocks for appropriate responses had to be experimented with. For illustration of which processes corresponds to the different tools, see Section 2.3 Figure 2.4, where the block "Process" is simulated by RealSim, whereas CENIT is responsible for "Model", "Estimator" and "Controller". In this thesis, online measurements during optimisation from the facility at Tiller is unavailable, and consequently has the original model been used as a replacement and simulated in RealSim. This design is beneficial as the original and reduced model behave differently from each other due to modelling errors, and will thus be a well reflection of the reality. However, as mentioned in Section 2.3, *Cybernetica AS* found that the original model was too computationally inefficient to additionally run a complex estimator such as a Kalman Filter. Consequently, during tuning and testing of the controller will the estimator be turned off and later for performance enhancement has only bias updating been introduced.

Lastly, in the original code are also interfaces for several integrators implemented. These include CVODE and Explicit Euler which are briefly described in Section 2.2. As CVODE is already implemented, this routine will be used to integrate the system as it usually accounts for possible stiffness, better accuracy and less simulation time. However, if the reduced model show significantly decreased stiffness, Explicit Euler may be considered as integration routine.

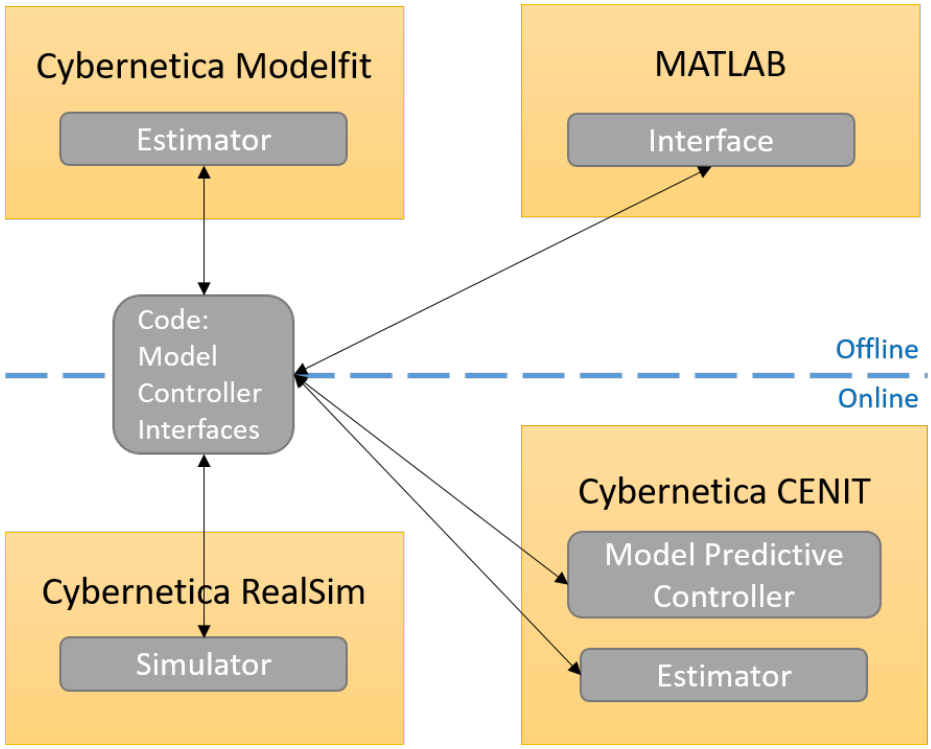


Figure 3.2: Overview of software and available interfaces utilised in this thesis for offline model validation and online optimisation.

# Chapter 4

# Model validation

Modelfit has been used to validate the reduced model against instrumental measurements from the Tiller facility and the original model. In Hotvedt (2017), was each of the reduced unit models for the absorber, desorber and heat exchanger separately analysed against the corresponding original unit model by running ballistic simulations from an initial value until steady state was reached. However, the influence of the reduced unit models on the complete model of the $CO_2$ capture facility was not verified. Consequently, in this chapter each of the unit models have first been substituted separately into the complete original model and the response analysed. These models with only one reduced unit model substituted into the original model are referred to as temporary models. The influence of the temporary model with the reduced heat exchanger has been analysed in Section 4.1, the temporary model with the reduced absorber model in Section 4.2 and the temporary model with the reduced desorber model in Section 4.3. Secondly, in the Section 4.4, have all the reduced unit models been substituted and the complete model response analysed. The simulations that have been performed in all the above mentioned sections are ballistic with no influence of controllers nor bias updating from instrumental measurements. In the last section however, Section 4.5, has bias updating with instrumental measurements been experimented with to further decrease modelling errors. The data set that has been used in all simulations (courtesy of SINTEF) illustrates a set of representative operating conditions from a test run at the real facility at Tiller, at which steps in some of the inputs have been induced. The most important changes in inputs may be seen in Figure 4.1. The inputs for the reboiler duty and mass flow of lean amine solution into the absorber are optimal inputs generated by the NMPC controller

through CENIT and is thus a consequence of the manual step changes in the inlet of flue gas and changes in inlet composition of $CO_2$ in the flue gas. The large spikes in the inlet composition of $CO_2$ is caused by the daily resetting of a propane burner which provides flue gas to the absorber in the Tiller facility.

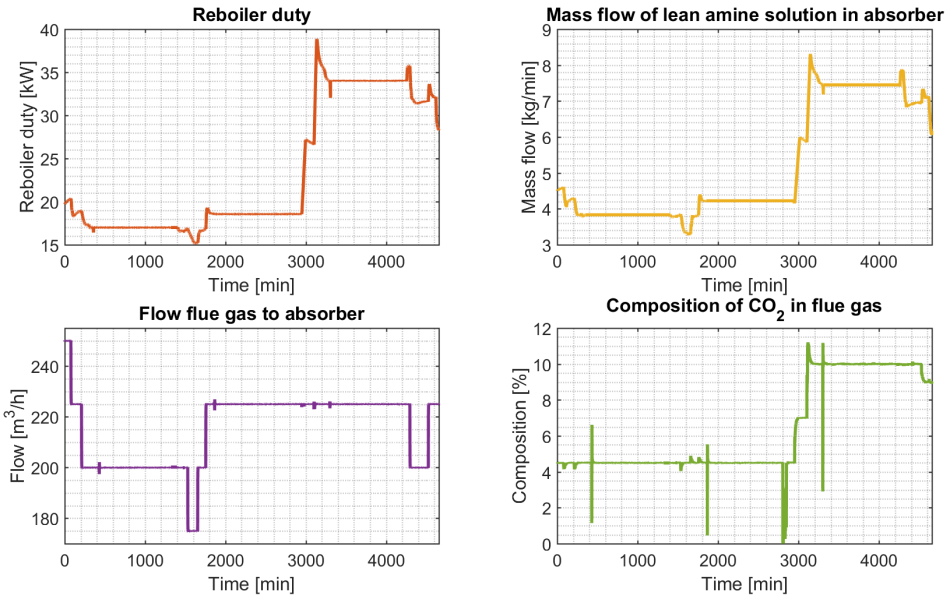


Figure 4.1: Overview of the most important inputs and steps in input during the ballistic simulations in Modelfit. Obtained from the data set provided by SINTEF.

One of the assumptions made in this chapter is treating the original model with the perfect model assumption. That is, neglecting modelling errors between the model and the true facility. Consequently, the goodness of fit of the reduced model response have been compared to the original model response instead of to instrumental measurements from the facility. Consequently, responses of variables in the models that have not been measured in the Tiller facility may be compared to each other. Two evaluation variables have been applied to investigate the goodness of fit; maximum and average absolute deviation defined in equation 4.1, Chapter 2.

$$\begin{aligned} \max|\tilde{D}| &= \max_k \left(|\boldsymbol{\phi}_{i,org,k} - \boldsymbol{\phi}_{i,red,k}|\right) \\ \text{avg}|\tilde{D}| &= \frac{\sum_{k=0}^{K} \left(|\boldsymbol{\phi}_{i,org,k} - \boldsymbol{\phi}_{i,red,k}|\right)}{K} \end{aligned} \tag{4.1}$$

Here $K = 4656$ samples, which are the number of samples in the data set. One sample represents one minute, thus the complete data set represents input and measurement values for more than three days. $\boldsymbol{\phi}$ is a generic vector with both controlled variables $\boldsymbol{z}$ and predicted measurements $\bar{\boldsymbol{y}}$ from the model, and $i$ is the index for the variable in question. The variables that have been analysed are the instantaneous capture ratio (CR) in the absorber column, the mass flow rate of $CO_2$ from the condenser, the concentration of $CO_2$ in the top of the absorber column and the temperature in the absorber column approximately one meter from the top. The first mentioned variable is a controlled variable which is derived using equation 4.2. Here $F_{abs,CO_2}$ is the molar flow of $CO_2$ which may be found using the relationship between molar flows and molar amounts in equation 2.1.

$$\text{CR} = 100 \times \frac{F_{g,abs,CO_2,in} - F_{g,abs,CO_2,out}}{F_{g,abs,CO_2,in}} \tag{4.2}$$

The capture ratio is a derived variable, and is hence not measured by instrumentation in the Tiller facility, but is still a very important variable. This is because the capture ratio often is used in optimisation and control and the variable must thus be able to reflect the conditions in the true plant. The three others variables are predicted measurements from the model where instrumental measurements from the Tiller facility have been made available by SINTEF. It has been decided that the mass flow rate of $CO_2$ from the condenser is, compared to the others, of most importance to yield correct results. This is because the variable is direct result of how much $CO_2$ has been captured from the exhaust gas and because the instrumental measurements for this variable is the most reliable measurements of those available.

Parameter adjustment have manually been experimented with in order for the reduced model to fit better to the original model. Three parameters have been adjusted in the different models; the heat transfer coefficient in the heat exchanger $\hat{h}_{hex}$ and two factors called the K-factors of $CO_2$. The last mentioned factors are multiplied with the overall mass transfer coefficients in the absorber and desorber, in order to change the overall mass transfer. They should ideally be set to 1, as not to enhance nor decrease the overall mass transfer coefficient in the column

found from correlations (Fløi, 2015, p. 71). However, in the original model, these factors were set less than 1 through parameter estimation such that the response of the original model would fit better to measurements. An overview of the final parameter adjustments for each of the temporary models with a separate reduced unit model substituted, in addition to the complete reduced model may be seen in Table 4.1. Notice that the K-factors for $CO_2$ had to be increased above one for well fit between the reduced model and the original model. However, in the model used for optimisation in Chapter 5 these factors will be set to their ideal values, unity, and thus may further parameter adjustments should be performed if the result deem inadequate. Several other parameters may also be adjusted, however, these three yielded noticeable changes with small adjustments and have was thus been focused on. To enhance the goodness of fit between the models, more parameters should be experimented with.

Table 4.1: Overview of parameter values in the original model and adjustments made in the temporary models with one unit model substituted and the total reduced model during model validation (hex = heat exchanger).

| | **Model** | | | | |
|---|---|---|---|---|---|
| **Parameter** | Original | Temp. w. hex | Temp. w. absorber | Temp. w. desorber | Reduced |
| $\hat{h}_{hex}$ | 0.3788 | 0.55 | 0.55 | 2 | 2 |
| K-factor$_{CO_2,abs}$ | 0.7 | 0.7 | 1 | 0.7 | 4 |
| K-factor$_{CO_2,des}$ | 0.5 | 0.5 | 0.5 | 0.5 | 2 |

Last but not least, have eigenvalue analyses been performed using the Stiffness Ratio in equation 2.15 which is calculated based on the eigenvalues of the estimated Jacobian matrix. The Jacobian is found in MATLAB using Listing 2.1 in Section 2.2 with a perturbation parameter of $\epsilon = 10^{-8}$. Stiffness is as explained in Section 2.2 an important property which for instance decides how small the step size in the integration routine must be for stability. The step size may also influence the simulation time. A stiffer system require a smaller step size and consequently would the simulation time increase. Consequently, it is of interest to investigate the stiffness of the reduced model. The analysis might determine whether simple integration routines such as Explicit Euler may be used on the system or if more advanced routines such as CVODE is necessary. Firstly however, have each of the separate reduced unit models from Hotvedt (2017) been investigated using the same constant input as for the simulations in Hotvedt (2017). The reason for this is to see whether the introduction of control volume discretisation instead of

the collocation method, in addition to change of state space adds stiffness to the unit models. If so, the unit models are also likely to influence the stiffness in the complete model. The stiffness ratio along with the absolute real maximum and minimum eigenvalue for each of the original unit models may be found in Table 4.2. As explained in Section 2.2, an $SR >> 1$ implies a stiff system. Consequently, the original unit models for the absorber and desorber are stiff. This is most likely due to having dynamical states for both gas and liquid in the same system. Gas dynamics are usually very quick whereas liquid dynamics are slow. Consequently, a large spread in eigenvalues of such systems is to be expected.

Table 4.2: Result of the eigenvalue analysis for the different separate original unit models; heat exchanger, absorber and desorber.

| **Unit model** | **max** $\lvert\Re(\lambda_i)\rvert$ | **min** $\lvert\Re(\lambda_i)\rvert$ | **SR** |
|---|---|---|---|
| Heat exchanger | 0.017 | 0.011 | 1.56 |
| Absorber | 17.4 | $1.2{\cdot}10^{-3}$ | $1.42 \cdot 10^{4}$ |
| Desorber | 1.56 | $1.5{\cdot}10^{-2}$ | $1.12{\cdot}10^{3}$ |

Thereafter, have each of the temporary models with one of the reduced units in addition to the complete reduced model been analysed regarding stiffness. The data set provided by SINTEF have been utilised such that the stiffness could be investigated for different operating conditions. The SR was thus analysed at four samples, two at which there are large changes in the responses and two at steady state. The samples chosen may thus not be representative for other operating areas. The SR's together with the absolute real maximum and minimum eigenvalue at each sample for the original model may be seen in Table 4.3. As one may see, are the SR's for the complete original model much larger at all samples than for the separate original unit models in Table 4.2. This suggests that other unit models apart from the heat exchanger, absorber and desorber, induce stiffness in the system. For instance the reboiler or the condenser, which also have dynamical states for both liquid and gas.

In addition to analysing the stiffness of the temporary reduced models and the complete reduced model against the original model, has the approximate simulation time in Modelfit for the ballistic simulations of each of the temporary and complete models been reported. As stated may the stiffness of the model influence the simulation time, and hence may this analysis give additional information about the system stiffness. On the other hand, will the complexity of the state space also influence the simulation time and is therefore likewise reported. Either way, the simulation time plays an important role for online optimisation where there is a real-time demand on how fast the system may be solved. Therefore, both

Table 4.3: Result of the eigenvalue analysis of the original model at different samples in the data set provided by SINTEF

| **Sample** | **max** $\lvert\Re(\lambda_i)\rvert$ | **min** $\lvert\Re(\lambda_i)\rvert$ | **SR** |
|---|---|---|---|
| 80 | $5.30{\cdot}10^{3}$ | $3.07{\cdot}10^{-7}$ | $1.73{\cdot}10^{10}$ |
| 1000 | $5.31{\cdot}10^{3}$ | $3.72{\cdot}10^{-6}$ | $1.43\ {\cdot}10^{9}$ |
| 3000 | $5.40{\cdot}10^{3}$ | $5.39{\cdot}10^{-5}$ | $1.00{\cdot}10^{8}$ |
| 4000 | $5.36{\cdot}10^{3}$ | $4.11{\cdot}10^{-5}$ | $1.30{\cdot}10^{8}$ |

the stiffness of the model in addition to state space complexity will determine whether the model is suitable for use in online optimisation. The original model in this thesis have a state space dimension of 448 and using the large data set provided by SINTEF, Modelfit used $\approx$ 26 seconds to simulate the model.

Even though this thesis treats the original model with the perfect model assumption, will there always exist modelling errors and hence will it be quite valuable to investigate how well the reduced model responses fit to instrumental measurements. The measurements from the real facility at Tiller are therefore also shown in the simulation results. A model that fits well to instrumental measurements without correction from measurements is of high importance, however, sometimes the parameters are difficult to tune. Introduction of a Kalman Filter for parameter estimation could update the parameters in the model such that the responses fits well with the measurements. However, a Kalman Filter may result in the parameters become infeasible or outside physical boundaries, which may cause more stiffness. If that is the case, bias updating with a time varying bias will be essential to obtain optimal solutions for the true facility. Bias updating, as explained in Chapter 5, does not update the parameters or states in the model directly but adjusts predicted measurements or derived variables instead to remove modelling errors. In this thesis, experimentation with a Kalman Filter has not been provided, however, to illustrate that bias updating may provide an equally well response if well-tuned, the last section, Section 4.5, show the results of simulation with a bias updating using instrumental measurements of the mass flow of $CO_2$ from the condenser.

## 4.1 Validation of the temporary model with the reduced heat exchanger

In Table 4.4 and Figures 4.2 and 4.3 may one see the result of the ballistic simulation of the temporary model in which only the reduced unit model for the heat exchanger has replaced the original unit model. Hotvedt (2017) found that a number of control volumes of $n = 2$ was necessary for the best match to the original model, however, testing the complete reduced model in this chapter, it was found that changing the number of control volumes to $n = 1$ gave insignificant differences. In order for the complete model response to fit nicely to the original model for both $n = 2$ and $n = 1$, $\hat{h}_{hex}$ had to be changed from $\hat{h}_{hex,org} = 0.3788$ to $\hat{h}_{hex,red} = 0.55$. A further increase in $\hat{h}_{hex}$ gave only minor improvements. As a result, the average absolute deviation decreased for all variables as seen in Table 4.4. On the other hand did some of the maximum absolute deviations increased slightly, for instance the capture ratio, yet this may be due to the disturbances causing rapid changes in the model responses.

Table 4.4: Maximum and average deviation of the capture ratio, mass flow of $CO_2$ from condenser, absorber temperature and $CO_2$ concentration in the top of the absorber comparing the temporary model with reduced heat exchanger against the original model. Without and with parameter adjustments.

| **Case** | **Variable** | $\boldsymbol{max\lvert\tilde{D}\rvert}$ | $\boldsymbol{avg\lvert\tilde{D}\rvert}$ |
|---|---|---|---|
| **Without parameter adjustment** | Capture ratio [%] | 8.40 | 1.38 |
| | Flow of CO2 from condenser $[\frac{kg}{h}]$ | 6.60 | 0.59 |
| | Absorber temperature $[°C]$ | 1.90 | 0.31 |
| | Concentration of CO2 in top of absorber [%] | 0.58 | 0.11 |
| **With parameter adjustment** | Capture ratio [%] | 9.11 | 0.15 |
| | Flow of CO2 from condenser $[\frac{kg}{h}]$ | 6.52 | 0.15 |
| | Absorber temperature $[°C]$ | 1.92 | 0.07 |
| | Concentration of CO2 in top of absorber [%] | 0.58 | 0.01 |

One may also notice that neither the original model response nor the temporary model fits perfectly to the instrumental measurements across the whole simulation horizon, even with parameter adjustment. In addition, one may see that the

responses in mass flow of $CO_2$ vapour from condenser and the temperature in the absorber column exhibits spikes in the solution which are not present in the measurement. These are most likely caused by the rapid changes in inlet composition of $CO_2$ in the flue gas. However, as the model will be used with a large time horizon in the optimisation problem, such disturbances causing rapid changes will not be significant.

Eigenvalue analysis of the reduced unit model of the heat exchanger gave the results in Table 4.5, whereas the results of the eigenvalue analysis of the complete temporary model may be seen in Table 4.6. As one may see comparing to the results for the original unit model of the heat exchanger in Table 4.2, did the introduction of control volumes in the heat exchanger increase the spread of the eigenvalues somewhat. However, the results in Table 4.6 suggests that the replacement of the original heat exchanger unit model with the reduced unit model in the complete model did little to the stiffness of the complete model. The SR in sample 80 and 1000 reduced slightly compared to the original in Table 4.3, on the other hand, did the SR in samples 3000 and 4000 increase slightly. Nevertheless, all the SR's are much larger than one, and the complete model is consequently still very stiff.

Table 4.5: Result of eigenvalue analysis of the reduced heat exchanger unit model

| **Model** | **max** $\lvert\Re(\lambda_i)\rvert$ | **min** $\lvert\Re(\lambda_i)\rvert$ | **SR** |
|---|---|---|---|
| Reduced heat exchanger | 0.022 | 0.002 | 10.8 |

Table 4.6: Result of the eigenvalue analysis of the temporary model with the reduced unit model for the heat exchanger. Analysed at different samples in the data set provided by SINTEF

| **Sample** | **max** $\lvert\Re(\lambda_i)\rvert$ | **min** $\lvert\Re(\lambda_i)\rvert$ | **SR** |
|---|---|---|---|
| 80 | $5.29{\cdot}10^{3}$ | $3.60{\cdot}10^{-6}$ | $1.47{\cdot}10^{9}$ |
| 1000 | $5.31{\cdot}10^{3}$ | $4.67{\cdot}10^{-6}$ | $1.14\cdot10^{9}$ |
| 3000 | $5.40{\cdot}10^{3}$ | $5.69{\cdot}10^{-5}$ | $1.46{\cdot}10^{8}$ |
| 4000 | $5.36{\cdot}10^{3}$ | $3.99{\cdot}10^{-5}$ | $1.34{\cdot}10^{8}$ |

The model reductions for the heat exchanger did not result in reduction of state space of the complete model, which therefore still has 448 states. However, the simulation time of the ballistic simulation in Modelfit became $\approx$ 24 seconds, which

is a reduction of 7.7%. This suggests that the calculation of the heat exchanger response has simplified, and that the slight increase in stiffness did not influence the simulation time.

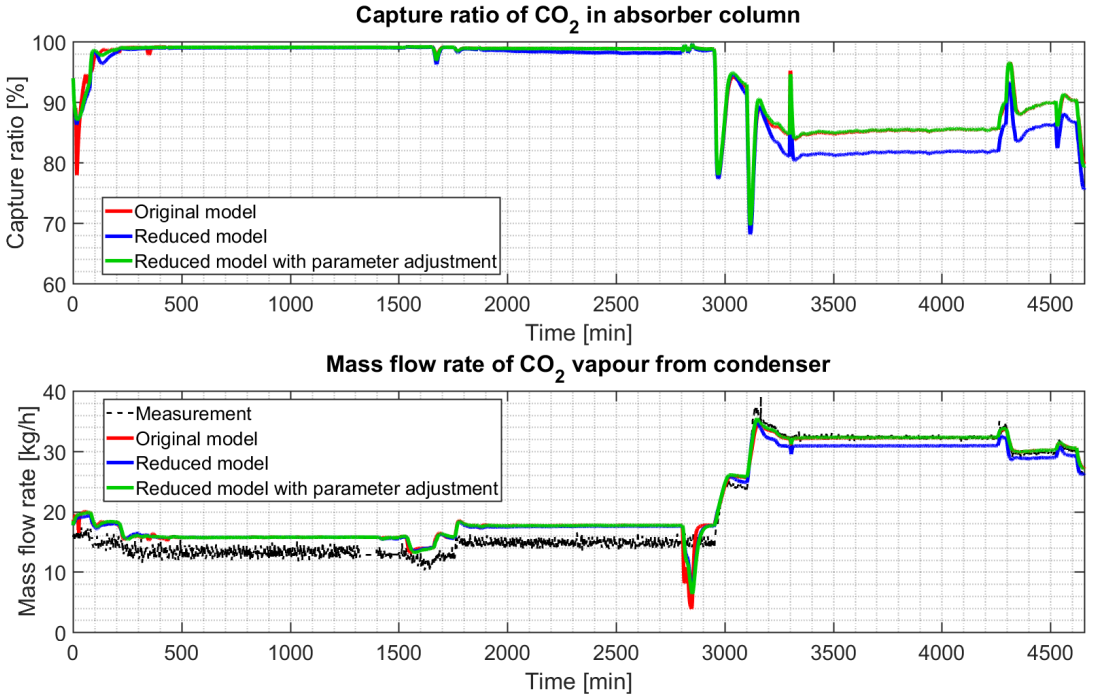


Figure 4.2: Response of the capture ratio in the absorber column and mass flow of $CO_2$ from the condenser in the temporary model with the reduced heat exchanger model substituted for the original unit model. Response compared to the original model and instrumental measurements.

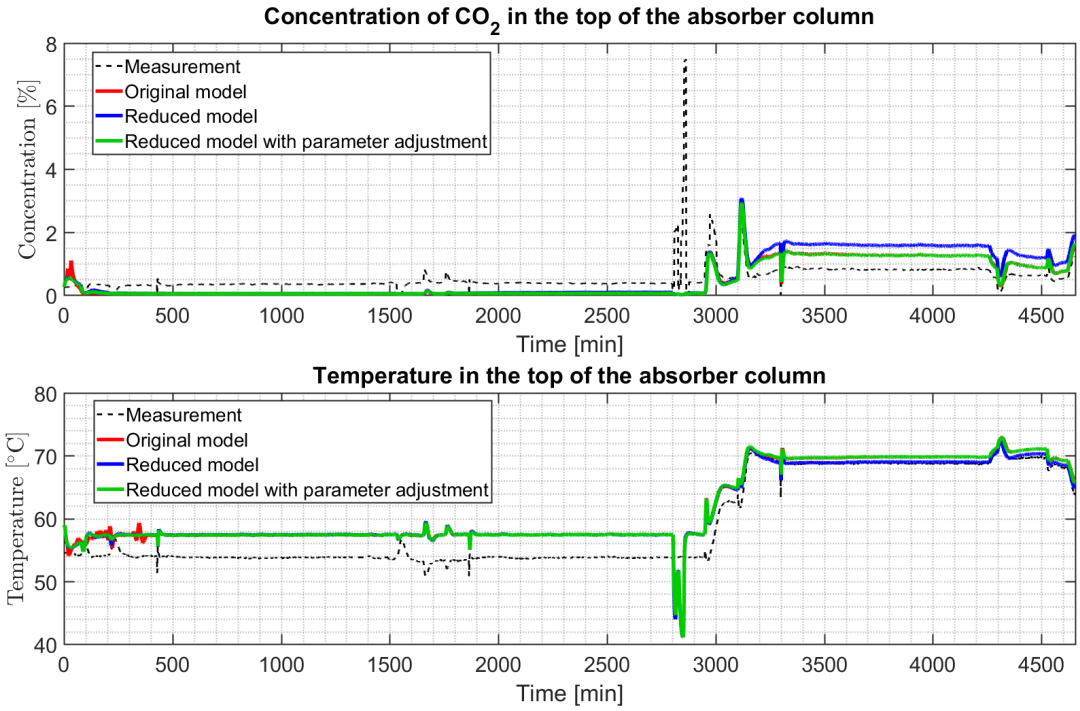


Figure 4.3: Response of the concentration of $CO_2$ and temperature in the top of absorber column in the temporary model with the reduced heat exchanger model substituted for the original unit model. Response compared to the original model and instrumental measurements.

## 4.2 Validation of the temporary model with the reduced absorber

The result of the ballistic simulations for the temporary model with only the reduced absorber unit model substituted for the original may be seen in Figures 4.4 and 4.5 and Table 4.7. Even though Hotvedt (2017) found that a number of control volumes of $n = 10$ was sufficiently accurate in the absorber, a number of control volumes of $n = 40$ was also tested in order to see if increasing the number of control volumes would affect the results.

Table 4.7: Maximum and average deviation of the capture ratio, mass flow of $CO_2$ from condenser, absorber temperature and $CO_2$ concentration in the top of the absorber comparing the temporary model with reduced absorber against the original model. Without and with parameter adjustments.

| **Case** | **Variable** | $\boldsymbol{max\lvert\tilde{D}\rvert}$ | $\boldsymbol{avg\lvert\tilde{D}\rvert}$ |
|---|---|---|---|
| **Without parameter adjustment n = 10** | Capture ratio [%] | 27.14 | 2.43 |
| | Flow of CO2 from condenser $[\frac{kg}{h}]$ | 10.99 | 0.52 |
| | Absorber temperature $[^\circ C]$ | 15.91 | 9.11 |
| | Concentration of CO2 in top of absorber [%] | 2.57 | 0.15 |
| **Without parameter adjustment n = 40** | Capture ratio [%] | 28.99 | 1.76 |
| | Flow of CO2 from condenser $[\frac{kg}{h}]$ | 8.65 | 1.78 |
| | Absorber temperature$[^\circ C]$ | 11.21 | 1.29 |
| | Concentration of CO2 in top of absorber [%] | 2.52 | 0.52 |
| **With parameter adjustment n = 10** | Capture ratio [%] | 29.45 | 1.46 |
| | Flow of CO2 from condenser $[\frac{kg}{h}]$ | 11.17 | 0.42 |
| | Absorber temperature$[^\circ C]$ | 16.37 | 8.93 |
| | Concentration of CO2 in top of absorber [%] | 2.83 | 0.10 |

As may be seen from the figures, only the response for the temperature in the absorber, bottom figure in Figure 4.5, yielded a better fit to the original model using $n = 40$ than $n = 10$ with or without parameter adjustment. However, considering the instrumental measurements, may one see that using $n = 40$ improved both the response of the mass flow rate of $CO_2$ from the condenser and the temperature in the absorber column. On the other hand, the response with $n = 40$ seems to be overestimating the concentration of $CO_2$ in the absorber column. Considering the average deviations in Table 4.7, may one see that besides from the temperature in the absorber column, using $n = 10$ in addition to parameter adjustment yielded somewhat better results to the original model than using $n = 40$. Consequently as it is of more importance the mass flow rate of $CO_2$ from the condenser to yield high accuracy, in addition to desiring a less complex state space, the solution with $n = 10$ and parameter adjustment seem sufficient. If the temperature in the absorber column was of more importance, a bias updating

for the temperature could be introduced to account for the large deviation using $n = 10$. The end parameter adjustment for the best fit became $\hat{h}_{hex,red} = 0.55$ and K-factor$_{CO_2,abs,red} = 1$ where the original K-factor$_{CO_2,abs,red} = 0.7$. One may additionally notice that the "spikes" in the solution are smoothed out, yielding less rapid changes.

The eigenvalue analysis of the reduced unit model of the absorber may be seen in Table 4.8 and the analysis of the temporary model with only the reduced unit model for the absorber substituted gave the results in Table 4.9. Comparing to result of the original unit model for the absorber in Table 4.2, one may see that the introduction of control volumes largely increased the stiffness of the system. From the results in Table 4.9 however, may one see that the reduced model of the absorber in the temporary model fortunately did not make much of a difference in terms of the stiffness compared to the original model. On the other hand, notice that the largest SR from the original in Table 4.3, sample 80 has been reduced. Even so, as the SR's are all much larger than unity is the total model still extremely stiff.

Table 4.8: Result of eigenvalue analysis of the reduced absorber unit model

| **Model** | **max** $\lvert\Re(\lambda_i)\rvert$ | **min** $\lvert\Re(\lambda_i)\rvert$ | **SR** |
|---|---|---|---|
| Reduced absorber | 7.20 | $9.04{\cdot}10^{-7}$ | $7.96{\cdot}10^{6}$ |

Table 4.9: Result of the eigenvalue analysis of the temporary model with the reduced unit model for the absorber. Analysed at different samples in the data set provided by SINTEF

| **Sample** | **max** $\lvert\Re(\lambda_i)\rvert$ | **min** $\lvert\Re(\lambda_i)\rvert$ | **SR** |
|---|---|---|---|
| 80 | $5.32{\cdot}10^{3}$ | $2.11{\cdot}10^{-6}$ | $2.52{\cdot}10^{9}$ |
| 1000 | $5.33{\cdot}10^{3}$ | $9.96{\cdot}10^{-7}$ | $5.25\ {\cdot}10^{9}$ |
| 3000 | $5.41{\cdot}10^{3}$ | $6.10{\cdot}10^{-6}$ | $8.86{\cdot}10^{8}$ |
| 4000 | $5.43{\cdot}10^{3}$ | $4.74{\cdot}10^{-6}$ | $1.15{\cdot}10^{9}$ |

Even though the reduced unit model for the absorber did not decrease the stiffness of the complete model significantly, was the state space complexity drastically reduced to 295 states, with the number of control volumes set to 10, compared to the original of 448 states. In addition were there a large reduction in simulation time of the ballistic simulation, $\approx 10$ seconds, a reduction of 61.5%. As the stiffness

is insignificantly reduced, is the smaller simulation time probably caused by the reduced state space in addition to the simplification of using control volumes instead of the collocation method as the results from Section 4.1 also suggests.

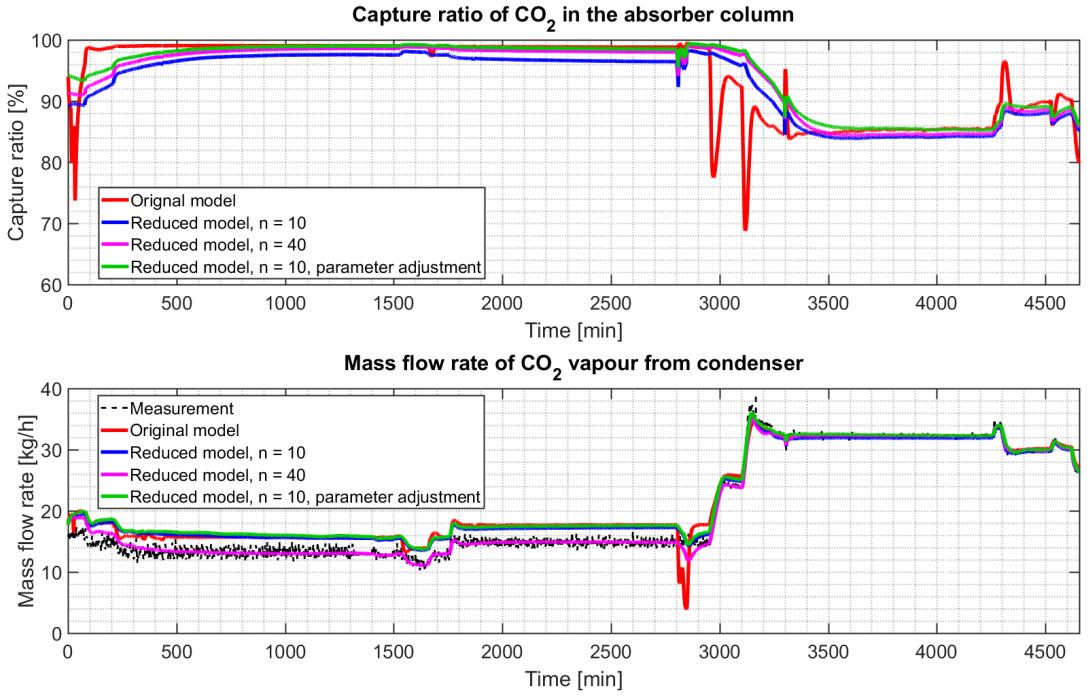


Figure 4.4: Response of the capture ratio in the absorber column and mass flow of $CO_2$ from the condenser in the temporary model with the reduced absorber model substituted for the original unit model. Response compared to the original model and instrumental measurements.

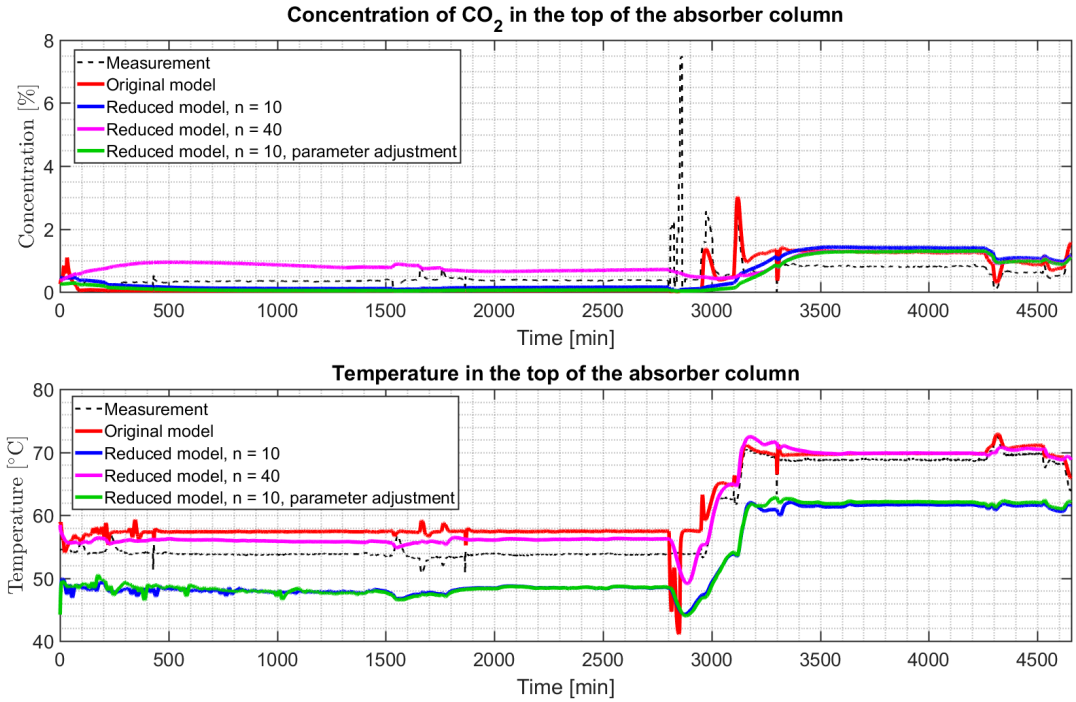


Figure 4.5: Response of the concentration of $CO_2$ and temperature in the top of absorber column in the temporary model with the reduced absorber model substituted for the original unit model. Response compared to the original model and instrumental measurements.

## 4.3 Validation of the temporary model with the reduced desorber

The reduced unit model for the desorber was also substituted separately into the original model and the results may be seen in Figures 4.6 and 4.7 in addition to Table 4.10.

Table 4.10: Maximum and average deviation of the capture ratio, mass flow of $CO_2$ from condenser, absorber temperature and $CO_2$ concentration in the top of the absorber comparing the temporary model with reduced desorber against the original model. Without and with parameter adjustments.

| **Case** | **Variable** | $\boldsymbol{max\lvert\tilde{D}\rvert}$ | $\boldsymbol{avg\lvert\tilde{D}\rvert}$ |
|---|---|---|---|
| **Without parameter adjustment n = 10** | Capture ratio [%] | 13.69 | 6.36 |
| | Flow of CO2 from condenser $[\frac{kg}{h}]$ | 4.52 | 1.90 |
| | Absorber temperature $[^\circ C]$ | 4.60 | 1.16 |
| | Concentration of CO2 in top of absorber [%] | 1.07 | 0.41 |
| **Without parameter adjustment n = 40** | Capture ratio [%] | 12.87 | 5.63 |
| | Flow of CO2 from condenser $[\frac{kg}{h}]$ | 6.51 | 1.78 |
| | Absorber temperature$[^\circ C]$ | 4.51 | 1.05 |
| | Concentration of CO2 in top of absorber [%] | 1.11 | 0.38 |
| **With parameter adjustment n = 10** | Capture ratio [%] | 11.42 | 3.18 |
| | Flow of CO2 from condenser $[\frac{kg}{h}]$ | 4.10 | 1.01 |
| | Absorber temperature$[^\circ C]$ | 3.64 | 0.64 |
| | Concentration of CO2 in top of absorber [%] | 0.60 | 0.21 |

As one may see, both the average and maximum deviation decreased after adjusting the parameters, however, it was harder to adjust the parameters such that the response fit well. What may also be seen is that increasing the number of control volumes to $n = 40$ did not improve the results of the four variables investigated. Consequently, for a better fit of the capture ratio and mass flow rate of $CO_2$ from the condenser, bias updating would be necessary. The end parameter adjustment became $\hat{h}_{hex,red} = 2$ whilst the K-factors were unchanged from their original values.

The result of the eigenvalue analysis of the reduced unit model for desorber may be found in Table 4.11 whereas the result for the temporary model with only the reduced unit model for desorber substituted may be seen in Table 4.12. As in Section 4.2 did the use of control volumes increase the stiffness of the desorber unit model largely, but decreased the large SR in sample 80 in the temporary

model compared to the original model.

Table 4.11: Result of eigenvalue analysis of the reduced unit model for desorber

| **Unit** | **max** $\lvert\Re(\lambda_i)\rvert$ | **min** $\lvert\Re(\lambda_i)\rvert$ | **SR** |
|---|---|---|---|
| Reduced desorber | 35.0 | $1.31{\cdot}10^{-4}$ | $2.67{\cdot}10^{5}$ |

Table 4.12: Result of the eigenvalue analysis of the temporary model with the reduced unit model for the desorber. Analysed at different samples in the data set provided by SINTEF

| **Sample** | **max** $\lvert\Re(\lambda_i)\rvert$ | **min** $\lvert\Re(\lambda_i)\rvert$ | **SR** |
|---|---|---|---|
| 80 | $5.35{\cdot}10^{3}$ | $2.24{\cdot}10^{-6}$ | $2.39{\cdot}10^{9}$ |
| 1000 | $5.35{\cdot}10^{3}$ | $2.05{\cdot}10^{-6}$ | $2.62\ {\cdot}10^{9}$ |
| 3000 | $5.44{\cdot}10^{3}$ | $2.69{\cdot}10^{-5}$ | $2.02{\cdot}10^{8}$ |
| 4000 | $5.52{\cdot}10^{3}$ | $2.09{\cdot}10^{-5}$ | $2.64{\cdot}10^{8}$ |

The reduced unit model for the desorber, with $n = 10$, decreased the state space complexity of the complete model to 376 states compared to 448 in the original. The simulation time also decreased to $\approx$ 17 seconds, a reduction of 34.6%.

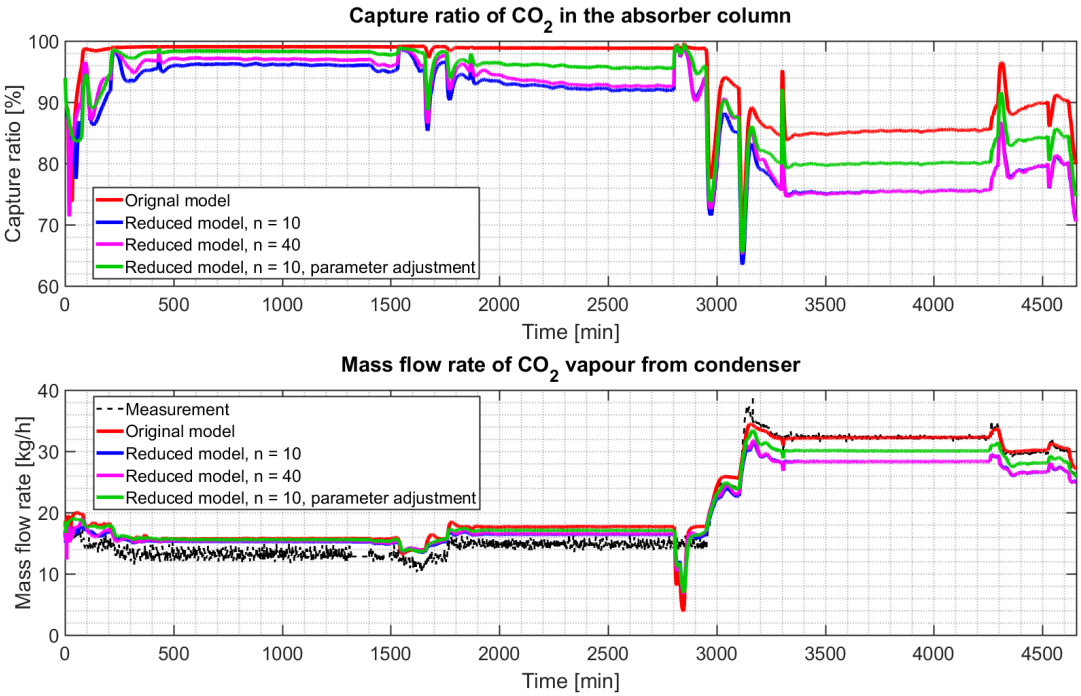


Figure 4.6: Response of the capture ratio in the absorber column and mass flow of $CO_2$ from the condenser in the temporary model with the reduced desorber model substituted for the original unit model. Response compared to the original model and instrumental measurements.

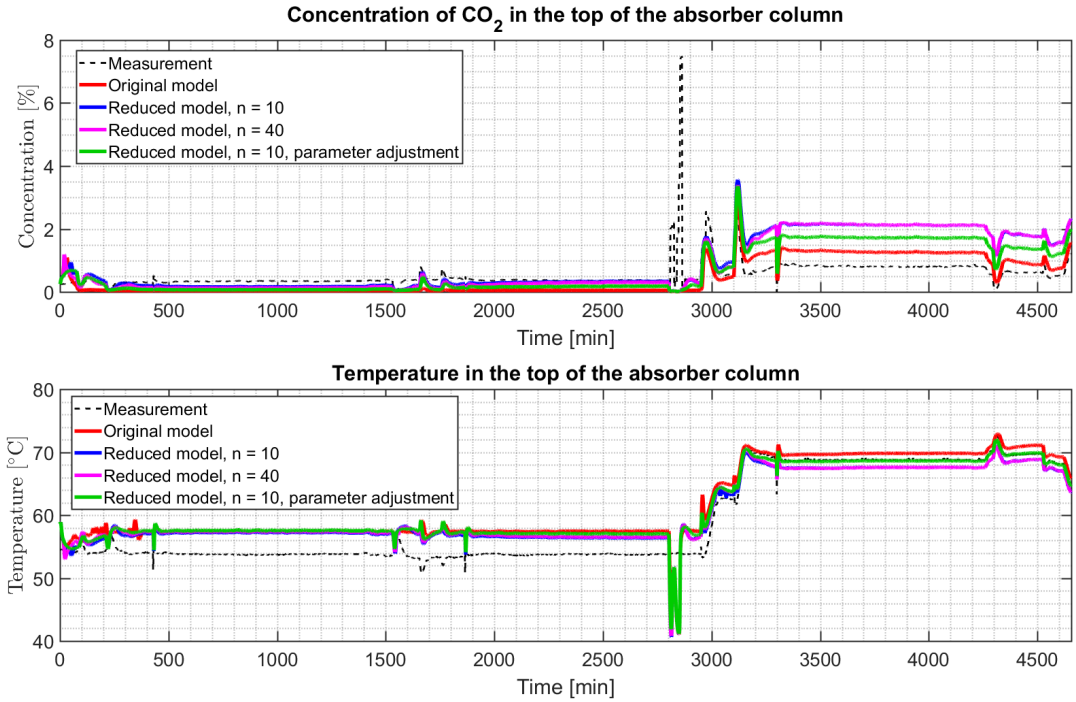


Figure 4.7: Response of the concentration of $CO_2$ and temperature in the top of absorber column in the temporary model with the reduced desorber model substituted for the original unit model. Response compared to the original model and instrumental measurements.

## 4.4 Validation of the complete reduced model

Finally, the complete reduced model was tested using the same data set as before, and the results may be seen in Figures 4.8 and 4.9, and Table 4.13. In this simulation the number of control volumes in the absorber and desorber was set to $n_{abs} = n_{des} = 10$, and the heat exchanger as previously, $n_{hex} = 1$. Similarly to the results in Section 4.3, did parameter adjustment decrease all of the average deviations even though a complete match was difficult to obtain. The end parameter adjustment became $\hat{h}_{hex,red} = 2$, K-factor$_{CO_2,abs,red} = 4$ and K-factor$_{CO_2,des,red} = 2$. However, increasing the $CO_2$ K-factors this much may

cause additional stiffness in the system as their ideal values are unity. Therefore, may bias updating be beneficial to remove modelling errors instead of increasing the K-factors above unity.

Table 4.13: Maximum and average deviation of the capture ratio, mass flow of $CO_2$ from condenser, absorber temperature and $CO_2$ concentration in the top of the absorber comparing the complete reduced model against the original model. Without and with parameter adjustments.

| **Case** | **Variable** | $\boldsymbol{max\lvert\tilde{D}\rvert}$ | $\boldsymbol{avg\lvert\tilde{D}\rvert}$ |
|---|---|---|---|
| **Without parameter adjustment** | Capture ratio [%] | 27.68 | 11.21 |
| | Flow of CO2 from condenser $[\frac{kg}{h}]$ | 11.10 | 3.18 |
| | Absorber temperature $[°C]$ | 14.63 | 8.96 |
| | Concentration of CO2 in top of absorber [%] | 1.87 | 0.71 |
| **With parameter adjustment** | Capture ratio [%] | 25.25 | 2.32 |
| | Flow of CO2 from condenser $[\frac{kg}{h}]$ | 12.63 | 0.85 |
| | Absorber temperature $[°CWi]$ | 14.82 | 7.47 |
| | Concentration of CO2 in top of absorber [%] | 2.38 | 0.17 |

The eigenvalue analysis of the complete reduced model gave the results in Table 4.14. As the unit models insignificantly changed the stiffness when substituted into the complete model, Sections 4.1-4.3, the results found was expected. Similar to before, has the SR in sample 80 been reduced but the other SR's increased. Consequently, other unit models in the complete model are probably causing the large stiffness, for instance the reboiler or condenser. On the other hand, one must keep in mind that the samples chosen for investigation may not be representative in all operating modes. As the reduction in stiffness is negligible, will CVODE be used as integration routine when solving the reduced model in optimisation in Chapter 5.

It found simulating that Modelfit used $\approx 7$ seconds on the complete simulation, which is reduction in simulation time of 73.1% from the original. The introduction of all the model reductions suggested by Hotvedt (2017) resulted in the reduced model having 223 states compared to the 448 states of the original model. It was mentioned in Section 2.2 that solving a system using CVODE may be time consuming if the state space is large. Therefore, the decrease in simulation time is

Table 4.14: Result of the eigenvalue analysis of the complete reduced model at different samples in the data set provided by SINTEF

| **Sample** | **max** $\lvert\Re(\lambda_i)\rvert$ | **min** $\lvert\Re(\lambda_i)\rvert$ | **SR** |
|---|---|---|---|
| 80 | $5.34{\cdot}10^{3}$ | $1.43{\cdot}10^{-6}$ | $3.74{\cdot}10^{9}$ |
| 1000 | $5.33{\cdot}10^{3}$ | $7.87{\cdot}10^{-7}$ | $6.78\ {\cdot}10^{9}$ |
| 3000 | $5.43{\cdot}10^{3}$ | $3.25{\cdot}10^{-6}$ | $1.67{\cdot}10^{9}$ |
| 4000 | $5.48{\cdot}10^{3}$ | $2.18{\cdot}10^{-6}$ | $2.52{\cdot}10^{9}$ |

most likely caused by the reduced state space, in addition to the simplification of using control volumes for spatial discretization instead of the collocation method. Conclusively, as the simulation time drastically reduced, the reduced model is better suitable for online optimisation than the original model, even though the stiffness of the complete model was insignificantly changed. A table summarising the reduction in state space complexity and the simulation time for the different temporary models with only one unit model substituted in addition to the original model and the reduced model may be found in Table 4.15.

Table 4.15: Overview of state space dimension, simulation time and reduction of simulation time of the different temporary and complete models

| **Model** | **Dimension** | **Simulation time [s](red. [%])** |
|---|---|---|
| Original | 448 | $\approx 26$ |
| Temporary model w. red. heat exchanger | 448 | $\approx 24$ (7.7) |
| Temporary model w. red. absorber | 295 | $\approx 10$ (61.5) |
| Temporary model w. red. desorber | 376 | $\approx 17$ (34.6) |
| Total reduced | 223 | $\approx 7$ (73.1) |

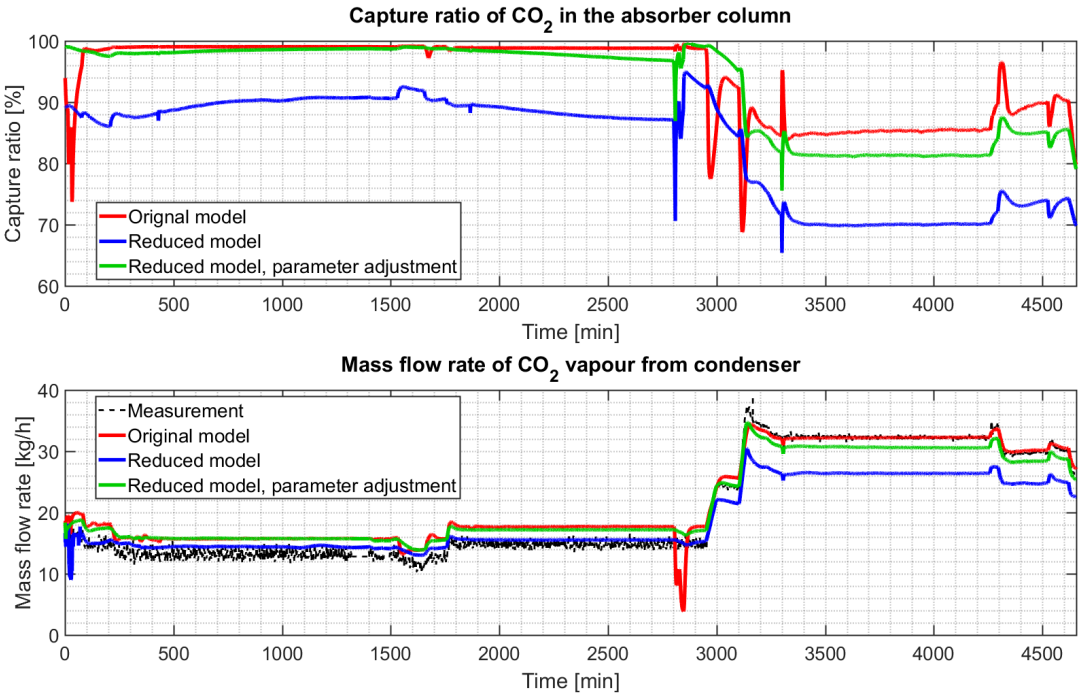


Figure 4.8: Response of the capture ratio in the absorber column and mass flow of $CO_2$ from the condenser in the complete reduced model. Response compared to the original model and instrumental measurements.

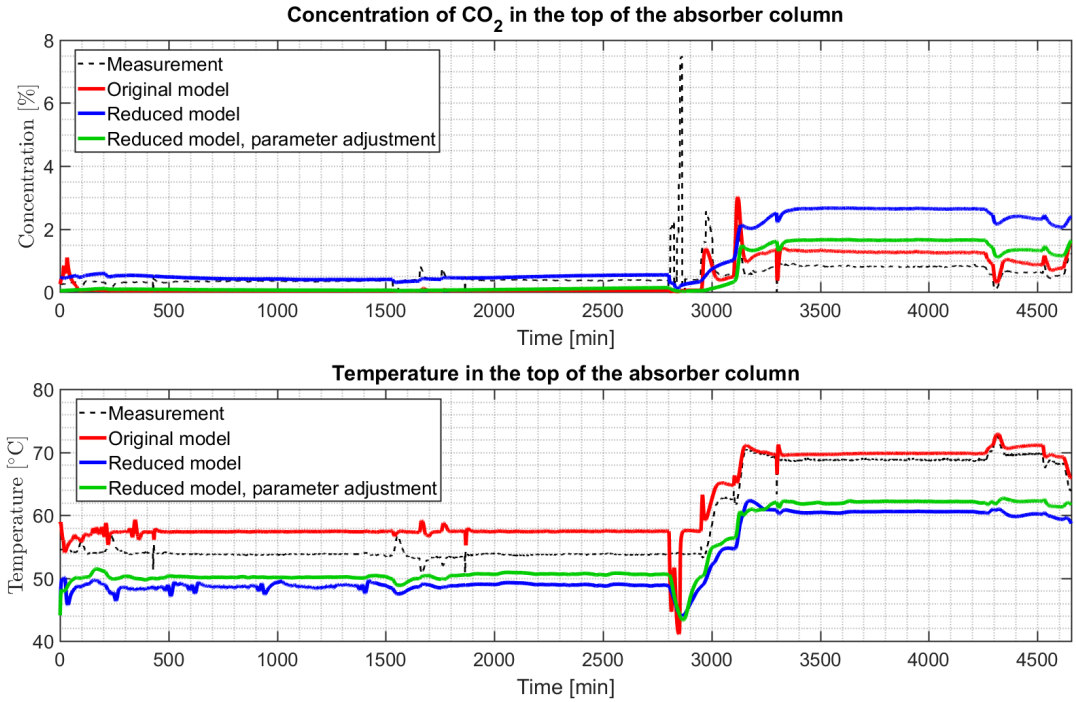


Figure 4.9: Response of the concentration of $CO_2$ and temperature in the top of absorber column in the complete reduced model. Response compared to the original model and instrumental measurements.

## 4.5 Reduced model response with bias updating

As mentioned in the beginning of Chapter 4, a Kalman Filter for parameter adjustment has not been experimented with due being time consuming and very complex. However, as mentioned may a simple estimator such as bias updating be introduced instead to reduce modelling errors, see Section 2.3 for explanation of bias updating. An example of this is bias updating using the measurement of the mass flow of $CO_2$ from the condenser. Notice how in Section 4.4, Figure 4.8 the response for mass flow of $CO_2$ from the condenser in the reduced model show a deviation from the original model response and measurement. Inclusion of bias updating however, results in the responses in Table 4.16 and Figures 4.10

and 4.11. The original model and the reduced model responses for the mass flow from condenser fits better with the measurement. The bias updating is further used to update the capture ratio and the concentration of $CO_2$ in the top of the absorber column, however only the capture ratio in the reduced model show significant better fit to the original model. Notice, comparing Figure 4.9 to Figure 4.11 that it seems that the concentration of $CO_2$ in the top of the absorber is updated too much as both the original and reduced model responses now lies above the measurement and not below. Further, there are no noticeable changes in the absorber temperature. Comparing the maximum and average absolute deviation with bias updating in Table 4.16 to the complete reduced model in Section 4.4, Table 4.13 may one see that the average absolute deviation for all variables, except the temperature in the absorber, are highly improved and yields even less deviation than the results for the complete reduced model with parameter adjustments. The still large maximum absolute deviation is most likely due to the rapid disturbances in the responses. This suggest that bias updating using only one measurement may not remove modelling errors in all variables, and in fact induce new errors. Consequently, should bias updating with several measurements be experimented with for sufficient reduction of modelling errors in all states. As mentioned in Section 2.3, may therefore a Kalman Filter be beneficial in such circumstances because it may automatically determine which states or parameters needs updating analysing all available measurements. Experimentation with Kalman Filter however, will be a topic of future work with the reduced model.

Table 4.16: Maximum and average deviation of the capture ratio, mass flow of $CO_2$ from condenser, absorber temperature and $CO_2$ concentration in the top of the absorber comparing the complete reduced model against the original model. With bias updating from measurements of the mass flow of $CO_2$ from the condenser.

| **Case** | **Variable** | $\boldsymbol{max\|\tilde{D}\|}$ | $\boldsymbol{avg\|\tilde{D}\|}$ |
|---|---|---|---|
| **With bias updating** | Capture ratio [%] | 29.54 | 1.20 |
| | Flow of CO2 from condenser $[\frac{kg}{h}]$ | 11.68 | 0.55 |
| | Absorber temperature $[°C]$ | 14.64 | 8.97 |
| | Concentration of CO2 in top of absorber [%] | 1.92 | 0.08 |

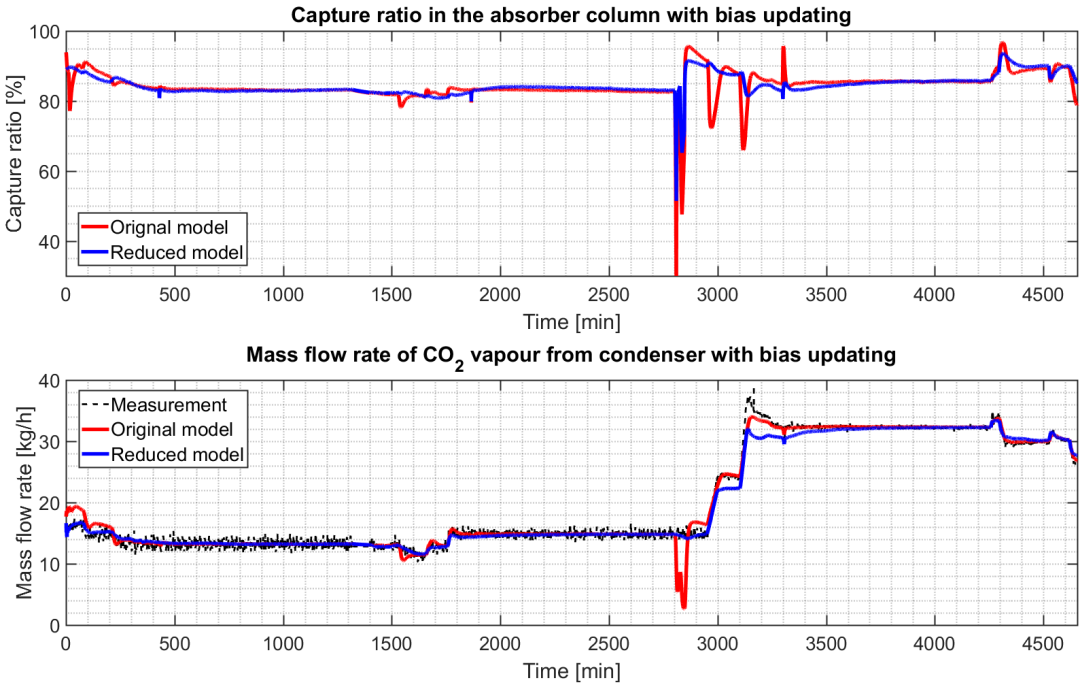


Figure 4.10: Response of the capture ratio in the absorber column and mass flow of $CO_2$ from the condenser in the reduced model where bias updating has been included. Response compared to the original model and instrumental measurements.

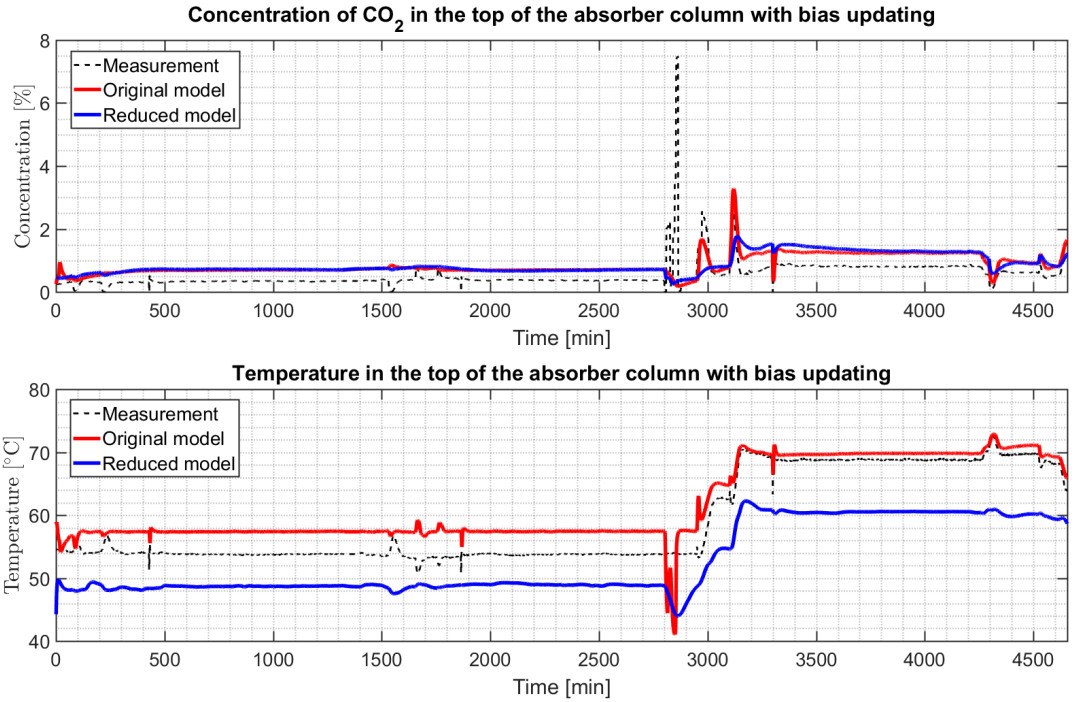


Figure 4.11: Response of the concentration of $CO_2$ and temperature in the top of absorber column in the complete reduced model where bias updating has been included. Response compared to the original model and instrumental measurements.

# Chapter 5

# Simulation results from optimisation

The optimisation problem that has be set up in this thesis is a Dynamic Real-Time Optimisation problem, which utilises single-level Nonlinear Model Predictive Control with both economic and regulatory objectives in the objective function. This type of controller is described in Section 2.3.2. The dynamic model in the optimisation problem has been the complete reduced model of the Tiller facility which was validated against the original model in Chapter 4. The algorithm has been designed such that the total cost related to the energy consumption in the reboiler is minimised, while an overall, or accumulated, capture ratio ($\text{CR}_{acc}$) should reach a minimum specified reference, $\text{CR}_{acc}^{ref}$, after 24 hours. These two variables will be controlled variables in the optimisation problem, and has been defined as follows, in equation 5.1.

$$\begin{aligned} CR_{acc} &= 100 \cdot \frac{\int_0^k (F_{g,abs,CO_2,in} - F_{g,abs,CO_2,out})dt}{\int_0^k F_{g,abs,CO_2,in}dt} \\ \text{Cost} &= \int_0^k \psi \cdot RDdt \end{aligned} \tag{5.1}$$

$\psi$ is here the price of energy in $[\frac{NOK}{kWs}]$, RD is the reboiler duty in $[kW]$ and $k$ is the current sample. Notice that, due to only being interested in the result after 24 hours, one evaluation point for both the cost and the $\text{CR}_{acc}$ will be needed and may be placed 24 hours ahead. However, as the prediction horizon $N$ is receding in an standard (N)MPC controller, the evaluation point will be

moving in time. The way to achieve the evaluation point at precisely $k = 24h$ is therefore by "freezing" the controlled variables at this point in time. That is, after simulating 24 hours, the updating of $\mathrm{CR}_{acc}$ and cost is stopped. Consequently, even though the optimisation problem operates with a receding horizon, the effect will be that of a shrinking horizon which shrinks by one time sample each sample $N_{k+1} = N_k - \Delta k$.

By having the optimisation problem focusing on the accumulated $CO_2$ capture ratio after 24 hours, a flexible mode is established in which the regeneration of MEA, and thus the instantaneous capture ratio (CR), defined in Chapter 4 equation 4.2, may vary during the prediction horizon. The algorithm may consequently utilise the knowledge of a daily varying price of energy and alter the regeneration of MEA correspondingly. During high peaks of the energy price, less regeneration may be performed such that less energy is used, inducing lower costs. More MEA regeneration may hence be performed in low peaks of the electricity price to keep the accumulated capture ratio at a certain percentage after 24 hours. However, the instantaneous CR should stay within certain bounds for optimal controlling. A too low CR may cause an unwanted shutdown of the facility that require large amounts of energy for start-up. Furthermore, an instantaneous capture ratio close to 100% increases the uncertainty of the model and might induce inconvenient large modelling errors. Consequently, a lower and upper constraint of CR(min,max) = (75,96)% have been introduced to prevent such conditions.

Two manipulated variables have been chosen to optimise for optimisation; the reboiler duty (RD) and the mass flow of lean amine into the absorber, $F_{l,abs}$. By the use of these two MV's, will there exist an optimal combination such that the reboiler duty may be minimised as much as possible but still achieve the regulatory goal. As explained in Section 2.3, input blocking will be used to decrease the degrees of freedom of the optimisation problem. The price of energy changes every hour during the day and ideally should therefore 24 input blocks be applied. However, it was found during simulations that 12 input blocks evenly spread throughout the day yielded adequate responses. The time between each input block will therefore be 2 hours, and thus should first-order hold instead of zero-order hold be utilised as described in Section 2.3. The initial point used for all simulation cases of the optimisation problem is a known steady-state solution with a capture ratio of $\approx 95\%$. One may argue that the initial point rather should be an endpoint of a previous simulated case where the system reached its reference value. However, this initial point along with the needed inputs were provided by *Cybernetica AS* and as long as all simulation cases uses the same initial point, they may be compared to each other and conclusions may be established. An overview of the CV's and MV's used in the DRTO along with their initial values,

may be found in Table 5.1.

Table 5.1: Overview of manipulated and controlled variables in the optimisation problem

| | **Variable** | **Abbreviation** | **Unit** | **Initial** |
|---|---|---|---|---|
| **MV** | Reboiler duty | RD | kW | 19.3 |
| | Mass flow of lean amine into absorber | $F_{l,abs}$ | $\frac{\text{kg}}{\text{min}}$ | 4.97 |
| **CV** | Accumulated Capture Ratio of CO2 in absorber column | $\text{CR}_{acc}$ | % | 94.8 |
| | Total energy costs | Cost | NOK | 0 |
| | Capture Ratio | CR | % | 94.8 |

To make the variable energy price function authentic, data regarding the energy price in Trondheim, Norway, was collected from *Nord Pool, Market Data* (2018). The energy price will also be dependent on outside temperature. Therefore, were the energy prices for the hottest and coldest day ( *Yr*, 2018) from the period April 2017 to April 2018 in Trondheim selected for further analysis. The hourly varying price of these two days has been illustrated in Figure 5.1. As may be seen, the energy prices from the hottest day did not change the shape of the price function. Consequently, only the energy prices from the coldest day have been used in the optimisation. An outside algorithm predicting the day-by-day energy prices based on weather forecasts and previous data from *Nord Pool, Market Data* (2018) could be developed in order to make the optimisation problem even more authentic. Additionally could daily varying prices for $CO_2$ emissions also be included. An algorithm for energy price prediction is a suggestion for future work.

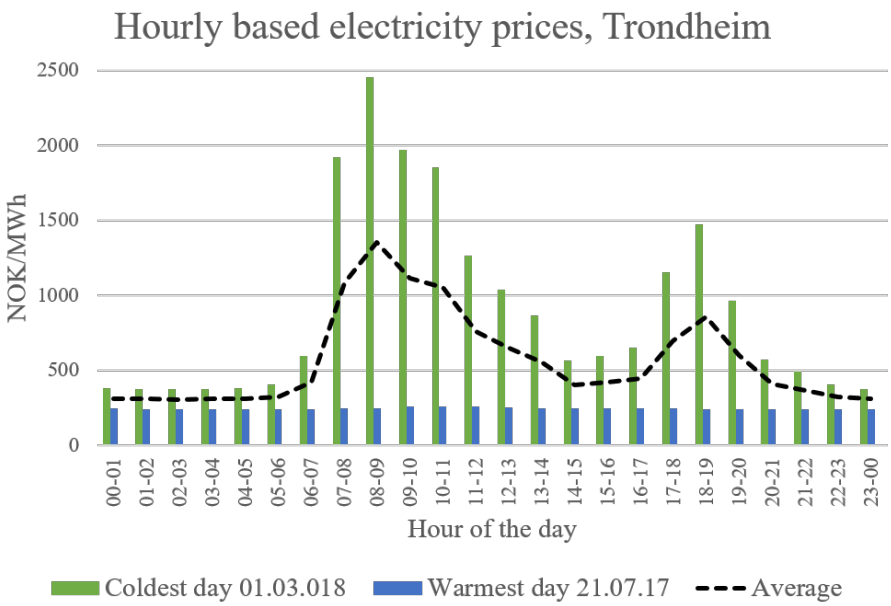


Figure 5.1: Illustration of a variable price of energy during 24 hours, data collected from *Nord Pool, Market Data* (2018)

Several variants of the optimisation problem have been tested. To be able conclude something about the performance of the DRTO with a varying degree of regeneration, has a base case using a fixed mode of operation also been implemented. In the fixed mode, the accumulated capture ratio has been forced constant throughout the simulation horizon, such that the MEA regeneration also remain constant. In addition has the cost been minimised as much as possible. Two different fixed values for the accumulated capture ratio were tested; 91% and 85%. Further description along with results of the cost for the base case may be found in Section 5.1. The idea behind comparing two different fixed mode scenarios against their corresponding flexible modes is that for the lower reference value, the DRTO will in the flexible mode be able to vary the CR to a much larger degree than for the higher reference value as the bounds on the CR is set to (75,96). Consequently, may the percentage decrease in cost be larger for the lower reference value scenario. Thus, the cases with the lower reference value will be an example of how much may be saved if allowing a somewhat smaller accumulated capture ratio than the often specified standard of more than 90%.

Both methods for the DRTO; infeasible soft-constraint and unreachable setpoints, explained in Section 2.3, were attempted for the flexible mode, however, it was found that the tuning related to the infeasible soft-constraint method required less effort. This is due to objective function having fewer quadratic weight penalties and more linear (exact) weight penalties, which makes it easier to compare the regulatory and economic objectives against each other. Setting the linear weights for the regulatory objectives sufficiently larger than for the economic objectives will ensure fulfilment of the regulatory objectives, while minimising the economic as much as possible. For the flexible mode simulations, has a solution been accepted if the end accumulated capture ratio was in the range $\mathrm{CR}_{acc}^{ref} \pm 0.2\%$ after 24 hours. The result of the infeasible soft-constraint method without disturbances and for fixed exhaust inlet conditions may be seen in Section 5.2. It is also of interest to see if the algorithm is robust enough to re-plan the optimal solution if abrupt changes in either the exhaust inlet conditions or the energy prices occur. Consequently, a simulation case where the composition of $CO_2$ in the exhaust gas increases has been performed and reported in Section 5.3 and a simulation case where the electricity price suddenly increases has been investigated in Section 5.4. In addition, one case where stricter physical constraints on the reboiler duty have been imposed, has been experimented with and may be seen in Section 5.5.

The optimisation cases have been simulated using *Cybernetica AS* software RealSim and CENIT. As mentioned in Chapter 3 has the original model been used in RealSim as a plant replacement model to simulate the facility. The results from Chapter 4 suggests that a bias updating using measurements is necessary if the reduced model should fit the responses of the original model. This may be introduced into the model, using the predicted measurements from RealSim. However, tuning of the controller will be simpler if measurements are disregarded and the model optimised based on the perfect model assumption, neglecting modelling errors. On the other hand, it is of importance to keep an eye on the values in the simulator in order to avoid a complete mismatch to the simulated facility. Consequently, will the $\mathrm{CR}_{acc}$ from RealSim be reported and compared to the results from CENIT to be certain that the facility's accumulated capture ratio is at least not lower than the reference value. On the other hand, is it of interest to see how the DRTO behaves under influence of bias updating and consequently has this been experimented with in Section 5.6. Furthermore, as explained in Section 1.3, is it assumed that the low-level controllers work perfectly. This means that the optimal MV trajectories calculated by CENIT will be implemented.

Through CENIT's MMI, may one analyse optimal predicted trajectories, history, current values and perform online adjustment of constants and tuning parameters. An example is illustrated in Figure 5.2 where both history, illustrated with negative time, and predicted trajectories, positive time, are visible. The values that have

already been implemented in the facility are values up until time zero, whereas the predictions are given from time zero and up until the complete receding prediction horizon $N$. Notice here, how the cost and $\mathrm{CR}_{acc}$ have been frozen after 24 hours of simulation time yielding a shrinking horizon effect. In Figure 5.2 this is approximately 17 hours into the future. However, the instantaneous CR and MV's have not been frozen and consequently, in Figure 5.2b, the CR after 17 hours into the future is not reflected in $\mathrm{CR}_{acc}$. However, the predictions after this point in time will not be considered in the objective function as the algorithm only optimises the problem during the first 24 hours. That is, each day is optimised isolated without regarding the solutions for the previous or the coming day.

A great amount of tuning was experimented with in order to achieve the goal of the optimisation problem. Not only have the weights for deviation penalisation in the controller been adjusted several times, but the number of input block's and evaluation points for sufficient response have been investigated. Common for all simulation cases described in the subsections below is the use of one QP iteration and at most 10 line searches in the SQP algorithm to solve the nonlinear problem. As explained in Section 2.3, are few QP iterations often accepted if the time between each sample is small. In all the simulation cases has a sample time of 3 minutes been utilised. On the other hand, a brief experimentation on increasing the number of QP iterations was performed out of curiosity. Increasing the number of QP iteration resulted, as expected, in the same optimal end result, although fewer samples where required before the algorithm settled at the optimal solution. This suggest that the SQP algorithm yields convergence towards optimum already in the first QP iteration. Consequently, as a larger number of QP iterations increased the solving time but did little to the end result, one QP iteration was used in the simulation cases. After finding the best possible combination of tuning parameters were the cases simulated throughout the simulation horizon without online adjustment.

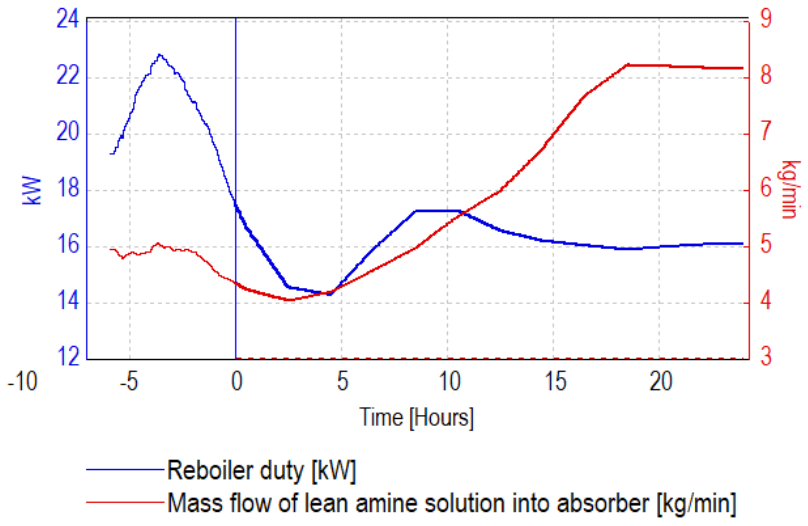


(a) Manipulated variables

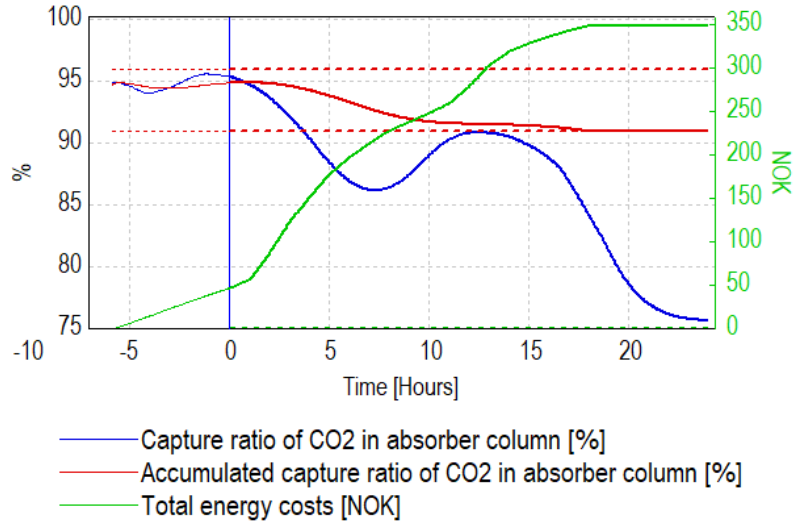


(b) Control Variables

Figure 5.2: Illustration of MV's and CV's with history and predictions from CENIT MMI. Negative time illustrates history whereas positive time are predictions into the future.

## 5.1 Fixed mode of operation

As mentioned, in order to analyse the performance of the DRTO, a base case using a fixed mode of operation has been established for comparison to the flexible mode investigated in Section 5.2. In the base case, the DRTO forces the accumulated capture ratio to stay at a reference value, $CR_{acc}^{ref}$, throughout the horizon whilst manipulating the reboiler duty and mass flow to minimise the cost. Two reference values were inspected; 91% and 85%. To achieve the goal of the base case, an infeasible soft-constraint method was utilised because it yielded only small fluctuations in the accumulated capture ratio compared to the unreachable setpoint method that was also attempted. Hence, the minimum and maximum constraint of the accumulated capture ratio was set to $CR_{acc}$(min,max) = ($CR_{acc}^{ref}$,$CR_{acc}^{ref}$) and violations penalised. To minimise the cost, Cost(min,max) = (0,0) was enforced. Decreasing the number of degrees of freedom, input blocking and control variable evaluation points, explained in Section 2.3, were also implemented. The input blocking was set equal for all MV's, the first change after 30 minutes and further every second hour. The CV evaluation points however, were chosen differently for the $CR_{acc}$ and the Cost, with the $CR_{acc}$ being evaluated every fourth hour, while the cost only evaluated after 24 hours. Additionally were the constraints on the CR applied to avoid shutdown and too high model uncertainties. The base case is summarised below.

Case: Basic

**Goal:**
Maintain an accumulated capture ratio of $\mathrm{CR}_{acc}^{ref}$ throughout horizon
Minimise Cost

**MV's:** RD, $F_{l,abs}$

**CV's:** $\mathrm{CR}_{acc}$, Cost, CR

**CV setpoints:**
N.A.

**CV constraints:**
$\mathrm{CR}_{acc}$: [$\mathrm{CR}_{acc}^{ref}$,$\mathrm{CR}_{acc}^{ref}$]
Cost: [0,0]
CR: [75,96]

**MV input blocking:**
RD: first after 30min, then every 2 h
$F_{l,abs}$: first after 30min, then every 2 h

**CV evaluation points:**
$\mathrm{CR}_{acc}$: every 4 hour
Cost: after 24 h
CR: every 4 hour

The results obtained for the base case using $\mathrm{CR}_{acc}^{ref} = 91\%$ may be seen in Figure 5.3. Figure 5.3b shows how the algorithm forces the instantaneous capture ratio to remain at 91% after an initial transient. Figure 5.3a illustrates how the reboiler duty and the mass flow were not able to vary much due to the strict $\mathrm{CR}_{acc}$ requirement. The end cost after 24 hours became $\mathrm{Cost}_N = 384$NOK. The result for $\mathrm{CR}_{acc}^{ref} = 85\%$ may be seen in Figure 5.4. Also here did the DRTO manage to keep the CR at 85% after initial transient. Notice how the RB and $F_{l,abs}$ have settled lower than for $\mathrm{CR}_{acc}^{ref} = 91\%$, which is expected. Resultantly, the cost became smaller and the end value became $\mathrm{Cost}_N = 353$NOK. The results for the two base cases are summarised in Table 5.2.

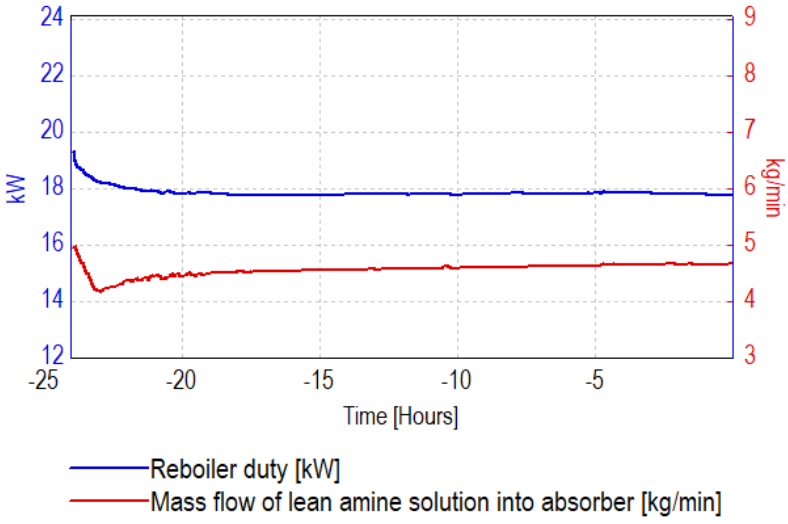


(a) Manipulated variables

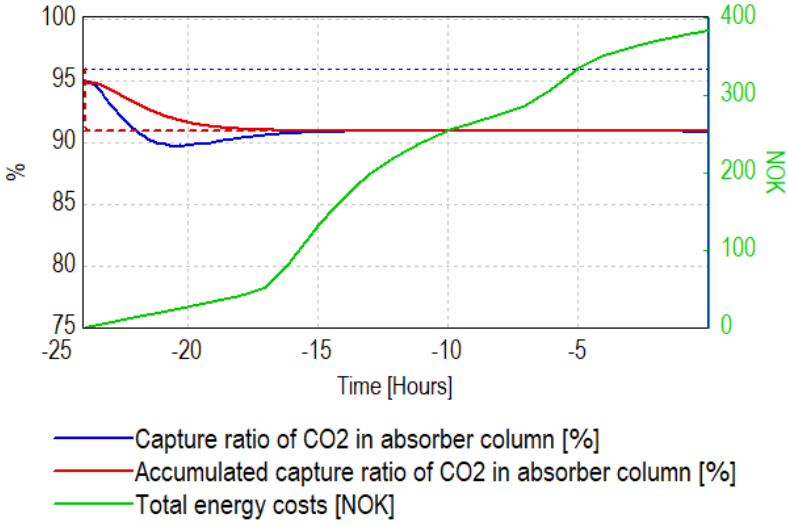


(b) Control Variables

Figure 5.3: Result of basic case where the accumulated capture ratio is held constant through the horizon after an initial transient. $\mathrm{CR}_{acc}^{ref} = 91\%$

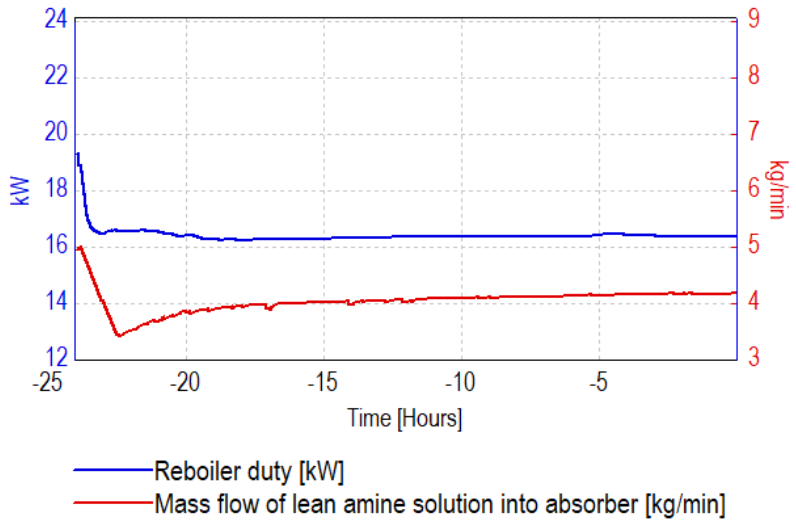


(a) Manipulated variables

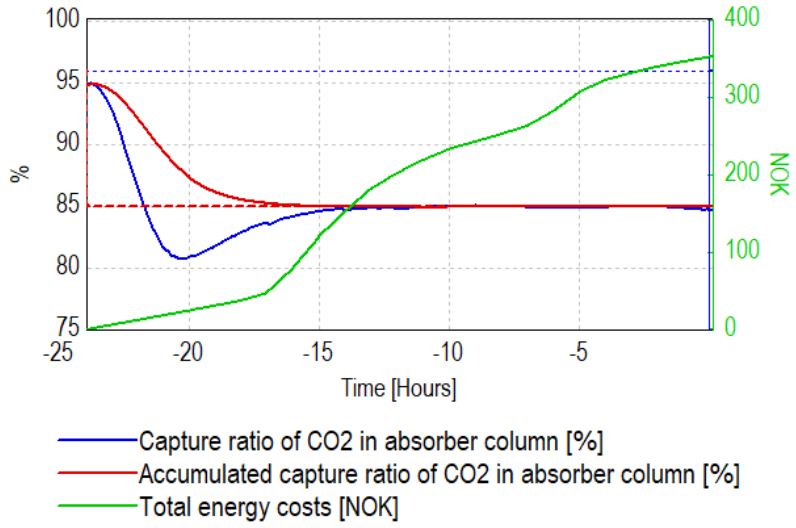


(b) Control Variables

Figure 5.4: Result of basic case where the accumulated capture ratio is held constant through the horizon after an initial transient. $\mathrm{CR}_{acc}^{ref} = 85\%$

## 5.2 Flexible mode of operation

The infeasible-soft constraints method were utilised also for the flexible mode due to easier tuning of the controller. However, the unreachable setpoint method was experimented with and yielded well results. However, not as good as the results from the infeasible-soft constraints method in this section. For the interested reader, may the simulation case using the unreachable setpoint method be found in the Appendix, Section A.1. For the flexible mode using the infeasible soft-constraint method, constraints on the $\mathrm{CR}_{acc}$ were set to $\mathrm{CR}_{acc}$(min,max) = ($\mathrm{CR}_{acc}^{ref}$,96) with only one evaluation point, at $k = 24$ hours. Consequently, will the accumulated capture ratio in addition to the instantaneous capture ratio be allowed to vary around $\mathrm{CR}_{acc}^{ref}$ during the prediction horizon, hopefully minimising the cost significantly. Such constraints on the $\mathrm{CR}_{acc}$ should make the algorithm find and optimal solution yielding an end accumulated capture ratio at the the reference value, the lowest bound. This is because less $\mathrm{CR}_{acc}$ always induce less cost, such that even though the end $\mathrm{CR}_{acc}$ is allowed between the bounds, the algorithm should force $\mathrm{CR}_{acc}$ to the minimum to also minimise cost. Equivalently to the base case, were two reference values; $\mathrm{CR}_{acc}^{ref} = 91\%$ and $\mathrm{CR}_{acc}^{ref} = 85\%$ experimented with. As before were the infeasible soft-constraints set on the cost, Cost(min,max) = (0,0), and constraints set on the CR, CR(min,max) = (75,96). However, for the CR in this case, a CV evaluation point where set every 6 hour. The number and length of the input blocks are the same as in the base case. A summary of the flexible mode simulation case may be found below.

Case: Flexible mode, infeasible-soft constraint method

**Goal:**
Achieve accumulated capture ratio of $CR_{acc}^{ref}$ after 24 h
Minimise Cost

**MV's:** RD, $F_{l,abs}$

**CV's:** $CR_{acc}$, Cost, CR

**CV setpoints:**
N.A.

**CV constraints:**
$CR_{acc}$: [$CR_{acc}^{ref}$,96]
Cost: [0,0]
CR: [75,96]

**MV input blocking:**
RD: first after 30min, then every 2 h
$F_{l,abs}$: first after 30min, then every 2 h

**CV evaluation points:**
$CR_{acc}$: after 24 h
Cost: after 24 h
CR: every 6 hour

The result of the simulation using $CR_{acc}^{ref} = 91\%$ may be found in Figure 5.5 whereas for $CR_{acc}^{ref} = 85\%$ in Figure 5.6. The resulting end cost became $Cost_N = 343$NOK and $Cost_N = 307$NOK for the two cases respectively, which yielded a cost reduction from the basic case of 10.9% and 13.0%. The results show as suggested earlier, that a lower reference value would grant the instantaneous capture ratio to vary to a larger degree than for the higher reference value such that the cost reductions increased. The resulting cost and cost reductions for the different cases may be seen in Table 5.2. In both cases, may one see that the optimal solution for the reboiler duty varies in agreement with the price of energy in Figure 5.1. When the energy price has its lowest peaks the reboiler duty has its highest peaks and vice versa. From Figure 5.6 it may seem that the CR violates the constraints enforced of [75,96]. However, keep in mind that the CR has evaluation points only every 6 hours such that the CR is allowed to be outside the bounds between the evaluation points. In addition, if the penalisation weight on this variable is sufficiently lower than for the other CV's, deviations from constraints may be accepted in order to comply with the constraints of the other CV's. If it is undesired for the CR to be outside the bounds, the number of evaluation points may be increased and the

penalisation weight may be set higher.

It is worth noticing that the initial point used in the simulation cases in this section and in the previous induces a warm start for the cost minimisation. The algorithm may thus focus on decreasing the $CR_{acc}$ towards reference point, hence use less energy than if the initial point was lower. This has been experimented briefly with in which an initial point of 91% and 80% accumulated capture ratio were used. The resulting end cost became, as expected, larger for both cases. With $CR_{acc}^{init} = 91\%$ the end cost became $Cost_N = 350$NOK and for $CR_{acc}^{init} = 80\%$ the end cost became $Cost_N = 410$NOK. The resulting optimal trajectories for both cases may be found in the Appendix, Section A.2 and A.3.

Aforementioned, as bias updating was excluded for tuning purposes, is it of importance to keep an eye on the $CR_{acc}$ in the simulator such that it is not below the reference value at the end of the simulation horizon. However, it was found that the $CR_{acc}$ in RealSim was always greater than the $CR_{acc}$ in CENIT after 24 hours, see Table 5.2, which suggest that the algorithm uses more energy than necessary. Consequently, could bias updating benefit cost minimisation as measurements from the simulated facility would be taken into account. The algorithm would be able to use less reboiler duty as the accumulated capture ratio in RealSim may be lowered to achieve the reference value. Keep in mind however, that even though the total operational cost could be lowered introducing bias updating, would the cost reductions in percentage be the same as bias updating would cause a decrease of the $CR_{acc}$ in RealSim also for the base cases. Simulation with bias updating is briefly experimented with and the results may be seen in Section 5.6.

Table 5.2: Summary of cost, cost reduction and accumulated capture ratio in RealSim for different optimisation cases

| **Case** | **Capture goal [%]** | **Cost [NOK]** | **Cost red. [%]** | **$CR_{acc}$ [%] (RealSim)** |
|---|---|---|---|---|
| Basic | 91 | 384 | ∼ | 95.4 |
| | 85 | 353 | ∼ | 89.5 |
| Infeasible s.-c. | 91 | 342 | 10.9 | 93.7 |
| | 85 | 307 | 13.0 | 87.7 |
| Unreachable setpoint | 91 | 348 | 9.4 | 94.3 |

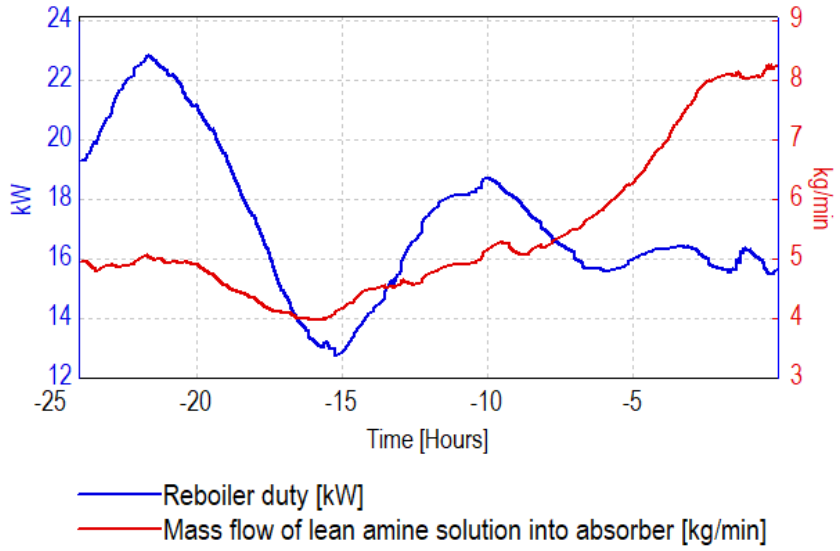


(a) Manipulated variables

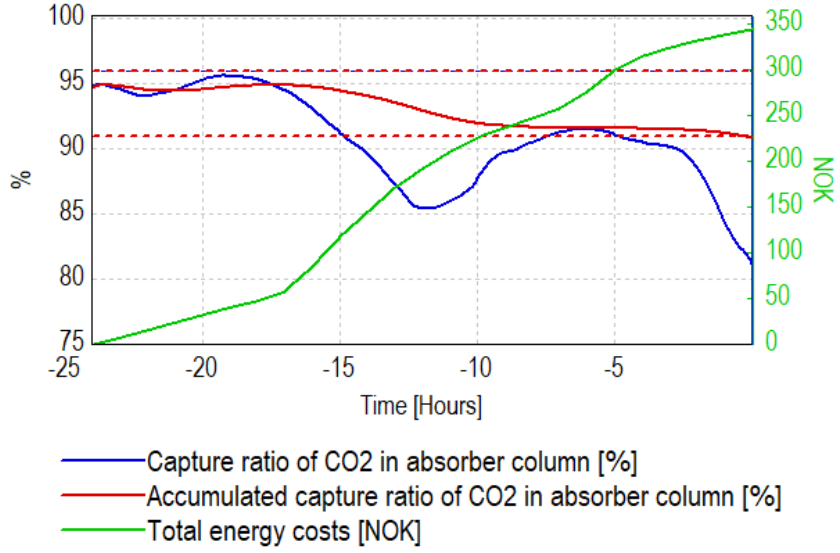


(b) Control Variables

Figure 5.5: Result of MV's and CV's for the flexible mode using the infeasible soft-constraint method with $\mathrm{CR}_{acc}^{ref} = 91\%$

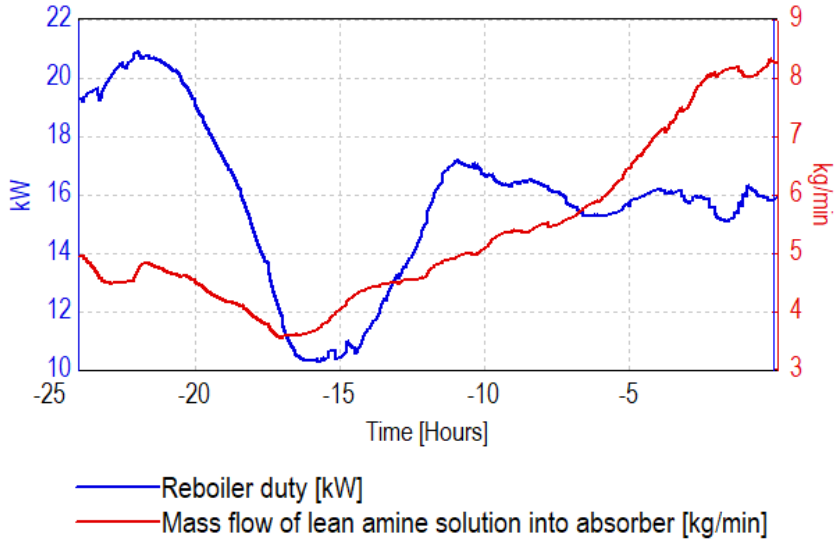


(a) Manipulated variables

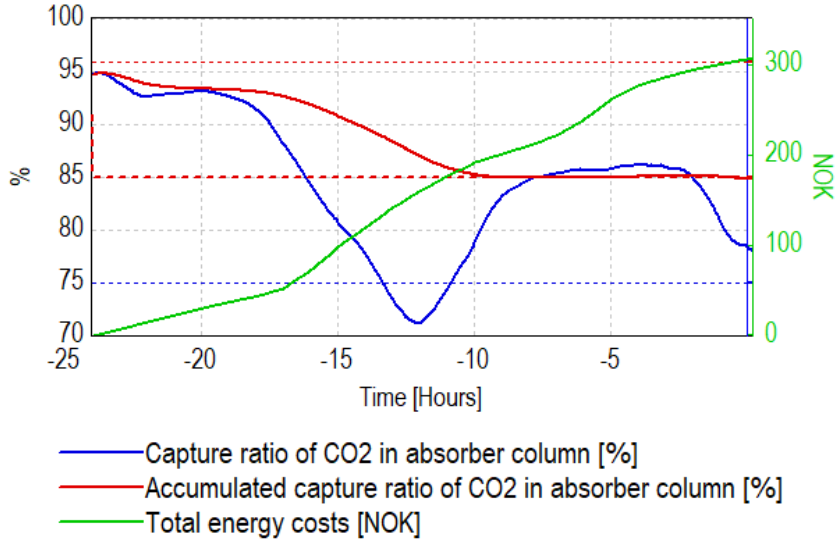


(b) Control Variables

Figure 5.6: Result of MV's and CV's for the flexible mode using the infeasible soft-constraint method with $\mathrm{CR}_{acc}^{ref} = 85\%$

One effect to notice from the flexible mode with infeasible soft-constraints is how $F_{l,abs}$ increases towards the end of the prediction horizon, both in Figures 5.5a and 5.6a and for the cases with the different initial points in the Appendix A.2 and A.3. Why the algorithm chooses this as optimal is not evident, however, one idea is as follows. There are several ways of instantly increasing the CR in the absorber column and two of these are; increasing the circulation rate of the liquid solution $F_{l,abs}$ and increasing the MEA regeneration by increasing the reboiler duty. Due to the shrinking horizon effect caused by freezing the optimisation variables, the algorithm optimises one day isolated without regarding the previous or the coming day. One should expect the reboiler duty to increase towards the end of the simulation horizon as the energy price decreases. However, as the accumulated capture ratio is above the reference value towards the end of the simulation horizon, the algorithm may relax the costly regeneration step and rather increase $F_{l,abs}$ sufficiently to achieve an accumulated capture ratio of $\text{CR}_{acc}^{ref}$ at $k = 24$hours.

A consequence of the combination of $F_{l,abs}$ and RD at the end of the prediction horizon is a quite low instantaneous capture ratio. This effect is not ideal if the simulations were to continue into the next day, as the delayed regeneration of the MEA would have to be performed to increase the CR. In fact, a two-day simulation has been investigated and the simulation results may be seen in the Appendix, Section A.4. Notice how the cost is reset after 24 hours due to minimising the cost during each 24 hours. As expected, the end cost after simulating day two became $\text{Cost}_N = 411$NOK as CENIT started with an instantaneous capture ratio of less than 91% and consequently had to use more energy to reach the goal of $\text{CR}_{acc}^{ref} = 91\%$. One solution to this problem is to introduce end constraints on for instance the inputs or the instantaneous capture ratio to force a desired condition at the end of the horizon. This may however, influence the minimisation of cost on the current day. Another solution may be to expand the prediction horizon to several days and use evaluation points every 24 hours. However, this would result in either increasing the time between each input block if the same number of input blocks where to be used, or increase the number of input blocks to yield the same length of each input block. Thus a trade-off between solving time and sensitivity to change in price would occur. A prediction horizon of 48 hours, although without the evaluation point after 24 hours, was experimented briefly with and the simulation result may be seen in the Appendix A.5. It was chosen to increase the number of input blocks to maintain the same sensitivity, which drastically increased solving time. As may be seen, the algorithm chose to utilise the low energy price around the beginning of a new day and increase the reboiler duty instead of relaxing it. This is as expected, as the algorithm now have to reach the reference after 48 hours. The inclusion of the evaluation point after

24 hours, could further make the $CR_{acc}$ reach its reference at the beginning of each new day, most likely without the low CR towards the end of the prediction horizon.

Simulating several days after each other, one should expect that the optimal solution would converge such that two consecutive days look similar to each other with the same initial point and same end point. However, after simulating 7 days in a row, day 6 and day 7 still became slightly different from each other. For instance the initial point at the beginning of a new day for the CR and the RB. The simulated optimal trajectories may be found in the Appendix, Section A.6. The reason for this may be the use of only one QP iteration to solve the nonlinear optimisation problem, which may give somewhat different results each time. Simulating even longer may show a convergence of the optimal solution, however, another problem may thus occur. The optimal solution may then experience loss of sensitivity for the variables consisting of integrals such as the accumulated capture ratio, equation 5.1. Notice, how the cost is reset each 24 hours because of minimising the cost through every day, however, the accumulated capture ratio is not reset as to avoid large, unrealistic jumps in the $CR_{acc}$ from one sample to the next. Not resetting this variable will result in, as time increases, the integral being made up of numerous samples such that changes in the instantaneous capture ratio will have little influence on the accumulated capture ratio. This may in fact be illustrated comparing Figure A.4b to Figure A.6b. The CR for day 6 in Figure A.6b is very similar to day 2 in Figure A.4b, however, the $CR_{acc}$ in A.4b varies much more than in Figure A.6b. A solution to this problem is either resetting the accumulated capture ratio now and then, or, as the time goes by, throw away a certain amount of old samples.

## 5.3 Flexible mode with an abrupt change in the carbon dioxide composition of the inlet exhaust gas

In order to test the robustness of the optimisation algorithm, several cases has been experimented with and one of these is a case where an abrupt change in the $CO_2$ composition of the inlet exhaust gas is induced. The aim of testing the robustness is to see whether CENIT will be able to re-plan the optimal solution to account for abrupt disturbances. The flexible mode case in Section 5.2 with $CR_{acc}^{ref} = 91\%$ was carried out, and the change in $CO_2$ composition was manually performed after approximately 11.5 hours of simulation. At this time of the day, the results from Section 5.2, Figure 5.5b, show that the instantaneous capture

ratio is quite low and by increasing the $CO_2$ composition at this point, one should expect CENIT to re-plan such that the CR increases sufficiently to reach the goal of $CR_{acc}^{ref} = 91\%$. From the results in Figures 5.7, one may see that the optimal solution is as expected. At 11.5 hours into the day, the $CO_2$ inlet composition is changed from 4.3% to 7%, which is a very large change. However, if the algorithm is able to re-plan and reach the goal considering such a large change, then smaller changes will not cause problems either. As a consequence to the increase in composition, do both the reboiler duty and $F_{l,abs}$ increase, such that the reference value for the accumulated capture ratio is achieved after 24 hours. Notice however, that the instantaneous capture ratio drops instantly after the change in composition. This is due to the inlet flow of $CO_2$ gas to the absorber becoming much larger than before and due to the inputs not being able to change abruptly to increase the absorption rate. Correspondingly, due to more utilisation of energy, does also the end cost increase to $\text{Cost}_N = 468\text{NOK}$. For sufficient test of robustness of the DRTO for disturbances in $CO_2$ inlet composition, should the composition also be changed at different times and it should be decreased and increased with different amounts. One additional simulation case was performed changing the composition to 7% after 19 hours of simulation instead of 11.5 hours. This is shown in the Appendix, Section A.7. Unfortunately, due to the instant drop in the CR after the change, the goal of $CR_{acc}^{ref} = 91\%$ is not reached at the end of simulation. Had the change in composition been less, the reference value for $CR_{acc}$ been lower, for instance 85%, or the rate of change of the input been allowed larger, the goal might have been reached. Consequently, one may see that the algorithm is not robust for all conditions, and is most probably limited by physical properties, such as the rate of change of inputs.

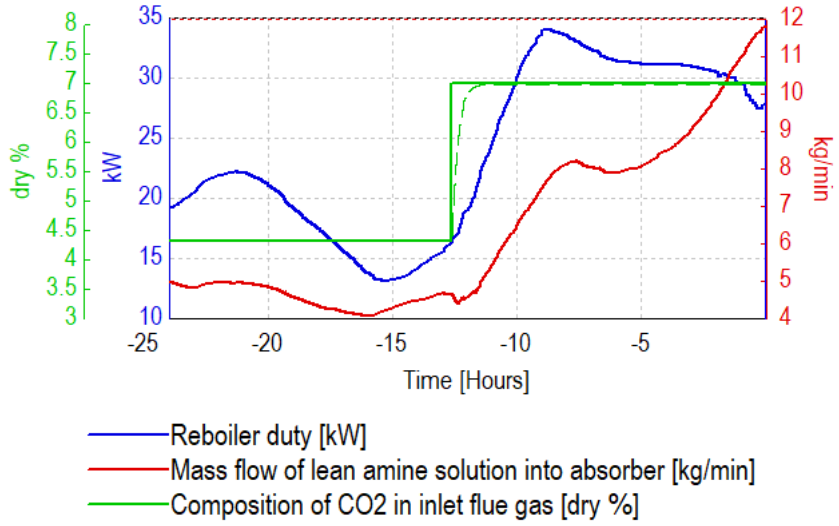


(a) Manipulated variables and $CO_2$ composition

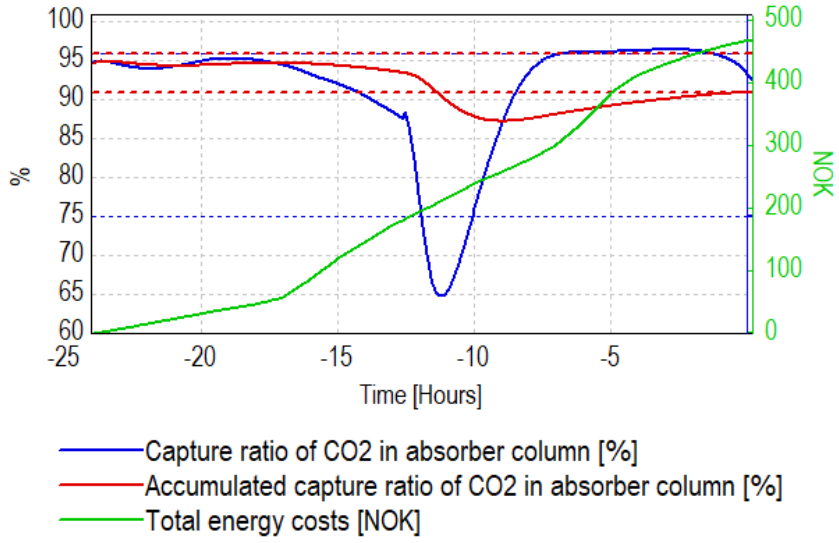


(b) Control Variables

Figure 5.7: Result of MV's and CV's for the flexible mode with an abrupt change in exhaust inlet $CO_2$ composition after 11.5 hours. $CR_{acc}^{ref} = 91\%$.

## 5.4 Flexible mode with an abrupt change in the price of electricity

In this section, the robustness of the DRTO to an abrupt change in electricity price was investigated. As with the case in Section 5.3, the flexible mode case from Section 5.2 was utilised with a $\mathrm{CR}_{acc}^{ref} = 91\%$. After approximately 4.5 hours into the simulation, the electricity price was manually increased by thrice the amount such that the algorithm had to re-plan its optimal solution according to the new predictions of the energy price. The results may be seen in Figure 5.9. Comparing with the results from the flexible mode in Section 5.2 Figure 5.5, may one see that the reboiler duty is lower around 10 hours into the simulation where the electricity price has its highest peak for the case with increased price. Correspondingly, does the instantaneous capture ratio become smaller around this point in time than in the flexible mode simulation case without disturbances in Section 5.2 Figure 5.5b. This is as expected as it is much more costly to use energy after the increase, and the algorithm should take more advantage of the low peaks in the electricity price. However, in order to still reach the goal of $\mathrm{CR}_{acc}^{ref} = 91\%$, the instantaneous capture ratio around 20 hours into the simulations becomes larger for the case with increased price in Figure 5.9b than the case without in Figure 5.5b. A case where the price of electricity increased after 12 hours of simulation was also investigated and the simulation results may be found in the Appendix Section A.8. Comparing these results to that of Figure 5.5 for the flexible mode without disturbances, there are only minor differences in the MV's and CV's except for the cost which is larger as expected. The reason for only minor difference is probably due to the increase in price occurring after the highest peak in the original energy price curve in addition to having less time left to focus on cost reductions compared to the case in Figure 5.9 where the change in price occurs earlier. The cost at the end of the prediction horizon is further weighted significantly lower than the $\mathrm{CR}_{acc}$ so that the algorithm chooses to fulfil the goal of the $\mathrm{CR}_{acc}$ to a larger extent than cost minimisation. These two cases show that the algorithm is robust to increases in the electricity price and manages to reach its most important goal of $\mathrm{CR}_{acc} = CR_{acc}^{ref}$. On the other hand, different shaped price curves should also be tested for proper conclusions of the robustness to changes in the electricity price. In fact, out of curiosity was one case investigated where a different price curve was utilised throughout the simulation horizon, and for the interested reader the simulation results may be seen in Appendix A.9. The DRTO managed to achieve the reference accumulated capture ratio also in this case.

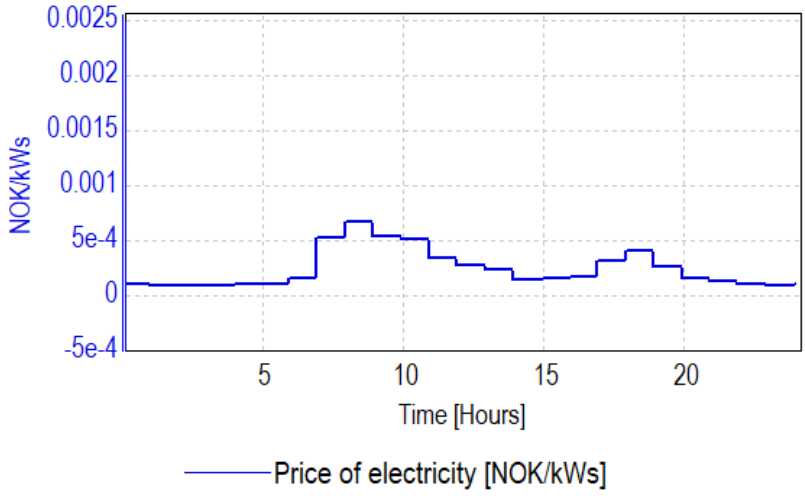


(a) Price of electricity before increase

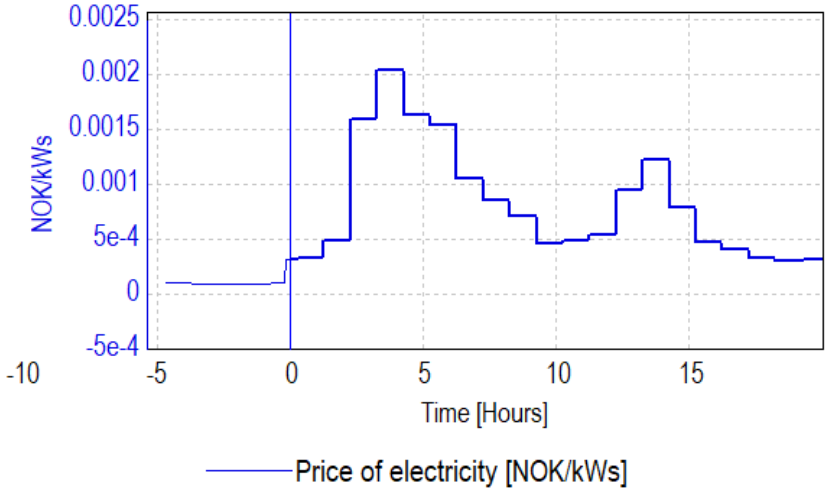


(b) Price of electricity after increase

Figure 5.8: Illustration of electricity price before and after increase for the flexible mode with an abrupt change in electricity price after 4.5 hours. $\mathrm{CR}_{acc}^{ref} = 91\%$.

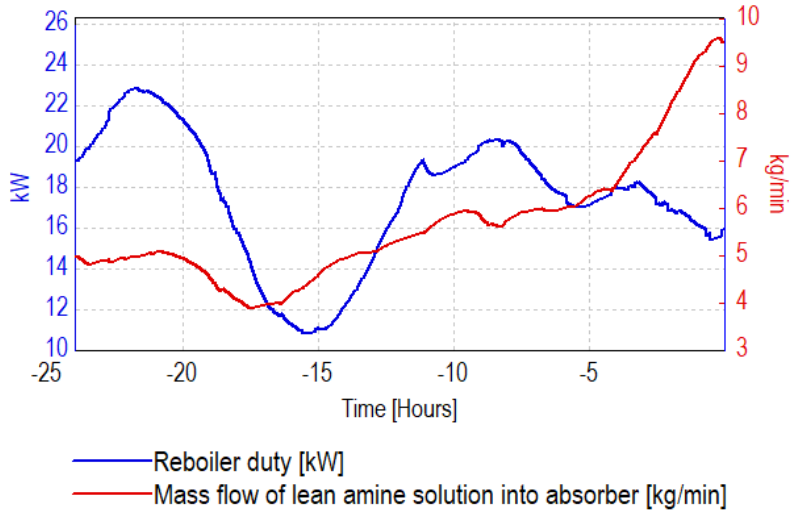


(a) Manipulated variables

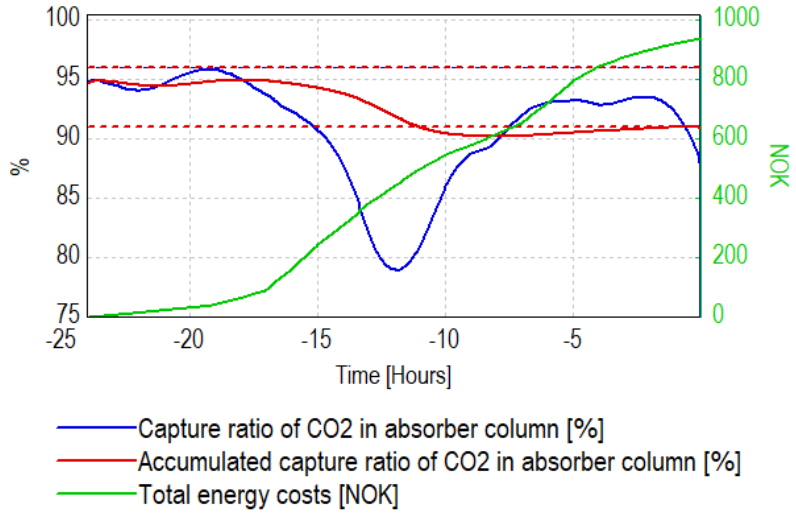


(b) Control Variables

Figure 5.9: Result of MV's and CV's for the flexible mode with an abrupt change in electricity price after 4.5 hours. $\mathrm{CR}_{acc}^{ref} = 91\%$.

## 5.5 Flexible mode with strict constraints on the reboiler duty

Another way to test the robustness of the DRTO is to enforce strict constraints on one of the manipulated variables in the optimisation problem, to see if the DRTO is able to find an optimal solution in a much stricter environment. This is investigated using the flexible optimisation case with a goal of 91% in addition to setting much stricter constraints on the reboiler duty, RD(min,max) = (10,18)kW. The maximum constraint applied here, is obviously a violation considering the results from the previous subsections in which the reboiler duty often increases above this limit. Hence, one should expect the optimal trajectories to change considerably. The result of the simulation may be seen in Figure 5.10. Notice how the reboiler duty is restricted by the upper constraint of 18kW. Consequently, the reboiler duty cannot decrease as much as in Section 5.2 during the highest peak in the electricity price, as it cannot increase too much during low peaks in the electricity price. The result became an end cost of $\text{Cost}_N = 369$NOK. This is nevertheless an increase in cost reduction from the basic case of 4.7%. Further, one may see that the DRTO was able to regulate the accumulated capture ratio to the goal of 91% at the end of the prediction horizon.

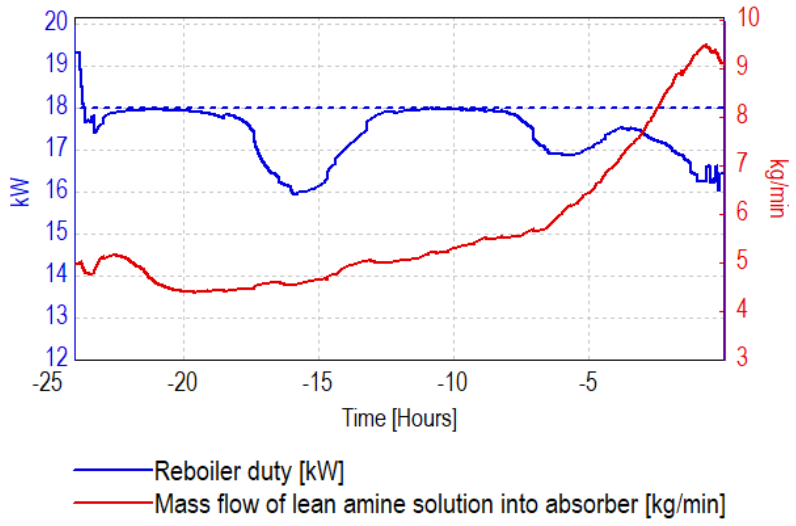


(a) Manipulated variables

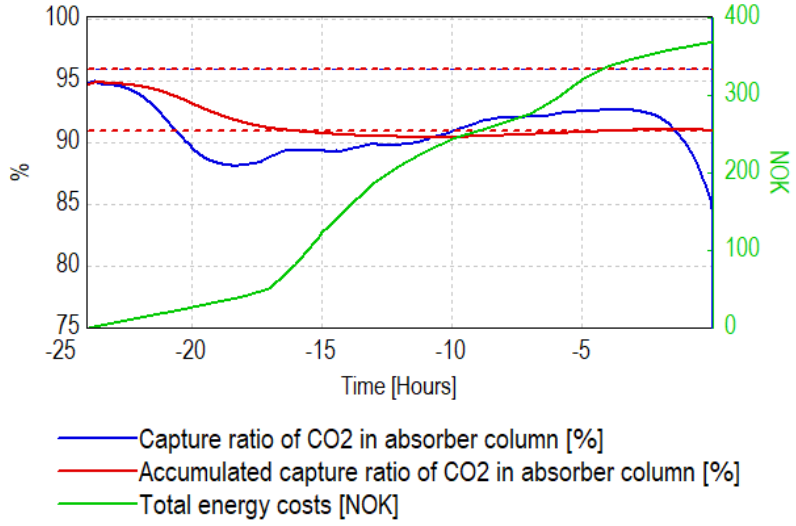


(b) Control Variables

Figure 5.10: Result of MV's and CV's for the flexible mode with strict constraints on the reboiler duty. $CR_{acc}^{ref} = 91\%$.

## 5.6 Flexible mode with bias updating

As previously, bias updating was excluded for simplicity during tuning and testing of the controller. However, as seen from the result in Table 5.2, using the original model as the simulated facility in RealSim resulted in a $\text{CR}_{acc}$ which was several percentage points above the $\text{CR}_{acc}$ in CENIT. This suggest that the optimisation algorithm uses more energy in the reboiler than necessary yielding a higher end accumulated capture ratio than the reference value in the simulated facility. Consequently, may further cost minimisation be accomplished if bias correction is introduced to adjust the deviation in the $\text{CR}_{acc}$. As in Section 4.5 was bias updating using measurements of the mass flow of $CO_2$ from the condenser utilised. Yet now predicted measurements from the original model are utilised instead of instrumental measurements. Of course, in a real setting where the algorithm is to control a plant, the measurements will be instrumental once again. In the Tiller facility, the normal range for this variable is 15-20 $\frac{kg}{h}$. The flexible simulation case from Section 5.2 with $\text{CR}_{acc}^{ref} = 91\%$ was run and the results may be seen in Figure 5.11. The estimated bias is illustrated in Figure 5.11c. Notice that the values for the bias is at most 4% of the normal range of the mass flow of $CO_2$ from condenser. Some differences from the flexible case in Section 5.2 are noticeable, for instance, the instantaneous capture ratio becomes larger at the beginning of simulation such that it therefore may be less between 10 to 15 hours of simulation where the energy price is largest. Also notice how both the reboiler duty and the $F_{l,abs}$ are larger at the end of horizon than in Section 5.2, Figure 5.5a. One could claim that it is more logical for the reboiler duty to increase towards the end of the simulation horizon as the energy price becomes cheap once again. However, the optimisation algorithm obviously found, in Section 5.2, that increasing $F_{l,abs}$ was enough to capture the remaining $CO_2$ before end of simulation horizon without increasing RD. In this case on the other hand, $F_{l,abs}$ had to be increased even more, and most likely not enough by itself to reach the goal as the RD also increases considerably. The bias updating resulted in the $\text{CR}_{acc}$ in the simulator to become 92.6% which is smaller than in Section 5.2 (95.4%) and hence less energy have been utilised throughout the simulation. Therefore, the resulting end cost became smaller, in fact $\text{Cost}_N = 335$NOK. On the other hand, additionally tuning will be required for the $\text{CR}_{acc}$ in RealSim reaching the reference value and further enhance cost minimisation.

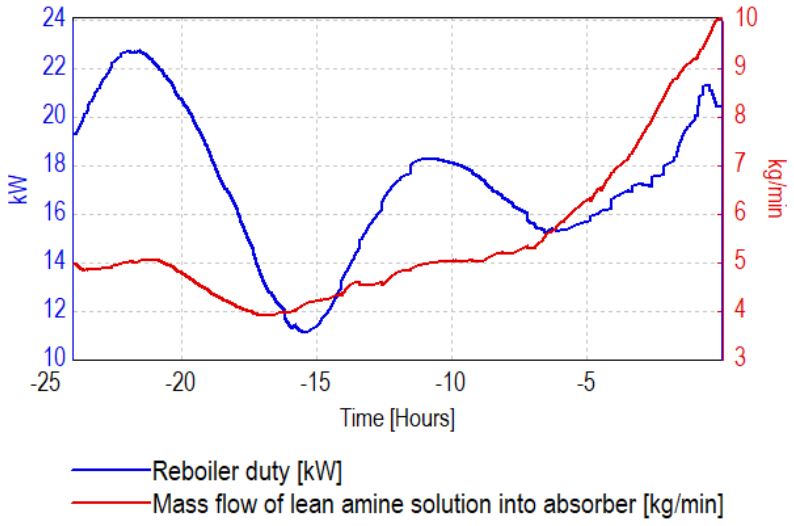


(a) Manipulated variables

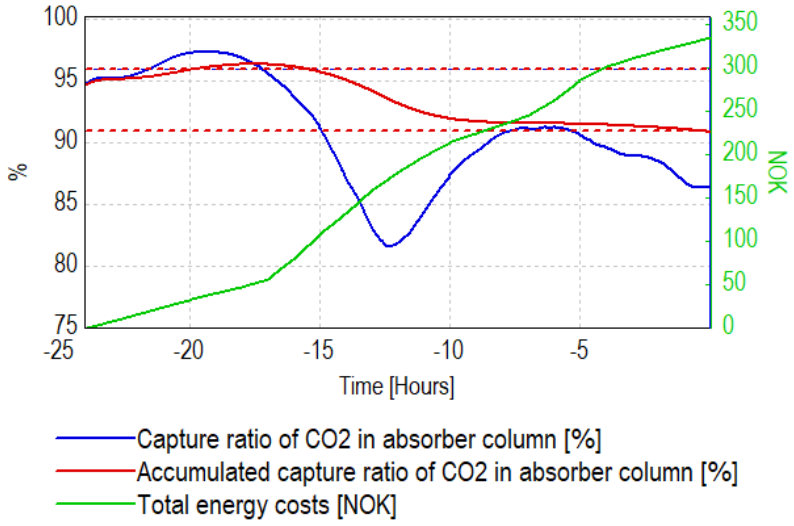


(b) Control Variables

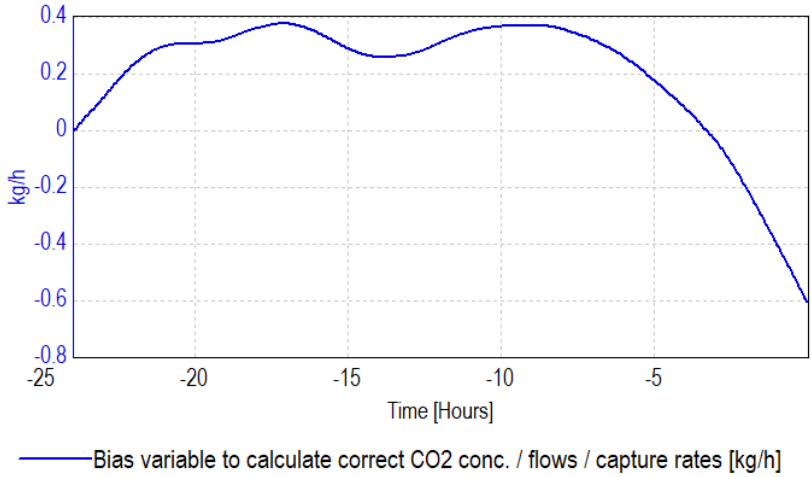


(c) Bias for mass flow of $CO_2$ from condenser

Figure 5.11: Result of MV's and CV's for the flexible mode with bias updating from measurement included. $CR_{acc}^{ref} = 91\%$.

# Chapter 6

# Discussion

Even though results from Chapter 4 and Chapter 5 are satisfactory both when it comes to responses for the reduced model compared against the original model and the performance of the DRTO, are there several assumptions made to achieve the results and several improvements exists that should be considered. For instance, the complete reduced model of the $CO_2$ capture facility has only implemented the model reductions suggested by Hotvedt (2017) for the unit models absorber, desorber and heat exchanger. Further experimentation with the remaining unit models may be performed to reduce the state space and possible decrease the simulation time additionally. Whether or not stiffness of the model may be improved by further model reductions are difficult conclude as dynamical states for both gas and liquid will persist and consequently will a natural spread in eigenvalues still exist. As was seen, the reduced unit models of the heat exchanger, absorber and desorber did increase the stiffness of the unit models. However, it must be kept in mind that the stiffness was analysed only at certain operating conditions and may not be representative for others. Moreover, the approximation of the Jacobian in Listing 2.1 was done using finite differences which has a smaller accuracy than for instance the central differences scheme which may also influence the stiffness results. Furthermore, explained in Section 2.2 could the Jacobian matrix be estimated well only if the problem was well scaled. However, the reduced unit models, the complete temporary models with only one reduced unit model substituted and the total reduced model all have states for both temperature and molar amounts, whereas the states in the original model are scaled with a reference value to yield dimensionless variables. Both the operating conditions and the way the Jacobian is estimated may influence the result of the eigenvalue

analyses. Ideally, should the states in the reduced model be well scaled, the Jacobian estimated with higher accuracy and the eigenvalue analysis repeated for several operating conditions before conclusions are made about the stiffness of the system.

Moreover, both in Chapter 4 and in Chapter 5 have the original model been used under the perfect model assumptions, that is, ignoring any modelling errors between the original model and measurements. Consequently, have the reduced model been compared and adjusted to fit the original model better. However, measurements from a facility, although only a simulated facility in Chapter 4, have been accessible and briefly included in the analysis, but not utilised to its full extent. In Chapter 4 have the data set with measurements provided by SINTEF only been used to illustrate that bias updating is significant to remove modelling error. However, the data set could instead be used in a Kalman Filter for proper parameter estimation, such that modelling error would significantly reduce. On the other hand, it must be kept in mind that a Kalman Filter may result in infeasible parameters. Consequently, should in an in depth study of Kalman Filter for parameter estimation be investigated as it result in both advantages and disadvantages and is therefore a suggestion for future work with the reduced model. Additionally, in Chapter 5 was the original model run in the simulator RealSim but only briefly used for bias updating due to simplifying the tuning of the controller. In Section 5.6, was bias updating included to illustrate that it may lead in further cost minimisation, however, only one case was experimented with and the results still showed an accumulated capture ratio much larger than the needed reference. Consequently, should further investigation with bias updating be performed, for instance, with several other measurements in addition to the mass flow of $CO_2$ from the condenser. Moreover, instead of bias updating, could the responses from the simulator be used in a Kalman Filter for online parameter or state estimation. As previously mentioned did *Cybernetica AS* find the original model to be too computationally inefficient to include a Kalman Filter in online optimisation. However, it has been shown from results that the reduced model improves the efficiency and reduces the simulation time. Therefore, inclusion of a Kalman Filter may be possible for the reduced model. Consequently, this is a recommendation for future work. Regarding the results for the reduction in simulation time of the reduced model compared to the original model in Chapter 4, was this analysis only approximate to illustrate that the model reductions induces simulation time reductions. Exactly how much time will be saved by the introduction of control volumes and the reduction in state space complexity should be further investigated with proper tools before conclusions are made.

In Chapter 5, did the DRTO yield very good results with more than 10% cost reductions comparing the fixed and flexible mode. However, as discussed in

Section 5.2, one should keep in mind that due to the high initial point of the CR and $CR_{acc}$, the optimal solution was subject to a warm start as the algorithm could focus on decreasing the accumulated capture ratio towards reference. Had another initial point been utilised for both basic case and flexible mode case might the reductions in cost have been less. Moreover, did the shrinking horizon effect result in each day being optimised separately such that the MV's end point yielded a less optimal solution for the coming day. Suggestions for improvements were made, however not experimented sufficiently with. Testing the robustness of the DRTO showed that the algorithm was robust in several scenarios. On the other hand, was the algorithm only tested for certain specific cases and for proper conclusions about the robustness of the DRTO, further experimentation with steps in inputs, strict constraints and different shapes for the curve of the price of electricity should be performed.

Furthermore, was it assumed that the low-level controllers in the facility that for instance control liquid levels, behaved perfectly. Such an assumption is acceptable for this thesis as the simulator for the facility simulates another model with the same low-level controllers implemented. However, if a true facility had been controlled using CENIT, the assumption of perfect low-level controllers may be less adequate. In addition, it was assumed that one QP iteration was sufficient to yield good results for the optimal solution. As explained in Chapter 5, additional QP iterations was experimented briefly with and resulted in the optimal solution settling after fewer samples than with only one QP iteration as expected. However, one might be tempted to increase the time between samples as the price of energy only changes once an hour. If so, will it be of more importance for the optimisation algorithm to find the true optimum at each sample, and thus should the number of QP iterations be increased.

As mentioned in Section 2.3, the SQP algorithm is only able to guarantee convergence to a local solution and attempts at analysing the optimisation problem considering global solutions were not performed. Even though the optimisation problem in this thesis is highly nonlinear, are there existing methods for global analysis. If the optimisation problem was to be further experimented with, such global analysis should be attempted. However, as explained in Section 2.3, a well designed objective function is often enough to make the optimisation algorithm find the global optimum. Therefore, as the DRTO is fully able to reach the reference in addition to minimising the cost, may one most probably conclude that the local optimum found is also the globally optimal solution.

Lastly, only one technique for cost minimisation has been investigated, namely a time-varying MEA regeneration throughout the 24 hours. Other techniques are also possible to investigate such as exhaust gas venting, amine storage or a

combination of techniques. Which technique provides the most cost reductions should be experimented with and is a suggestion for future work.

# Chapter 7

# Conclusion

The results from Chapters 4 and 5 are very promising when it comes to firstly, modelling a complete $CO_2$ capture facility using molar amounts as state variables and discretising in space using control volumes, and secondly, optimisation of the model using a Dynamic Real-Time Optimisation Algorithm incorporating both control and economic objectives. Results from Chapter 4 show that the complete reduced model decreased the complexity of the state space with 225 states compared to the original model, in addition to decreasing the simulation time by $\approx 73\%$. On the other hand, the stiffness of the reduced model did not improve significantly. In fact, the separate reduced unit models for the absorber, desorber and heat exchanger had a higher degree of stiffness than the original unit models. Fortunately, the introduction of the reduced unit models did not increase the stiffness of the complete system largely. This is most likely due to having several other unit models in the complete system with both slow and fast dynamics that contribute to stiffness, such as the reboiler or condenser. The reduction in simulation time was thus concluded to be caused by the reduction in state space complexity and simplified spatial discretization using control volumes instead of the collocation method. Moreover, the model reductions induced modelling errors between the reduced model and the original model. On the other hand, Section 4.5 showed that by including bias updating from instrumental measurement of the mass flow of $CO_2$ from the condenser, the modelling errors were significantly removed in variables such as the capture ratio. These results suggest that further modelling errors may be removed by additional feedback from instrumental measurements.

Results from Chapter 5 suggests that optimising a $CO_2$ capture facility during 24

hours with the aid of a DRTO is highly feasible. It was shown that the DRTO was able to reach a specific reference value for the accumulated capture ratio after 24 hours whilst minimising the cost related to the energy consumption in the reboiler. The DRTO was able to utilise the knowledge of an hourly varying price of energy to vary the costly solvent regeneration accordingly, and thus the capture ratio, such that the resulting end cost after 24 hours became less than if the DRTO held the regeneration at a constant level. Two specified reference values for the accumulated capture ratio was experimented with; 85% and 91%, and the resulting cost reductions became 13.0% and 10.9% respectively comparing the end cost of the variable regeneration mode to the fixed regeneration mode. Results testing the robustness of the DRTO showed that the algorithm is robust to abrupt changes in $CO_2$ composition of the inlet exhaust gas, except for large changes occurring close to the end of the simulation horizon. The DRTO was also robust to abrupt increases in the energy price, and was additionally able to handle stricter constraints on the energy utilisation in the reboiler. However, analysing the behaviour of the simulated facility, where the original model was run, showed that due to the modelling errors between the reduced model and the original model, the DRTO utilises unnecessary energy for solvent regeneration resulting in the accumulated capture ratio in the simulator becoming larger than the reference value. Consequently, bias updating using the measurements of the $CO_2$ mass flow from condenser in the simulator was introduced to further enhance cost minimisation.

Consequently, utilising the results from this thesis may drive carbon capture technology one step closer at becoming desirable for companies to invest in. However, there will always be an extra energy demand associated with a connected carbon capture plant, and until the cost of operating the plant is less than the fee of greenhouse gas emissions, there will always exist those who prefer trading for emission allowances. On the other hand, due to the increased focus on reduction of greenhouse gas emissions on a global basis, the results of this thesis may contribute towards an increasing focus on the CCS technology. Especially in Norway, where most of the electricity production comes from the use of renewable sources could CCS greatly benefit reduced emissions of $CO_2$, contributing towards stalling of global warming and its disastrous consequences on a global basis.

# Chapter 8

# Future work

Several extensions and further experimentation of this thesis have been suggested throughout the thesis and are repeated in this chapter. As mentioned in Chapter 4 are there several unit models in the complete model that have not been investigated considering model reductions. Further model reductions may introduce additional modelling errors and larger deviations from measurements. However, it may also lead to additional decrease in simulation time. On the other hand, model reductions must be taken with care, as too large modelling errors are unacceptable. Additionally, discussed in Chapter 6, is the simulation time analysis only approximately done in Modelfit and proper tools should be utilised for exact conclusions of simulation time reductions comparing the reduced model to the original model.

Furthermore, was a Kalman Filter not experimented with in this thesis, neither for parameter estimation in Chapter 4, nor for state estimation and feedback in Chapter 5. As previously explained did *Cybernetica AS* found that the original model was too computational inefficient for online parameter estimation using a Kalman Filter. However, results from Chapter 4 suggests that the reduced model greatly decreased the simulation time and consequently could a successful inclusion of an online Kalman Filter be more probable. At least, a Kalman Filter for offline parameter adjustment during model validation should be further experimented with, as no real-time demand exist for offline model validation.

Moreover, has only one technique for cost minimisation been experimented with, namely time-varying solvent regeneration. Other techniques may also be investigated, such as solvent storage or exhaust gas venting or a combination. In

fact, at the Tiller facility, there exists two storage tanks, see Figure 1.1 in which solvent could be stored during high peaks of the energy curve. Such techniques should also be experimented with in order to see which technique result in most reductions in cost.

As mentioned in Chapter 5, were the energy prices for the coldest day the last year utilised in the optimisation. However, the energy price will change from day to day and will be dependent on the season. Consequently, should an outside algorithm predicting the energy price curve for the day based on for instance weather forecasts and previous data from *Nord Pool, Market Data* (2018) be introduced to make the optimal solution of optimisation more authentic. Additionally could the $CO_2$ emission fee which is daily varying also be included.

Lastly, as mentioned in Chapter 6 has a global analysis of the optimisation problem not been provided due to the system equations being highly nonlinear. However, there exists solutions for global analysis of nonlinear, non-convex problems, and further investigations of the optimisation problem should attempt such an analysis to see whether the local optimum found is also a global optimum, which has only been assumed in this thesis due to good results of the DRTO.

# Bibliography

Arce, A., Dowell, N. M., Shah, N. and Vega, L. (2012). Flexible operation of solvent regeneration systems for co2 capture processes using advanced control techniques: Towards operational cost minimisation, *International Journal of Greenhouse Gas Control* **11**: 236–250.

Arora, S., Dhaliwal, S. and Kukreja, V. (2005). Solution of two point boundary value problems using orthogonal collocation on finite elements, *Applied Mathematics and Computation* **171(1)**: 358–370.

Brown, R. and Hwang, P. (2012). *Introduction to Random Signals and Apllied Kalman Filtering, 4th edition*, John Wiley and Sons, nc.

Carbon Capture and Storage Association (2018). Post-combustion capture, `http://www.ccsassociation.org/what-is-ccs/capture/post-combustion-capture/`. Accessed: 2018-02-22.

Computation (2018). Sundials: Suite of nonlinear and differential/algebraic equation solvers, cvode, `https://computation.llnl.gov/projects/sundials/cvode`. Accessed: 2018-03-13.

Cybernetica AS (2018). Technology: Model predictive control, `http://cybernetica.no/`. Accessed: 2018-03-07.

EnergiNorge (2016). Eu krever okt elektrifisering i norsk transportsektor, *EnergiNorge* .

European Commission (2018a). The eu emissions trading system (eu ets), `https://ec.europa.eu/clima/policies/ets_en`. Accessed: 2018-02-02.

European Commission (2018b). Paris agreement, `https://ec.europa.eu/clima/policies/international/negotiations/paris_en`. Accessed: 2018-02-02.

Flø, N. E., Kvamsdal, H. and Hillestad, M. (2015). Dynamic simulation of post-combustion co2 capture for flexible operation of the brindisi pilot plant, *International Journal of Greenhouse Gas Control* **48**: 204–2015.

Flø, N. E. (2015). *Post-combustion absorption-based $CO_2$ capture: modeling, validation and analysys of process dynamics*, PhD thesis, Norwegian University of Science and Technology.

Foss, B. and Heirung, T. A. N. (2016). Merging optimization and control, *Technical report*, Norwegian University of Science and Technology, Trondheim, Norway. Accessed: 2018-02-22.

FrontlineSolvers (2018). Global optimisation methods, `https://www.solver.com/global-optimization`. Accessed: 2018-05-14.

Geankoplis, C. (1993). *Transport processes and unit operations, 3th edition*, Prentice-Hall International, Inc.

Gravdahl, T. and Egeland, O. (2002). *Modeling and Simulation for Automatic Control*, Marine Cybernetics AS.

Hotvedt, M. (2017). *Modelling and simulation of absorber, desorber and heat exchanger in a post-combustion, amine-based co2 capture facility*, Project thesis, Norwegian University of Science and Technology, Trondheim.

Laird, C., Åkesson, J., Lavedan, G., Prölß, K., Tummescheit, H., Velut, S. and Zhu, Y. (2012). Nonlinear model predictive control of a co2 post-combustion absorption unit, *Chemical Engineering Technology* **35(1)**: 445–454.

Manaf, N., Qadir, A. and Abbas, A. (2017). The hybrid mpc-minlp algorithm for optimal operation of coal-fired power plants with solvent based post-combustion co2 capture, *Petroleum* **3(1)**: 155–166.

Maree, J. P. and Imsland, L. (2011). On combining economical performance with control performance in nmpc, *The International Federation of Automatic Control* .

Moody, T. (2007). Chapter 5: Stiff systems, `http://www4.ncsu.edu/~mtchu/Teaching/Lectures/MA583/chapter5.pdf`.

Nocedal, J. and Wright, S. J. (2000). *Numerical Optimisation, 2nd edition*, Springer.

*Nord Pool, Market Data* (2018). `https://www.nordpoolgroup.com/`. Accessed: 2018-03-02.

Oliveira, V. d. (2016). Economic model predictive control – historical perspective and recent developments and industrial examples, http://folk.ntnu.no/skoge/publications/thesis/2016_de-oliveira/Trial%20lecture/TrialLecture.pdf. Accessed: 2018-04-18.

Olivier, J., Schure, K. and Peters, J. (2017). Trends in global co2 and total greenhouse gas emissions: 2017 report, *Technical Report 2674*, Netherlands Environmental Assessment Agency, The Hague. Accessed: 2018-02-02.

Sahraei, M. H. and Ricardez-Sandoval, L. (2014). Controllability and optimal scheduling of a co2 capture plant using model predictive control, *International Journal of Greenhouse Gas Control* **30**: 58–71.

Seborg, D., Edgar, T. and Mellichamp, D. (2004). *Process Dynamics and Control, 2nd edition*, John Wiley & Sons, Inc.

SINTEF (2017). Co2 laboratory, tiller, https://www.sintef.no/en/all-laboratories/co2-laboratory-tiller/. Accessed: 2018-04-17.

Smith, N., Miller, G., Aandi, I., Gadsden, R. and Davison, J. (2013). Performance and costs of co2 capture at gas fired power plants, *Energy Procedia* **37**: 2443–2452.

SSB (2017). Utslipp av klimagasser, https://www.ssb.no/natur-og-miljo/statistikker/klimagassn/aar-endelige. Accessed: 2018-02-02.

Strand, S. and Sagli, J. (2004). Mpc in statoil - advantages with in-house technology, *Elsvier* **37 (1)**: 197–103.

Wang, Y., Zhao, L., Otto, A., Robinius, M. and Stolten, D. (2017). A review of post-combustion co2 capture technologies from coal-fired power plants, *Science Direct, Energy Procedia* **114**.

Westerberg, A. and Piela, P. (1994). Equational-based process modelling, http://chemeng.in.coocan.jp/ce/WhitmanCME1923.pdf.

Willersrud, A., Imsland, L., Hauger, S. and Kittilsen, P. (2013). Short-term production optimization of offshore oil and gas production using nonlinear model predictive control, *Elsevier, Journal of Process Control* **23 (2)**: 215–223.

Withman, W. (1923). A preliminary experimental confirmation of the two-film theory of gas absorption, *Chemical and Metallurgical engineering* **29(4)**.

World Meterological Organization (2017). Wmo statement on the state of the global climate in 2017, http://ane4bf-datap1.s3-eu-west-1.amazonaws.com/wmocms/s3fs-public/ckeditor/files/2017_provisional_statement_

text_-_updated_04Nov2017_1.pdf?7rBjqhMTRJkQbvuYMNAmetvBgFeyS_vQ. Accessed: 2018-02-02.

Xie, H.-B., Zhou, Y., Zhang, Y. and Johnson, J. K. (2010). Reaction mechanism of monoethanolamine with co2 in aqueous solution from molecular modeling, *Journal of Physical Chemistry A* **114**: 11844–11852.

*Yr* (2018). https://www.yr.no/place/Norway. Accessed: 2018-03-02.

Zhang, Y., Kostyukova, O. and Chong, K. (2011). A new time-discretization for delay multiple-input nonlinear systems using the taylor method and first order hold, *Discrete Applied Mathematics* **159(9)**: 924–938.

# Appendix A

# Extra optimisation cases

## A.1 Flexible mode, unreachable setpoint method

**Case: Flexible mode, unreachable setpoint method**

**Goal:**
Achieve accumulated capture ratio of 91% after 24 h
Minimise Cost

**MV's:** RD, $F_{l,abs}$

**CV's:** $CR_{acc}$, Cost, CR

**CV setpoints:**
$CR_{acc}$: 91
Cost: 0

**CV constraints:**
$CR_{acc}$: [75,96]
CR: [75,96]

**MV input blocking:**
RD: first after 30min, then every 2 h
$F_{l,abs}$: first after 30min, then every 2 h

**CV evaluation points:**
$CR_{acc}$: after 24 h
Cost: after 24 h
CR: every 6 hour

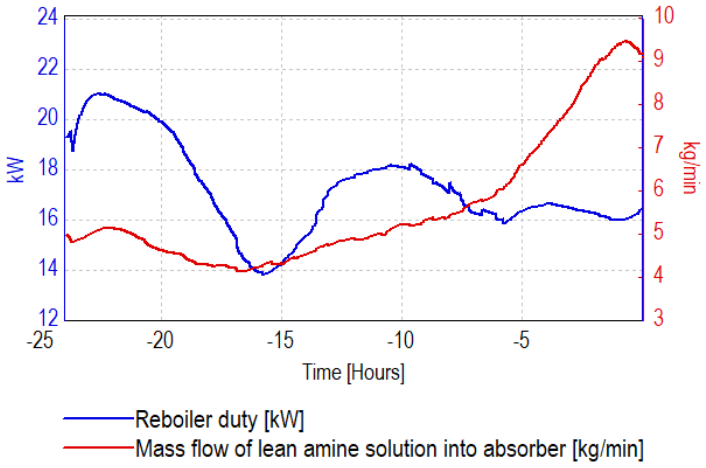


(a) Manipulated variables

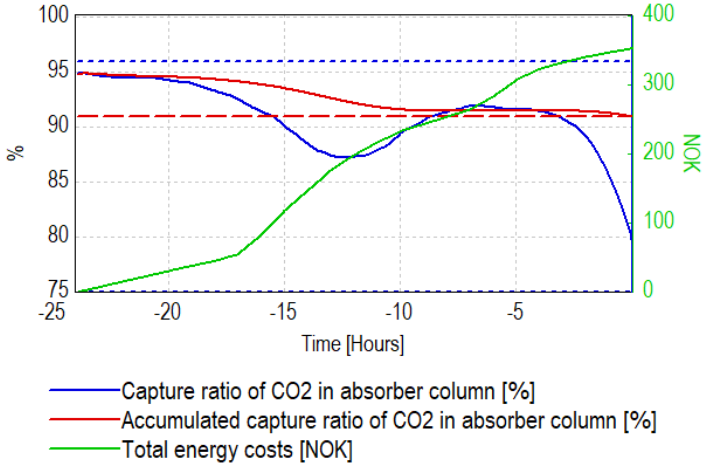


(b) Control Variables

Figure A.1: Result of MV's and CV's for the unreachable setpoint method with $\mathrm{CR}_{acc}^{ref} = 91\%$

## A.2 Flexible mode, infeasible soft-constraints, initial starting point at CR = 91%

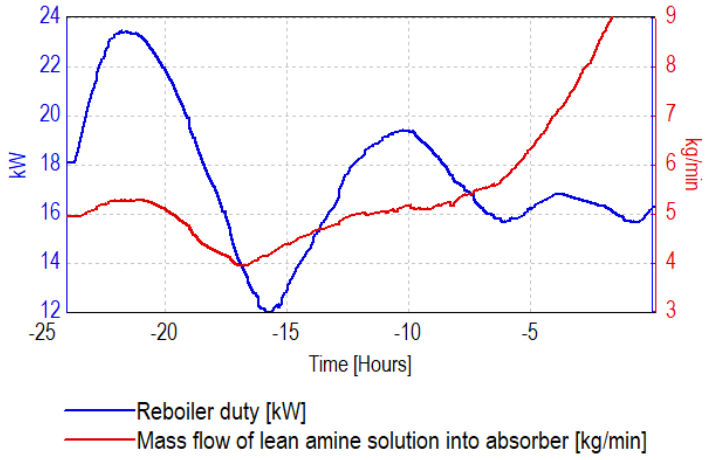


(a) Manipulated variables

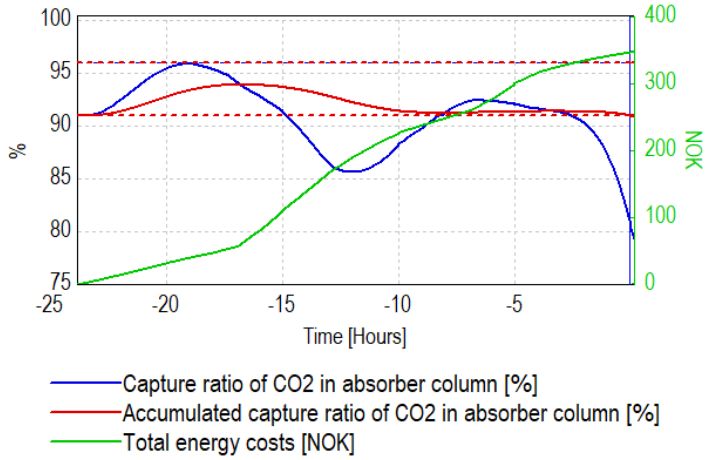


(b) Control Variables

Figure A.2: Result of MV's and CV's for the flexible mode with $\mathrm{CR}_{acc}^{ref} = 91\%$, initial starting point at $CR = 91\%$

## A.3 Flexible mode, infeasible soft-constraints, low initial starting point for CR

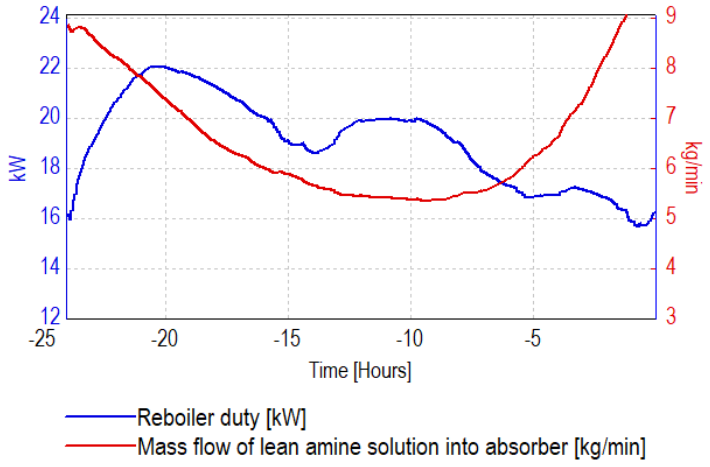


(a) Manipulated variables

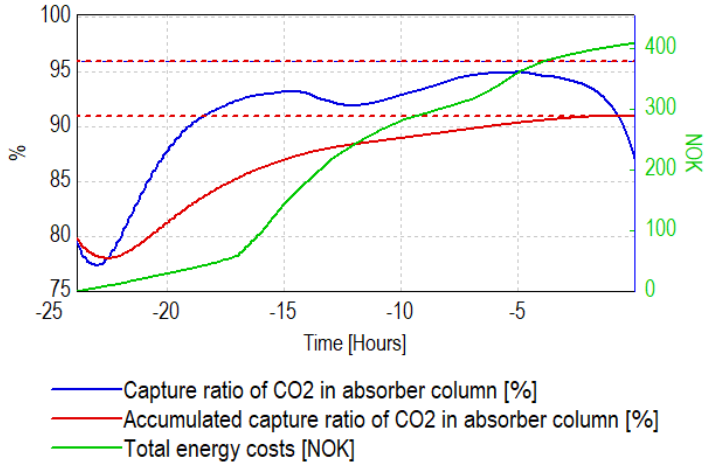


(b) Control Variables

Figure A.3: Result of MV's and CV's for the flexible mode with $CR_{acc}^{ref} = 91\%$ and a low initial starting point

## A.4 Flexible mode, two days simulation

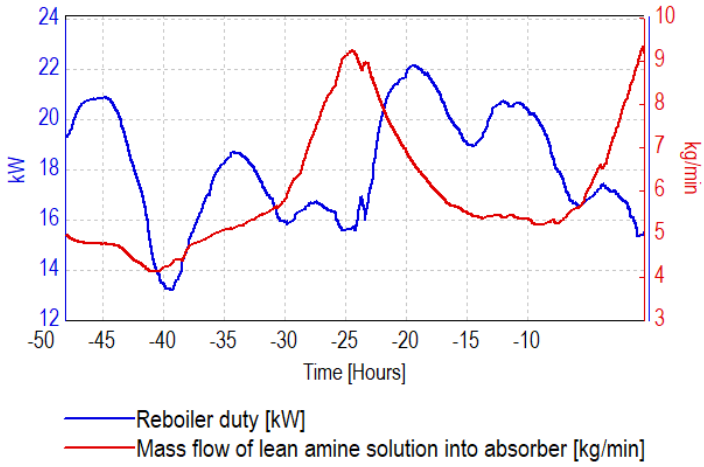


(a) Manipulated variables

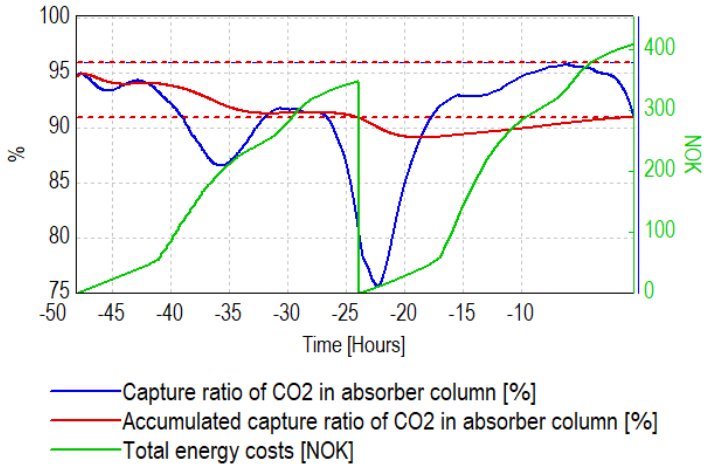


(b) Control Variables

Figure A.4: Result of MV's and CV's for the flexible mode with $CR_{acc}^{ref} = 91\%$ after two days simulation.

## A.5 Flexible mode, prediction horizon of 48 hours

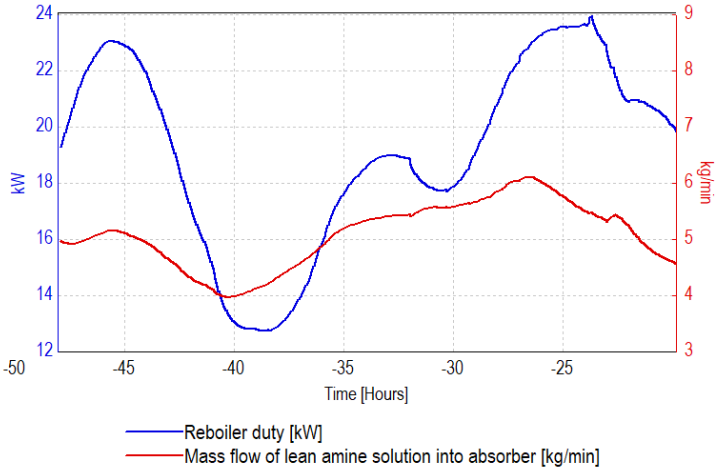


(a) Manipulated variables

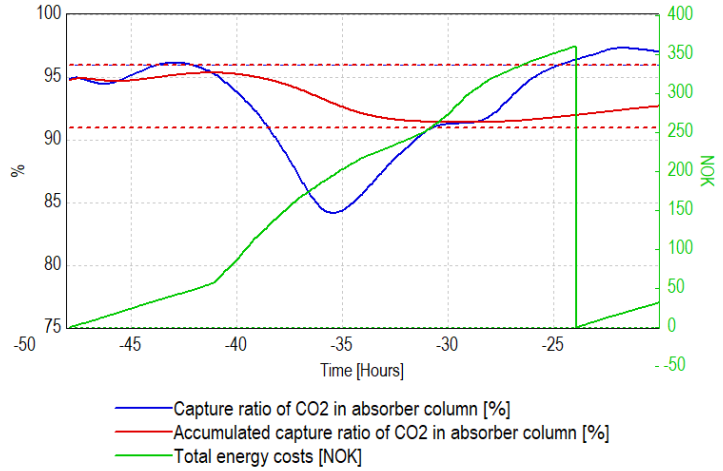


(b) Control Variables

Figure A.5: Result of MV's and CV's for the flexible mode with $CR_{acc}^{ref} = 91\%$ and prediction horizon of 48 hours

## A.6 Flexible mode, day 5-7 after 7 days simulation

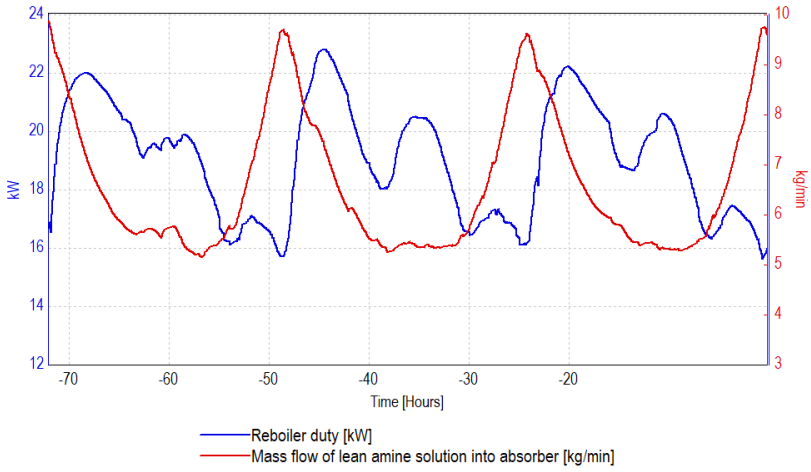


(a) Manipulated variables

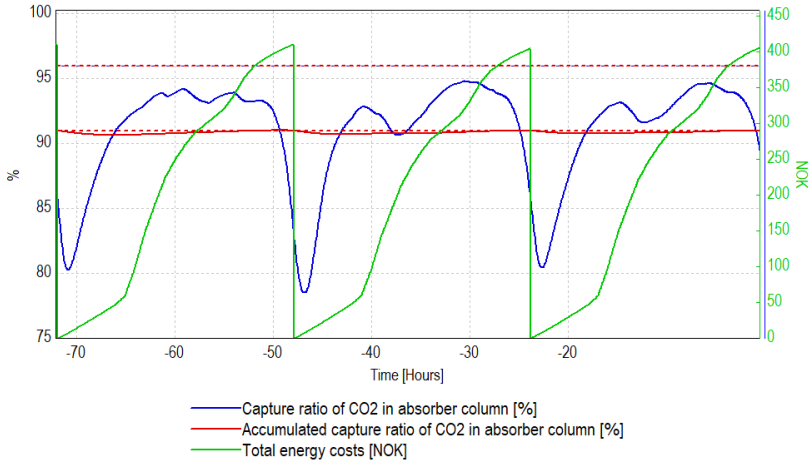


(b) Control Variables

Figure A.6: Result of MV's and CV's for the flexible mode with $CR_{acc}^{ref} = 91\%$ after 7 days of simulation. Illustrated are day 5-7.

## A.7 Flexible mode, abrupt change in composition of carbon dioxide in the exhaust gas after 19 hours

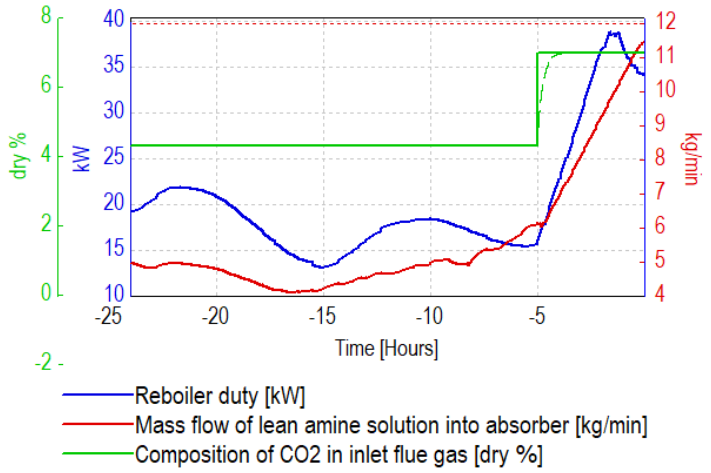


(a) Manipulated variables

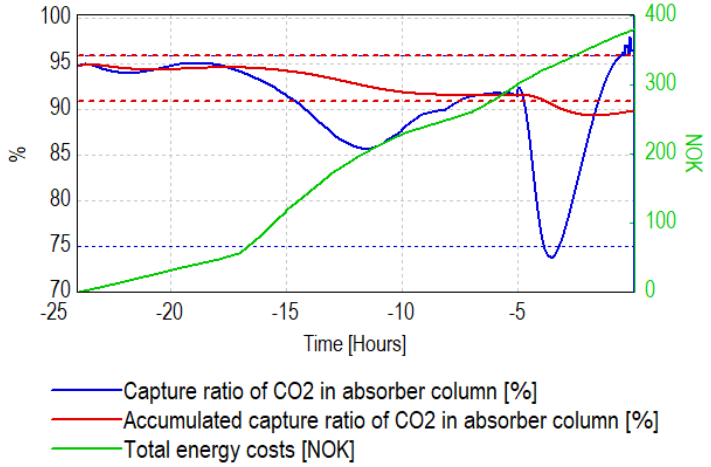


(b) Control Variables

Figure A.7: Result of MV's and CV's for the flexible mode with $CR_{acc}^{ref} = 91\%$ and an abrupt change in $CO_2$ composition in the exhaust gas after 19 hours

## A.8 Flexible mode, abrupt change in electricity price after 12 hours

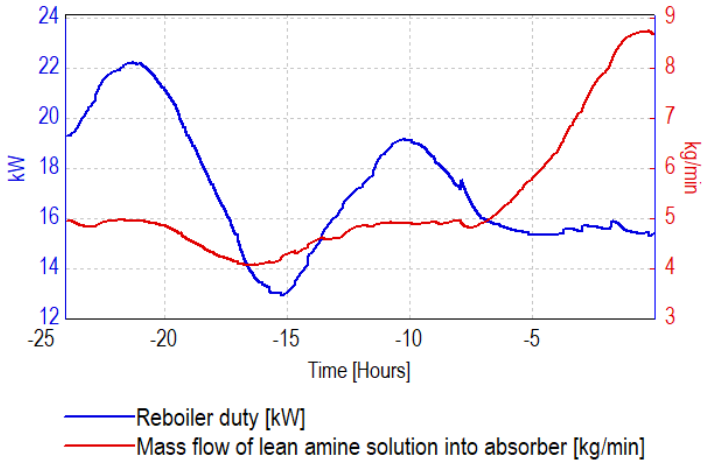


(a) Manipulated variables

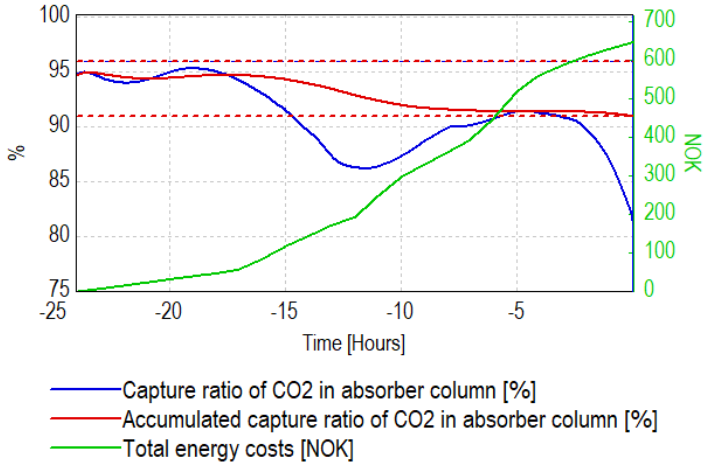


(b) Control Variables

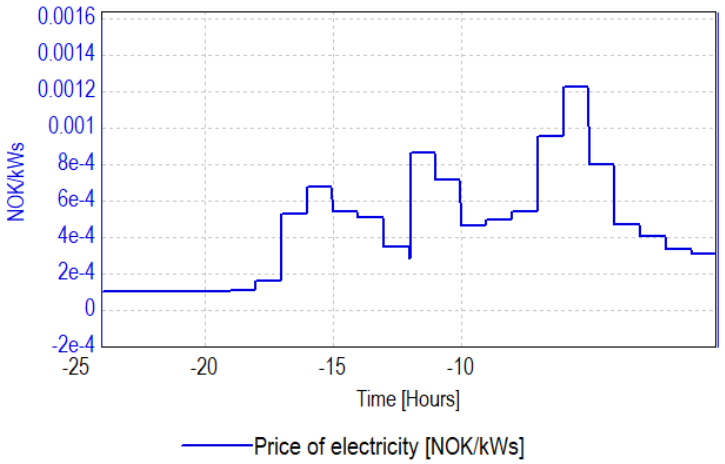


(c) Electricity price curve with increase after 12 hours simulation

Figure A.8: Result of MV's and CV's for the flexible mode with $CR_{acc}^{ref} = 91\%$ and an abrupt change in price after 12 hours

## A.9 Flexible mode, different shaped electricity price curve

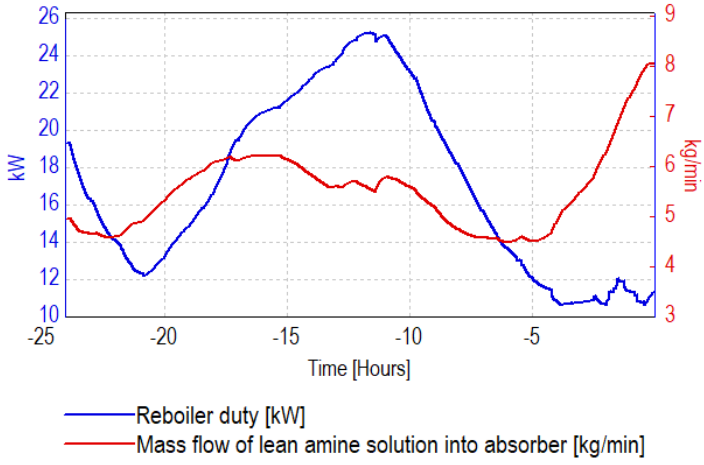


(a) Manipulated variables

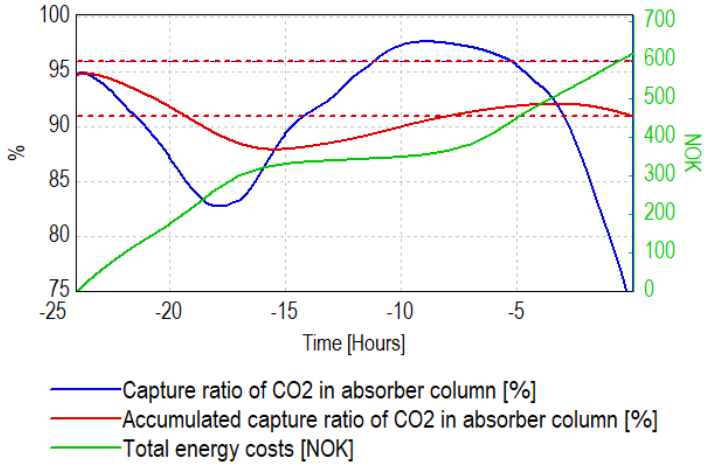


(b) Control Variables

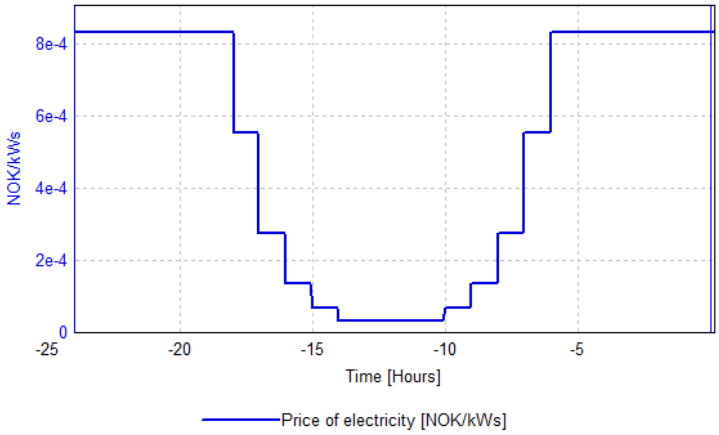


(c) Electricity price curve

Figure A.9: Result of MV's and CV's for the flexible mode with $CR_{acc}^{ref} = 91\%$ and a different shaped price of electricity

# Appendix B

# Conference paper, draft

# Dynamic Real-Time Optimisation of an Amine-Based, Post-Combustion $CO_2$ Capture Facility using Single-Level NMPC

**Mathilde Hotvedt** [*] **Svein O. Hauger** [**] **Fredrik Gjertsen** [***] **Lars Imsland** [****]

[*] *Engineering Cybernetics Department, NTNU, Trondheim, Norway (e-mail: mathilde.hotedt@gmail.com).*
[**] *Cybernetica AS, Trondheim, Norway*
[***] *Cybernetica AS, Trondheim, Norway*
[****] *Engineering Cybernetics Department, NTNU, Trondheim, Norway*

**Abstract:** A complete model of an amine-based post-combustion CO2 capture facility has been attempted optimised considering the energy consumption related to the costly liquid amine regeneration process in the facility. The dynamic model used for optimisation is a reduced version of a previous modelled facility by *Cybernetica AS*, where molar amounts has been used as state variables and control volumes have been utilised for spatial discretisation. The two models have been validated against each other and parameter adjustments performed for the reduced version to fit better to the original. The results show that the reduced version yields adequate responses with parameter adjustments although deviations from the original is visible such that bias update through measurements are necessary for a good fit. The two models have also been analysed considering stiffness, and it was found that the reduced model yielded negligible reduction in stiffness. However, the model reductions yielded a decrease in state space complexity resulting in a simulation time reduction of 73%. The reduced model was optimised using a dynamic real-time optimisation algorithm that merged economic, cost related to energy consumption, and regulatory objectives, obtaining an accumulated capture ratio of 91% after 24 hours. Results comparing a fixed case with constant amine regeneration to a flexible case with a variable amine regeneration according to the natural periodicity of the electricity price show a cost reduction of 10.9% for the flexible case.

*Keywords:* Model-based control, optimisation, Post combustion CO2 capture, Model Predictive Control, cost minimisation, process control

## 1. INTRODUCTION

The year of 2017 had numerous extreme weather conditions such as hurricanes, floods and draughts, and was according to WMO (World Meterological Organization, 2017) among the three warmest years on record. WMO states that the climate changes are most likely caused by the increasing amount of human-made greenhouse gas emissions into the atmosphere, where the most prominent is $CO_2$. There are several ways to reduce the emissions of $CO_2$ to the atmosphere, and a very promising technology is Carbon Capture and Storage (CCS), which according to Carbon Capture and Storage Association (2018) is able to capture on average 90% of the $CO_2$ in exhaust gas from power plants and industrial processes. However, Smith et al. (2013) found that having a $CO_2$ capture plant attached to the outlet of a power plant increased the operational costs of the power plant. Consequently, many companies chooses not to invests in carbon capture plants. In order to make CCS a more desirable technology, possible contribute towards reduced greenhouse gas emissions and stalling of global warming, is it of high importance to reduce the operational costs related to the capture process.

This paper will represent results obtained in a Master's thesis by Hotvedt (2018), regarding cost minimisation of an amine-based post-combustion $CO_2$ capture facility. A post-combustion facility attempts removal of the $CO_2$ from exhaust gas for instance through absorption with monoethanolamine (MEA) (Carbon Capture and Storage Association, 2018). In the absorption tower of the plant, the liquid MEA solution will come in contact with the exhaust gas such that the MEA absorbs the $CO_2$ component of the gas. In the desorption tower, the reverse process is occurring where the MEA solution is regenerated such that $CO_2$ is removed from the liquid solution resulting in a nearly pure stream of $CO_2$ gas out of the desorption tower whereas the liquid amine solution may be circulated back to the absorption tower to be used anew. The regeneration process in the capture facility is a very energy demanding process as the liquid solution must be heated sufficiently for the MEA to release the $CO_2$. The goal has therefore been to minimising the cost related to the energy consumption of the amine regeneration process while regulate the accumulated, or overall, capture ratio, to a specified reference level after 24 hours of simulation. A variable price of electricity has been implemented such that the algorithm may exploit the natural periodicity of

the price curve for less regeneration during high peaks and more regeneration during low peaks.

The model of the capture facility used for optimisation, is a model of an existing test facility located at Tiller, Trondheim (SINTEF, 2017). It will be based on a previous model from Flø (2015) that *Cybernetica AS* has further developed to use in online optimisation, referred to as the *original* model. Model reductions suggested by Hotvedt (2017) for three of the unit models, absorber, desorber and heat exchanger, has been implemented and the complete model referred to as the *reduced* model. The model reductions consisted of modelling each of the dynamical equations for the components in the liquid and gas using molar amounts as state variables in addition to control volumes for spatial discretisation. Therefore has firstly the reduced model been validated against the original model considering performance, system stiffness, state space dimension and simulation time. Theory regarding this topic may be seen in Section 2.1 and simulation results in Section 3.

The reduced model of the capture facility has thereafter been optimised considering cost minimisation related to the energy requirement of the amine regeneration process. Several papers, see Arce et al. (2012), Manaf et al. (2017), have attempted cost minimisation by the use of two-level control hierarchy, which the upper level provides economic setpoints to the lower level for regulatory performance. However, Maree and Imsland (2011) points out that a disadvantage with the two-level hierarchy is an often sub-optimal economic performance and suggests merging the objectives into one-level. One-level control hierarchy was experimented with by Willersrud et al. (2013) on a simplified multi-well oil production plant to yield optimal economic and satisfactory regulatory performance. Such a one-level control hierarchy is sometimes referred to as Dynamic Real-Time Optimisation (DRTO) or Economic MPC (EMPC). Consequently has a DRTO been used on the reduced model of the capture facility to obtain the goal described above. The infeasible soft-constraint method for merging the objectives has been utilised and described in Section 2.2 whilst the simulation results of the DRTO may be found in Section 4.

## 2. METHOD

### *2.1 Model validation and analysis*

The model validation has been performed treating the original model with the perfect model assumption, disregarding modelling errors from the true facility. This assumption has been made as the original model has yielded satisfactory responses when tested by *Cybernetica AS*. Consequently, has the reduced model been validated against the original model in several steps. Firstly, have the two model responses of certain variables been evaluated against each other using maximum and average absolute deviation defined in (1). Here $\phi$ represents a generic variable, subscripts $org$ and $red$ represent the variable in the original and reduced model, $i$ is the index for the variable in question and $K$ is the total number of samples.

$$\begin{aligned} \max|\tilde{D}| &= \max_k \left(|\phi_{i,org,k} - \phi_{i,red,k}|\right) \\ avg|\tilde{D}| &= \frac{\sum_{k=0}^{K}\left(|\phi_{i,org,k} - \phi_{i,red,k}|\right)}{K} \end{aligned} \tag{1}$$

The variables have been analysed in Modelfit using a pre-generated data set from SINTEF containing inputs and a few instrumental measurements for $K = 4656$ samples, representing more than 3 days. The inputs induces steps in the inlet flow of flue gas to the absorber and in the composition of $CO_2$ in the inlet flue gas, and the model responses are calculated based on these inputs. The two most important analysed variables have been the capture ratio in the absorber column, which is a derived variable $\mathbf{z} = h(\mathbf{x})$, and the mass flow of $CO_2$ from the condenser, which is a predicted measurement in the model $\bar{\mathbf{y}}$. The last mentioned variable does have a corresponding instrumental measurement in the data set. Manual parameter adjustment was performed to make the reduced model response fit better to the original model, and a simple estimator, bias updating from measurements, was introduced to illustrate the importance of including measurements in feedback for removal of modelling errors.

Secondly, has the system stiffness been investigated through an eigenvalue analysis. Stiffness is a property that usually occurs from having both fast and slow dynamics that results in a large spread in eigenvalues. Stiffness may influence the solving time of the system as the step size in integration routines must be set small to account for the fastest dynamics in the system. Stiffness may be analysed using the Stiffness Ratio defined in (2) from Moody (2007), where an $SR >> 1$ characterise a stiff system. $\lambda_i$ for $i \in R^m$ are the eigenvalues of the Jacobian matrix $J$ of the system, defined in (3), with dimension $m$ of the state variables $\mathbf{x}$. Here $\mathbf{g}$ represent the set of system differential equations.

$$SR = \frac{\max_i |\Re(\lambda_i)|}{\min_i |\Re(\lambda_i)|} \tag{2}$$

$$J = [\frac{\partial \mathbf{g}}{\partial x_1}, \frac{\partial \mathbf{g}}{\partial x_2}, \ldots, \frac{\partial \mathbf{g}}{\partial x_m}]^T_{|\mathbf{x_p}, \mathbf{u_p}} \tag{3}$$

For a nonlinear, high order system, the finite differences scheme in (4) from Nocedal and Wright (2000) may used to approximate $J$. Here, $\epsilon$ is the perturbation parameter and $\mathbf{e_i}$ a vector with 1 at position $i$ and 0 elsewhere. The perturbation parameter may be chosen $\epsilon = 10^{-8}$ if the problem is well scaled, see Nocedal and Wright (2000).

$$\frac{\partial \mathbf{g}}{\partial x_i} \approx \frac{\mathbf{g}(\mathbf{x} + \epsilon \cdot \mathbf{e_i}) - \mathbf{g}(\mathbf{x})}{\epsilon} \tag{4}$$

Lastly, was an analysis of the approximate simulation time in Modelfit performed. *Cybernetica AS* found using the original model in online optimisation that the original model was too time-consuming by itself to include complex estimators such as Kalman Filter for improved response through feedback from measurements of a real facility. Consequently, was it of interest to see whether the reduced model has decreased the simulation time and hence will be more suitable for online optimisation including a Kalman Filter.

### *2.2 Optimisation problem*

The optimisation problem for optimising the reduced model of the capture facility was to merge economic

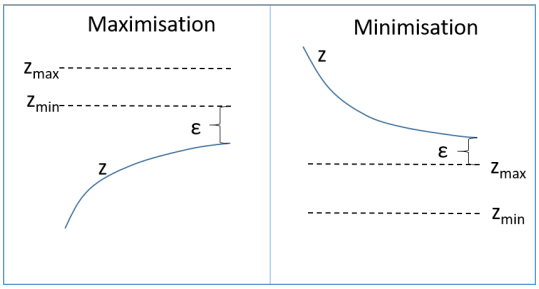


Fig. 1. Illustration of the infeasible soft-constraint method for single-level MPC

and regulatory objectives. Consequently, a Dynamic Real-Time Optimisation (DRTO) algorithm was implemented using single-level Nonlinear Model Predictive Controller. Constructing a single-level control hierarchy may be done using for instance the infeasible setpoint method or the infeasible soft-constraint method explored in Willersrud et al. (2013). The infeasible soft-constraint method has been implemented for this optimisation problem and is illustrated in Fig. 1. The infeasible soft-constraint method introduces out-of-bounds constraints on the economic objectives and takes advantage of slack variables in the objective function to make the optimisation problem feasible but minimise the deviation from the constraints as much as possible. In a minimisation problem the following will always hold as long as the variable $z$ is lower bounded and $-\rho_{opt}\mathbf{z}_{opt,max} \leq 0$. Here $\rho$ is a weight vector for the slack variables.

$$\begin{aligned} \mathbf{z}_{min} &\leq \mathbf{z}_{max} \leq \mathbf{z} \\ \varepsilon &= \mathbf{z} - \mathbf{z}_{max} \geq 0 \\ \rho^T \varepsilon &= \rho^T(\mathbf{z} - \mathbf{z}_{max}) \leq \rho^T \mathbf{z} \end{aligned} \tag{5}$$

Dividing the objectives into two, control objectives $z_{opt}$ and regulatory objectives $z_{reg}$ and utilising the derivation above, may one write the objective function in an (N)MPC scheme with $N$ as the prediction horizon as in (6). Notice how the objective function is independent of the bounds on the economic objectives such that these may be set arbitrarily. For minimisation the cost related to the energy requirement in the capture facility, may the bounds for instance be set to Cost (max,min) = (0,0). Additionally, if $Q_{reg}$ is set small, the objective function will in practice become an exact penalty function in which the regulatory and economic objectives may be weighed directly against each other. Setting $\rho_{reg}$ sufficiently larger than $\rho_{opt}$ will ensure fulfilment of the regulatory objectives but still optimise the economic objectives as much as possible.

$$\begin{aligned} \min_{\phi \in R^n} f(\phi) &= \sum_{i=0}^{N-1} (\mathbf{z}_{reg,i+1} - \mathbf{z}_{reg}^{ref}) Q_{reg} \\ &\cdot (\mathbf{z}_{reg,i+1} - \mathbf{z}_{reg}^{ref}) + \Delta \mathbf{u}_i^T R_\Delta \Delta \mathbf{u}_i \\ &+ \rho_{reg}^T \varepsilon_{reg,i+1} + \rho_{opt}^T \varepsilon_{opt,i+1} \\ &= \sum_{i=0}^{N-1} (\mathbf{z}_{reg,i+1} - \mathbf{z}_{reg}^{ref}) Q_{reg} \\ &\cdot (\mathbf{z}_{reg,i+1} - \mathbf{z}_{reg}^{ref}) + \Delta \mathbf{u}_i^T R_\Delta \Delta \mathbf{u}_i \\ &+ \rho_{reg}^T \varepsilon_{reg,i+1} + \rho_{opt}^T \mathbf{z}_{opt,i+1} \end{aligned} \tag{6}$$

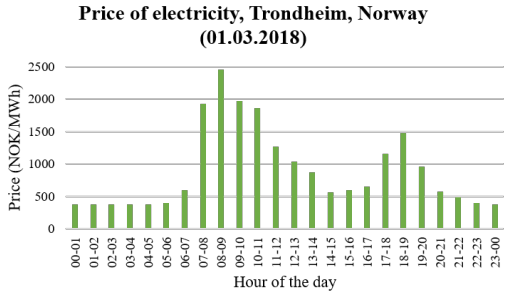


Fig. 2. Illustration of the varying price of electricity in Trondheim, Norway collected from Nord Pool (2018)

The regulatory objective in the optimisation problem of the capture facility is to achieve a specified reference value for the accumulated, or overall, capture ratio ($CR_{acc}$) at the end of prediction horizon $N = 24$ hours. In such a way will a flexible mode be established such that the amine regeneration process is allowed to vary considering a time varying price of electricity, which is illustration in Fig. 2. The data was collected from Nord Pool (2018). The price curve has two high peaks during the day, and consequently should the optimal solution illustrate less energy utilisation in the reboiler (reboiler duty) during these peaks for cost minimisation, whilst $CR_{acc}$ reaches its references after 24 hours.

The flexible mode will be compared to a fixed mode such that conclusions about cost reductions for the flexible mode may be investigated. In the fixed mode, $CR_{acc}$ is forced constant throughout the simulation horizon, to obtain a constant amine regeneration thus constant use of energy. Three controlled variables are utilised in the optimisation problem. The accumulated capture ratio, the cost related to the reboiler duty for amine regeneration, and the instantaneous capture ratio (CR), which should be kept inside bounds of CR (min, max) = (75, 96)% to avoid a complete shutdown of the capture facility for low capture ratio and to avoid large model uncertainties for large capture ratio. Controlled variable evaluation points will be utilised to decrease the number of constraints of the optimisation problem (Strand and Sagli, 2004). For the flexible mode may the Cost and $CR_{acc}$ have only one evaluation point due to obtaining the objectives after 24 hours. For the fixed mode however, several evaluation points for $CR_{acc}$ are needed throughout the horizon due to the stricter requirement of constant $CR_{acc}$, and 6 evaluation points evenly spread out during 24 hours have shown adequate results. To keep the CR within the bounds, 6 evaluation points were used also for this variable. There are two manipulated variables that the DRTO must find optimal solutions for, the reboiler duty (RD) and the mass flow of lean amine into the absorber $F_{l,abs}$. Input blocking has been utilised to reduce the degrees of freedom of the problem (Nocedal and Wright, 2000). As the price of electricity changes every hour of the day, 24 input block's would be ideal, however, 12 input block's evenly spread out have yielded sufficient performance.

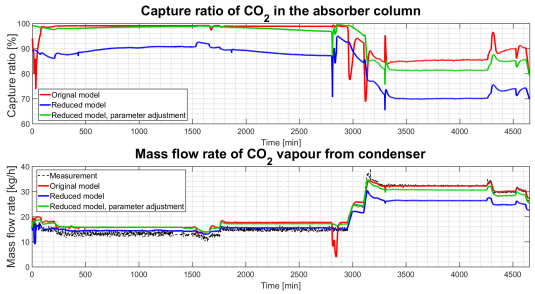


Fig. 3. Result of capture ratio in the absorber column and mass flow of $CO_2$ from the condenser comparing the original model against the reduced model

## 3. SIMULATION RESULTS OF MODEL VALIDATION

The simulation result of the capture ratio (CR) and mass flow of $CO_2$ from condenser ($F_{g,CO_2,cond}$) may be seen in Fig. 3, where the original model response, the reduced model response, and the reduced model response with parameter adjustments have been illustrated. In addition, illustrates the dashed line in the bottom figure of Fig. 3 instrumental measurements for the mass flow of $CO_2$ from condenser from the data set provided by SINTEF. The maximum and average absolute deviation of the two variables comparing the original model to the reduced model may be seen in Table 1.

Seen from the results, parameter adjustments reduced the average absolute deviation of the reduced model to the original model significantly although not removed completely. Notice how the reduced model response without parameter adjustment for $F_{CO_2,cond}$ seem to fit better to the instrumental measurements in the first 3000 samples, however, due to treating the original model as with the perfect model assumption, the response with parameter adjustment is superior. On the other had, it was difficult to remove the deviations completely with manual parameter adjustment. Consequently, was a simple estimator, bias updating, introduced such that feedback from instrumental measurements of the mass flow of $CO_2$ could be used to update the responses of the two variables such that the reduced model fit even better to the original. Seen from the two bottom lines in Table 1 did bias updating result in even less deviations. However, with bias updating the variables to be updated must be determined in advance of simulation and will consequently not remove modelling errors in all variables in the model. Consequently, should also a more complex estimator such as Kalman Filter be experimented with for parameter estimation.

The eigenvalue analysis of the original and the reduced model was performed at two samples in the data set and gave the results in Table 2 and Table 3 respectively. The two samples represent two different operation conditions where at sample 1000, the models are at an approximate steady state, whereas at sample 3000, dynamic changes are occurring. As may be seen, are both models highly stiff as $SR >> 1$ and in fact are the stiffness in the reduced model slightly higher than did the original model. On the other hand, did the model reduction result in a halving of the state space complexity and consequently a reduction in simulation time of approximately 73%, see Table 4. Conclusively, even though the stiffness increased slightly, may one state that the reduced model is more suitable for use in online optimisation as the solving time of the system is drastically reduced, and thus may it also be possible to include a complex estimator for state and parameter estimation in online estimation.

## 4. SIMULATION RESULTS FROM OPTIMISATION

The optimisation cases for the fixed and flexible mode were started from the same initial point using a reference of $CR_{acc}^{ref} = 91\%$, and 24 hours were simulated. The result of the manipulated and controlled variables for the fixed mode may be seen in Fig. 4 and Fig. 5 and the result for the flexible mode may be seen in Fig. 6 and Fig. 7. A solution was accepted if the accumulated capture ratio was within $CR_{acc}^{ref} \pm 0.2\%$. As may be seen was the DRTO able to force a constant $CR_{acc}$ through the horizon after an initial transient for the fixed mode, resulting in a constant reboiler duty. For the flexible mode was the DRTO able to vary the reboiler duty according to the price of electricity in Fig. 2, obtaining much energy utilisation during low peaks of the electricity price and vice versa. Consequently, allowing a flexible mode resulted in a cost reduction of 10.9%. Keep in mind that the simulation was run from a high initial point resulting in a warm start for the DRTO such that it could focus on decreasing the $CR_{acc}$ towards

Table 1. Maximum and average absolute deviation of the capture ratio and the mass flow of $CO_2$ from the condenser. Without and with manual parameter adjustment in addition to bias updating.

| Case | Variable | max $\mid \tilde{D} \mid$ | avg $\mid \tilde{D} \mid$ |
|---|---|---|---|
| Without parameter | CR [%] | 27.68 | 11.21 |
| adjustment | $F_{g,CO_2,cond}$ $[\frac{kg}{h}]$ | 11.10 | 3.18 |
| With parameter | CR [%] | 25.25 | 2.32 |
| adjustment | $F_{g,CO_2,cond}$ $[\frac{kg}{h}]$ | 12.63 | 0.85 |
| With bias | CR [%] | 29.54 | 1.20 |
| updating | $F_{g,CO_2,cond}$ $[\frac{kg}{h}]$ | 11.68 | 0.55 |

Table 2. Eigenvalue analysis of the original model for sample 1000 and 3000 from the data set provided by SINTEF

| Sample | max $\mid \Re(\lambda_i) \mid$ | min $\mid \Re(\lambda_i) \mid$ | SR |
|---|---|---|---|
| 1000 | $5.31 \cdot 10^{3}$ | $3.72 \cdot 10^{-6}$ | $1.43 \cdot 10^{9}$ |
| 3000 | $5.40 \cdot 10^{3}$ | $5.39 \cdot 10^{-5}$ | $1.00 \cdot 10^{8}$ |

Table 3. Eigenvalue analysis of the reduced model for sample 1000 and 3000 from the data set provided by SINTEF

| Sample | max $\mid \Re(\lambda_i) \mid$ | min $\mid \Re(\lambda_i) \mid$ | SR |
|---|---|---|---|
| 1000 | $5.33 \cdot 10^{3}$ | $7.87 \cdot 10^{-7}$ | $6.78 \cdot 10^{9}$ |
| 3000 | $5.43 \cdot 10^{3}$ | $3.25 \cdot 10^{-6}$ | $1.67 \cdot 10^{9}$ |

Table 4. Comparison of state space dimension and simulation time in Modelfit for the original and reduced model

| Model | State space dimension | Simulation time (s) |
|---|---|---|
| Original | 448 | $\approx 26$ |
| Reduced | 223 | $\approx 7$ |

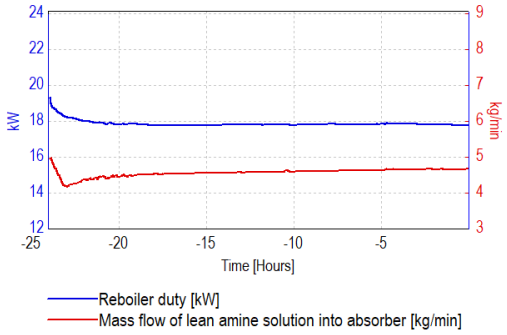


Fig. 4. Result of the Manipulated Variables for the fixed case with $CR_{acc}^{ref} = 91\%$

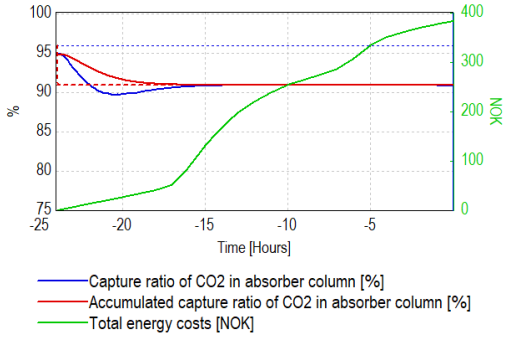


Fig. 5. Result of the Controlled Variables for the fixed case with $CR_{acc}^{ref} = 91\%$

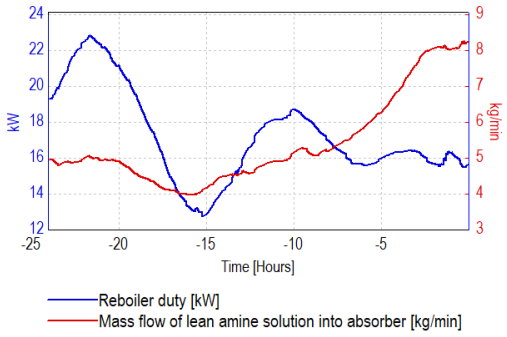


Fig. 6. Result of the Manipulated Variables for the flexible case with $CR_{acc}^{ref} = 91\%$

reference. Had a lower initial point been used may the cost reductions have been less.

The simulation results shown in Fig. 4-7 have not included bias updating with feedback from measurements due to simplifying the tuning of the controllers. However, in Hotvedt (2018), was bias updating experimented with using a simulator tool, RealSim, from *Cybernetica AS* to simulate the facility. Without bias updating, it was found that the facility in the simulator yielded a much larger end accumulated capture ratio than the reference, thus

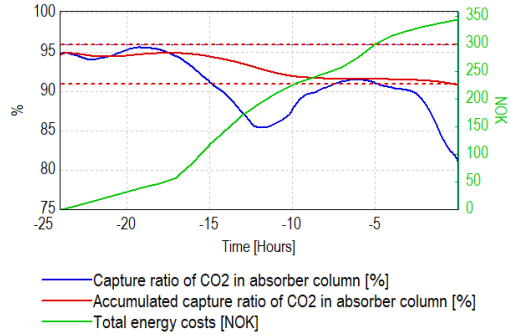


Fig. 7. Result of the Controlled Variables for the flexible case with $CR_{acc}^{ref} = 91\%$

suggesting an unnecessary use of reboiler duty. Inclusion of bias updating from $F_{g,CO_2,cond}$ resulted in a smaller end accumulated capture ratio and thus lower cost. Consequently may bias updating benefit cost minimisation. Furthermore, in Hotvedt (2018), were the robustness of the DRTO to an abrupt change in $CO_2$ composition of the inlet flue gas and an abrupt change in electricity price tested and the results were satisfactory. The DRTO showed able to achieve the reference value for the $CR_{acc}$ in most cases, except for changes in composition close to the end of simulation horizon. Stricter constraints on the reboiler duty was also tested, and results showed that the DRTO was capable of obtaining $CR_{acc}^{ref}$ also in a stricter environment, with the consequence of higher costs.

A Kalman Filter was unfortunately not experimented with for parameter and state estimation and correction. As mention, was the original model too time-consuming for use in online optimisation. However, as results from Section 3 show that the reduced model has a much shorter solving time, inclusion of a Kalman Filter may be possible and should be experimented with in future work with the capture facility. A Kalman Filter may, likewise to bias updating, enhance cost minimisation by adjusting the model to reflect the reality well, and contrary to bias updating, do so in a more automatic way without predetermination of which states or parameters to update.

## 5. DISCUSSION

Simulation results from Section 3 show that modelling a $CO_2$ capture facility using molar amounts as state variables for each of the components in the liquid and gas in addition to spatial discretisation using control volumes are very promising. Even though deviations from the original model is present, was it shown that the deviation could be removed significantly through either parameter adjustments or even better through bias updating using instrumental measurements from a real facility. On the other hand, did the reduced model induce slightly more stiffness to the system than originally. It must be kept in mind however, that the stiffness was only analysed at a few samples from the data set and may not illustrate the stiffness in other operation conditions. Furthermore, as both models are very stiff, should the extra stiffness in the reduced model not in particular influence the

solving of the system. In spite of increased stiffness, did the model reduction result in a halving of the state space dimension of the reduced model compared to the original model resulting in a simulation time reduction of 73%. Consequently, will the reduced model be more suitable for online optimisation. Results from Section 4 show that the use of a DRTO with a single-level NMPC for merging economic and regulatory objectives yield very satisfactory results. Comparing a flexible mode to a fixed mode of amine regeneration, a cost reduction of 10.9% was obtained. Future work with the model of the $CO_2$ capture facility should include experimentation with a Kalman Filter to further enhance cost minimisation.

## ACKNOWLEDGEMENTS

I would like to extend my greatest appreciation to *Cybernetica AS* for allowing me to work with such an important topic as CCS and for aiding me through the process of my Master's thesis.

## REFERENCES

Arce, A., Dowell, N.M., Shah, N., and Vega, L. (2012). Flexible operation of solvent regeneration systems for co2 capture processes using advanced control techniques: Towards operational cost minimisation. *International Journal of Greenhouse Gas Control*, 11, 236–250. doi:https://doi.org/10.1016/j.ijggc.2012.09.004.

Carbon Capture and Storage Association (2018). Post-combustion capture.

Flø, N.E. (2015). *Post-combustion absorption-based $CO_2$ capture: modeling, validation and analysys of process dynamics*. Ph.D. thesis, Norwegian University of Science and Technology.

Hotvedt, M. (2017). *Modelling and simulation of absorber, desorber and heat exchanger in a post-combustion, amine-based CO2 capture facility*. Project thesis, Norwegian University of Science and Technology, Trondheim.

Hotvedt, M. (2018). *Dynamic Real-Time Optimisation of an Amine-Based CO2 Capture Facility using Single-Level Nonlinear Model Predictive Control*. Master's thesis, Norwegian University of Science and Technology, Trondheim.

Manaf, N., Qadir, A., and Abbas, A. (2017). The hybrid mpc-minlp algorithm for optimal operation of coal-fired power plants with solvent based post-combustion co2 capture. *Petroleum*, 3(1), 155–166. doi: https://doi.org/10.1016/j.petlm.2016.11.009.

Maree, J.P. and Imsland, L. (2011). On combining economical performance with control performance in nmpc. *The International Federation of Automatic Control*.

Moody, T. (2007). Chapter 5: Stiff systems.

Nocedal, J. and Wright, S.J. (2000). *Numerical Optimisation, 2nd edition*. Springer.

Nord Pool (2018). Nord Pool, market data. `https://www.nordpoolgroup.com/`. Accessed: 2018-03-02.

SINTEF (2017). Co2 laboratory, tiller. `https://www.sintef.no`. Accessed: 2018-04-17.

Smith, N., Miller, G., Aandi, I., Gadsden, R., and Davison, J. (2013). Performance and costs of co2 capture at gas fired power plants. *Energy Procedia*, 37, 2443–2452.

Strand, S. and Sagli, J. (2004). Mpc in statoil - advantages with in-house technology. *Elsvier*, 37 (1), 197–103. doi: https://doi.org/10.1016/S1474-6670(17)38715-3.

Willersrud, A., Imsland, L., Hauger, S., and Kittilsen, P. (2013). Short-term production optimization of offshore oil and gas production using nonlinear model predictive control. *Elsevier, Journal of Process Control*, 23 (2), 215–223.

World Meterological Organization (2017). WMO statement on the state of the global climate in 2017. Accessed: 2018-02-02.